COMPLEX MICROBIOTA TARGETED REDERIVATION (CMTR) AS AN ALTERNATIVE METHOD TO STUDY EFFECT OF GUT MICROBIOTA ON HOST PHYSIOLOGY

A DISSERTATION PRESENTED TO THE FACULTY OF THE GRADUATE SCHOOL AT THE UNIVERSITY OF MISSOURI IN PARTIAL FULFILLMENT OF THE REQUIREMENTS FOR THE DEGREE DOCTOR OF PHILOSOPHY

BY

MARCIA L. HART

DR. CRAIG L. FRANKLIN AND AARON C. ERICSSON, DISSERTATION CO-MENTORS

DECEMBER 2016

The undersigned, appointed by the dean of the Graduate School, have examined the dissertation entitled

COMPLEX MICROBIOTA TARGETED REDERIVATION (CMTR) AS AN ALTERNATIVE METHOD TO STUDY EFFECT OF GUT MICROBIOTA ON HOST PHYSIOLOGY

presented by Marcia L. Hart,
a candidate for the degree of Doctor of Philosophy, and hereby certify that, in their opinion, it is worthy of acceptance.

_____
Craig Franklin, DVM, PhD

_____
Aaron Ericsson, DVM, PhD

_____
James Amos-Landgraf, PhD

_____
Susan McKarns, PhD

_____
Mark McIntosh, PhD

DEDICATION

This work is dedicated to my loving, and supporting family without whom I couldn't have accomplished this goal. Thank you for all of your support and never questioning my crazy quest for knowledge and love of "going to school".

ACKNOWLEDGEMENTS

I would like to acknowledge and thank the many people who have helped me along this incredible journey.

First and foremost, my co-mentors Craig Franklin and Aaron Ericsson for their excellent guidance during this process. Thank you for the encouragement and for truly listening to my ideas (which admittedly were sometimes a bit crazy).

The members of my committee Dr. Jim Amos-Landgraf,
Dr. Susan McKarns, and Dr. Mark McIntosh

Past and present colleagues at MU both in the Comparative Metagenomics lab and in the Comparative Medicine Program. You guys have been absolutely great to work with and I have appreciated our "over lunch" or "over grown up beverages" science and veterinary medicine chats.

The many mentors, faculty, and veterinarians who have helped me along this exciting journey. Without your encouragement and willingness to teach, my career story may have had a very different ending.

CONTENTS

LIST OF FIGURES

LIST OF TABLES

LIST OF ABBREVIATIONS

ANOVA: analysis of variance

AUC: area under the curve

B6 IL-10-/-: B6.129P2-*Il10*^{tm1Cgn}/J (B6 IL-10$^{-/-}$)

B6: C57L/6 mouse strain

C3H IL-10-/-: C3Bir.129P2(B6)-Il10^{tm1Cgn}/J

CD: Crohn's disease

CD1: Crl:CD1 or ICR mouse stock

CMTR: complex microbiota targeted rederivation

CRL: Charles River Laboratories

Crl:CD1: CD1 or ICR mouse stock

DNA: deoxyribonucleic acid

DPBS: Dulbecco's phosphate-buffered saline

ET: embryo transfer

FVB/J: Friend virus B NIH/Jackson Laboratories mouse strain

GI: gastrointestinal

GIT: gastrointestinal tract

GM: gut microbiota

GMCRL: gut microbiota Charles River Laboratories

GMHSD: gut microbiota Envigo (previously known as Harlan Laboratories)

GMJAX: gut microbiota The Jackson Laboratory

GMTAC: gut microbiota Taconic Biosciences

GWAS: genome wide associated study

hCG: human chorionic gonadotropin

HSD: Envigo (previously known as Harlan Laboratories)

IBD: inflammatory bowel disease

IP: intraperiotneal

IU: international unit

IV: intravenous

JAX: The Jackson Laboratory

NGS: next generation sequencing

OTU: operational taxonomic unit

PCA: principal component analysis

PCR: polymerase chain reaction

PERMANOVA: permutational analysis of variance

PMSG: pregnant mare serum gonadotropin

rRNA: ribosomal ribonucleic acid

SPF: specific pathogen free

TAC: Taconic Bioscience

ABSTRACT

Rodent models are invaluable tools to study the effects of differing gut microbiota (GM) on health and disease. Our laboratory has demonstrated that mouse GM profiles vary among animal vendors suggesting that subtle differences in GM may be an important experimental variable influencing reproducibility. To assess the role of microbiota on model phenotypes, complex microbiota targeted rederivation (CMTR) can be used. With CMTR, mice of the desired model are rederived using embryo transfer into surrogate dams with one or more desired GM profiles. Unfortunately, differing GM are often present in inbred strains of mice complicating CMTR as these strains frequently have poor reproductive indices and variations in maternal care which can add unwanted experimental variables. To overcome this, we exploited the benefits of outbred mice as surrogates by establishing colonies of CD1 mice with differing GM profiles. CD1 embryos were transferred into CD1 or C57BL/6 surrogate dams that varied by GM composition and complexity to establish three separate colonies. Using targeted next generation sequencing, female offspring were shown to have similar GM profiles to surrogate dams. Furthermore, breeding colonies of CD1 mice with distinct GM profiles were maintained for four generations, demonstrating stability of GM profiles within these colonies. We then compared changes in the phenotype of B6 IL-$10^{-/-}$ and C3H IL-$10^{-/-}$ mice rederived by CMTR using either CD1 colonies or the inbred strains from which the colonies were derived. Cecal and colonic histologic lesion scores differed significantly between groups, but no differences were seen when surrogate source of GM (CD1 vs inbred strain) was compared. These findings underscore that CMTR using outbred CD1

colonies will be an invaluable experimental resource for experiments desiring to assess the role of complex microbiota on model phenotypes.

CHAPTER 1:

Introduction

The human gastrointestinal tract (GIT) is one of the most densely populated ecosystems known, with an estimated number of microbes outnumbering human cells by a factor of 10. It is thought that these microbes carry as many as 150 times the genes contained in the human genome (1). To put this into perspective, humans have been described as a super-organism, consisting of 90% microbial cells and 99% microbial genes (2) which beg the questions "who are these microbes and what are they doing?". Despite their considerable volume, little is known about the true nature and function of these microbes in health and disease.

The majority of the gut microbiota (GM) is unculturable and it has only been within the last decade, with the advent of advanced sequencing technologies, that study of these microorganisms has been possible. It is becoming apparent that the GM plays an important role in both enteric and systemic disease (3, 4). However, the majority of these studies remain correlative largely due to difficulty in controlling experimental variables such as environment, genotype, and patient compliance (4) as well as reliance on biopsy and fecal sampling (5-7). Animal models can be an important means to control or modify these experimental variables. Unfortunately, the majority of studies are performed on rodents with an overly simplified GM composition thereby inadvertently limiting translatability to human populations who are colonized with diverse, complex GM profiles. To date, there is a paucity of reliable *in vivo* methods in which to study the effect of complex GM in translatable rodent models. To overcome these limitations we

implemented a new strategy that we named Complex Microbiota Targeted Rederivation (CMTR) to focus on the study of complex GM profiles in the IL-$10^{-/-}$ mouse model of inflammatory bowel disease (IBD). The studies in this dissertation describe the standardization of DNA extraction methods used to detect GM bacterial communities by next generation sequencing (chapter 2), development of outbred Crl:CD1 mice with defined, complex GM profiles that can be used for Complex Microbiota Targeted Rederivation (CMTR) (chapter 3), investigation into the utility of CMTR to improve consistency in disease phenotype of the Il-$10^{-/-}$ mouse model of inflammatory bowel disease (chapter 4), and outline smaller projects used to support these key studies (chapter 5). The author's objective for the research detailed within this body of work is to advance the field of microbiome research by providing an alternative method for studying the role of complex GM profiles and demonstrating their effect on disease phenotype in the IL-$10^{-/-}$ mouse model.

Gut Microbiota (GM)

The human body is colonized by a myriad of microorganisms. Composed predominantly of bacteria, these organisms are found in a variety of anatomic locations and are thought to have coevolved with their hosts over the last millennia (8). In addition to bacteria other microbes can also be found including archaea, fungi, viruses, and eukaryotes. Collectively these microorganisms and all of their genetic components are referred to as the *microbiome*. Individual microbial populations within a site are termed *microbiota* and are often preceded with a description of the anatomic location, such as gut microbiota (GM) which will herein be the term used to describe gut bacteria.

The gastrointestinal tract (GIT) is a long tube lined by a single layer of simple epithelium that runs from the oral cavity to the anus and is broken down into upper (oral cavity, esophagus, stomach, duodenum) and lower (ileum, jejunum, appendix/cecum, colon, anus) regions. Each segment within these regions is colonized by a number of microbes increasing in concentration and complexity from upper (predominantly aerobic bacteria) to lower (predominantly anaerobic bacteria), with the vast majority of bacteria colonizing the cecum and colon (9-11). In addition to longitudinal differences in colonization along the GIT, there are also axial differences in colonization from the luminal to mucosal surface (12). GIT bacteria are largely commensal, with many important host-microbe interactions occurring along the epithelial-bacterial interface. These interactions have been suggested to be important in many physiologic processes in health and disease including metabolism, immunity, organ development, and protection against pathogen infection (3, 13-15).

GM Colonization and Maturation

For decades, common dogma proposed that the intrauterine environment is sterile with early GM colonization occurring during and shortly following birth. However, both human and animal studies have demonstrated the presence of maternal gut associated bacteria such as *Escherichia coli* and *Enterococcus faecium* in the placenta and amniotic fluid suggesting that the GM may be colonized much earlier (16-19). Additional studies have shown that *Enterococcus*, *Streptococcus*, *Staphylococcus*, and *Propionobacterium* species can be isolated from umbilical cord blood (20). The bulk of these bacteria are thought to result from translocation of the mother's microbiota to the blood stream followed by colonization of the associated fetal tissues and fetus via the fetal circulatory

system. Interestingly, two studies indicate early fetal colonization with several bacterial phyla including *Actinobacteria*, *Proteobacteria*, *Bacteroidetes*, and *Firmicutes* in relative abundances that closely resemble the maternal oral cavity further implicating bacterial translocation from maternal GIT to fetus (21, 22). An alternative mechanism of fetal colonization is by fetal swallowing of maternal enteric bacteria present in the amniotic fluid. During normal fetal development, fetal swallowing of amniotic fluid occurs by 8 weeks of gestation (23). Ardissone *et al*. detected similar bacterial species in both meconium and amniotic fluid, suggesting that fetal ingestion of maternal bacteria is possible (24). Despite the possibility of early *in utero* colonization, it is thought that these bacteria make up a relatively small portion of the neonatal GM with the majority of colonization occurring during and shortly after birth.

Initial neonatal GM composition is predominantly of maternal origin, and is largely dependent on the mode of delivery. Whereas, vaginally delivered infants are colonized with bacteria of fecal and vaginal origin such as *Lactobacillus* spp., *Prevotella* spp., and *Escherichia coli*; cesarean delivered infants are colonized with bacterial species of maternal epidermal and hospital origin including species within genre *Staphylococcus*, *Propionobacterium*, *Clostridium* and *Corynebacterium* (25, 26). Infants delivered via cesarean-section have been shown to have a delay in gut colonization by phylum *Bacteroidetes* that may not resolve until 1-7 years of age when compared with vaginal delivery (27, 28). In addition to delivery mode several other factors are indicated to influence early postnatal GM development including gestational age (29), breast feeding vs. formula feeding (30), and environment (31, 32) .

The postnatal GM continues to develop throughout maturation with a general reduction in number of aerobes and facultative anaerobes and an increase in anaerobic bacterial populations such as *Bacteroides*, *Clostridium*, and *Bifidobacterium* spp. (33-35). Initially the neonatal GM is characterized by low diversity with a predominance of the phyla *Proteobacteria* and *Actinobacteria*. With postnatal ageing, a progression toward increased bacterial diversity and increased abundance of *Firmicutes* and *Bacteroidetes* occurs. It is thought that by 2-5 years of age, this shift in bacterial population more closely resembles an adult GM (36, 37).

The healthy adult GM has individual specificity and is thought to be generally stable throughout adulthood (34, 38, 39) with temporal fluctuations in composition occurring in response to change in diet, antibiotic use, disease, and environment (39-41). Endoscopic based studies of healthy individuals show esophageal bacterial populations with limited bacterial diversity dominated by *Streptococcus* spp. in the distal esophagus (42). Other genera such as *Prevotella*, *Actinomyces*, *Lactobacillus*, and *Staphylococcus* have been shown to be present but in lower relative abundance. In contrast to other body sites, increased bacterial diversity in the distal esophagus has been shown to correlate with disease (43). In the stomach there are a total of 10 genera with *Helicobacter pylori* (which can be commensal or pathogenic) accounting for the vast majority of taxa when present (44). Other taxonomic members are *Prevotella*, *Streptococcus*, *Veillonella*, and *Rothia* spp. with *Streptococcus* being the predominant genus when *H. pylori* colonization is absent (44). Little is known regarding the small intestine, as studies of this region of the GIT are limited to biopsies and ileostomy samples which are associated with diseased patients and provide little insight into the healthy GM (5, 10).

The greater number of studies performed on fecal samples from healthy volunteers suggest that the adult lower GIT is largely dominated by two phyla, *Firmicutes* and *Bacteroidetes* (8, 45, 46) with minor contributions by *Actinobacteria*, *Verrucomicrobia*, and *Proteobacteria*. In the colon, the majority of bacteria are within the phylum *Bacteroidetes* and belong to the genus *Bacteroides*, while a large number of bacteria within phylum *Firmicutes* are classified as *Clostridium coccoides* group (*Clostridium* clutster XIVa) or *Clostridium leptum* group (*Clostridium* cluster IV). In healthy individuals the abundance of the phylum *Proteobacteria* is markedly low, with a relatively high abundance of *Bacteroides*, *Prevotella*, and *Ruminococcus* species.

The microbiota of the elderly has been shown to have greater inter-individual variation than adults with a trend toward a decrease in GM diversity correlating with age, diet, and housing in a retirement community or institution (47-49). In general, there is an increase in facultative anaerobes such as *Proteobacteria* and *Bacilli*, and a decrease in specific bacterial populations such as *Faecalibacterium prausnitzii* and *Clostridium* cluster XIVa bacteria. Decreases in *Bacteroides*, *Bifidobacterium*, and *Enterobacteriaceae* with increases in *Clostridium* spp. have also been reported (47, 48).

Studies of normal, healthy GM composition lay the foundation for the relation of these differences to the disease state with the goal of targeted therapeutic intervention. Unfortunately, at all GM development stages a considerable amount of inter-individual variation has been observed (50, 51) making a generalized characterization of bacterial composition of the healthy GM challenging. In addition, most studies of the GM in healthy patients are largely reliant on fecal samples which are thought to poorly represent

the upper GIT and mucosal-associated bacteria along the GIT length. Although endoscopy and colonoscopy can be performed to obtain biopsy samples, these have been shown to greatly differ in bacterial composition from fecal samples (5-7).

16S rRNA Gene Sequencing

Early studies of the GM were largely dependent on cultivation techniques with bacterial communities being phylotyped based on growth in selective culture medium, metabolic product, substrate consumption, staining characteristics, and cell morphology. However, with an estimate of only 10-30% of the GM being culturable these studies were arguably limited. With the advent of affordable advanced molecular sequencing technologies, more in depth study of the GM has become increasingly possible. A considerable advantage of this technology is the use of bacterial DNA or RNA extracted directly from GIT tissue or fecal samples, without the need for bacterial culture techniques.

Current NGS methods are based on three types of strategies which include amplicon sequencing (for assessment of microbial composition), shotgun sequencing (for assessment of microbial gene content and potential function), and transcriptome sequencing (for assessment of microbial functionality) (52-54). One of the most common applications of amplicon sequencing in NGS technology is 16S ribosomal RNA gene sequencing. Amplicon sequencing utilizes specific primers targeted for polymerase chain reaction (PCR) amplification of the variable region of the16S rRNA gene. The 16S rRNA gene is a component of the 30S small subunit of the prokaryotic ribosome. This gene is highly conserved between species of bacteria (55) and is frequently used for phylogenetic studies (56).

In addition to conserved segments, the 16S rRNA gene contains hypervariable regions that allow specific bacterial identification. There are nine different 16S rRNA variable regions flanked by conserved segments in most bacterial species which can be used as targets for PCR primers based on sequencing application (57). Following amplification and assembly the DNA sequences are assembled into contiguous regions, identified by comparison with previously annotated sequences, and assigned operational taxonomic units (OTUs) based on sequence similarity. Various indices of abundance, richness, and diversity can then be used to compare and describe bacterial communities where these differences may be associated with human health and disease status. However, studies suggest that bias introduced in pre-sequencing sample processing steps such as DNA extraction, can mask true bacterial composition and over- or under-represent specific microbial populations (58). For example, sample or sample processing bias can lead to large discrepancies in the proportion of Gram negative bacteria observed in 16S rRNA sequencing when compared with traditional culture based or microscopic detection methods (59). To address this, we evaluated several DNA extraction methods on fecal samples from a variety of species used in current GM studies (Chapter 2).

Current Models Used to Study the GM

Due to limitations in sampling the human GM, there has been considerable research into the development of alternative *in vitro* and *in vivo* models. *In vitro* models such as batch fermentation, continuous culture, and artificial digesters can provide quick, cost-effective methods to study the GM (60). However, these methods are largely limited as they do not have an epithelial mucosal lining or host immunological and endocrine function. In addition, as the greater proportion of the GM is unculturable these systems

are ineffective at adequately representing the *in vivo* bacterial milieu. Several animal models for studying the GM have been proposed, with the majority of studies being performed in mice. Animal models offer several advantages over human clinical studies including fewer ethical constraints, environmental and genetic control, and GIT accessibility at necropsy. In addition, animal models are advantageous over *in vitro* models as they allow study of unculturable microbes and investigation on the effect of these microbes on host physiology.

Mouse models used to study the GM can be broken down into three basic categories; those that allow study of the absence of GM, the presence of simplified GM, or the presence of complex GM. Gnotobiotic (germ free mice) are mice that are generated and raised in microbial free environments. As such, these animals are not colonized by bacteria and allow a simplified approach to the study of host development, establishment and maintenance of the immune system, and GIT epithelial function in the absence of the GM. When these mice are monocolonized by gastric gavage with a single gut bacterial species, research into the effect of this bacterium on host physiology can be performed. However, with both germ free and monocolonized mice, experimental results must be carefully interpreted as these mice have physiologic and immunologic differences when compared with conventionally raised mice colonized with complex GM communities (61). To overcome these limitations, germ free mice can be colonized with a previously defined, simplified GM community known as altered Schaedler's flora (62). These mice are colonized with 8 pre-defined bacterial species, specifically *Lactobacillus* spp., *Lactobacillus murinus*, *Mucispirillum schaedleri*, *Eubacterium plexicaudatum*, *Firmicutes* bacterium, *Clostridium* spp. (ASF356), *Clostridium* spp. (ASF502),

Parabacteroides spp. (62). Although harboring a restricted GM, these mice have a normal pattern of physiologic and immunologic development than either germ free or monocolonized mice. However, as these mice are colonized with an overly simplified GM they do not adequately reflect the complex microbial interactions that may occur in humans thereby limiting translatability. To overcome the research limitations noted above, the use of humanized mice has been proposed. Humanized mice are germ free mice that are colonized by gastric gavage with human fecal sample(s) (63). These mice allow insight into the effect of human GM on the host. However, it should be noted that humanized mice do not harbor all GM bacterial species present in human samples (63, 64).

A caveat to all of the methods described above is the use of germ free mice in the generation of these models. As stated previously, germ free mice undergo development in the absence of GM and as such, have several physiologic abnormalities including deficits in immune development, intestinal associated metabolism, and epithelial gene expression (65-67). Because of these abnormalities, studies focused on these parameters can be hampered. Therefore, alternative strategies to generate mice that develop and mature in the presence of complex GM must be thoroughly explored. To help address this we proposed a new method we termed Complex Microbiota Targeted Rederivation (CMTR). We utilized surgical embryo transfer to generate outbred Crl:CD1 mouse colonies with vendor specific GM that varies in complexity and composition (Chapter 3). These colonies can be used for CMTR to generate isogenic mice harboring GM that varies in complexity and composition or, alternatively, could be used to generate

genetically disparate colonies of mice seeded with the same GM. As such, CMTR can be used as a method in further investigate the impact of complex GM on host physiology.

Inflammatory Bowel Disease (IBD)

Inflammatory bowel disease (IBD) is the term for a group of idiopathic, chronic, inflammatory conditions effecting the small and large segments of the GIT. There are two known primary forms of the disease, ulcerative colitis and Crohn's disease, which can be differentiated by the longitudinal pattern and location of inflammation along the GIT (68). Both clinical forms of the disease can be diagnosed at any age, ranging from young children to the elderly (69). However, the majority of cases are diagnosed in adolescence and early adulthood (69). The number of reported cases of IBD has been steadily increasing worldwide with the bulk of patients diagnosed in western industrialized countries. IBD is associated with substantial morbidity with long-term costs to patient, health care, and society highlighting the important health significance of this disease (70, 71)

The exact etiologic pathogenesis of IBD remains unknown but is suggested to involve a complex interaction between host genetic factors, environmental factors or microbial factors, and aberrant immune responses. Recent genome-wide association studies (GWAS) of the human genome have identified several genetic polymorphisms in innate-immune signaling genes suggesting abnormal interaction with host commensal or pathogenic bacteria (72, 73). Further implicating the GM in disease pathogenesis are animal studies demonstrating that the GM is necessary for the development of disease in germ free mice (74-76). In addition, transfer of GM from mice with colitis to healthy mice, induces disease in GM transfer recipients (77). Interestingly, mucosal T

lymphocytes in cases of IBD have been shown to be stimulated by commensal bacteria, suggesting that the GM may be a trigger for chronic GIT inflammation (78). Moreover, several clinical studies in patients have demonstrated that GM bacterial communities are disrupted (dysbiosis) (79, 80) and that antibiotic use can alter the clinical course of disease in a subset of these patients (81).

IBD patients have demonstrated decreases in GM diversity with an overall unstable bacterial composition as compared to healthy volunteers (80). Alterations in GM diversity have been suggested to be the result of a break down in healthy host-microbe mutualism with a significant shift from bacterial symbiont (beneficiary) to pathobiont (disease causing) populations (82). These studies indicate that a decrease in the relative abundance of phyla *Bacteroidetes* and *Firmicutes* with significant increases in *Actinobacteria* and *Proteobacteria* are associated with IBD clinical presentation (79, 83-85). Most notably, there is considerable decrease in *Clostridium* IV bacterial species within phylum *Firmicutes*. Specifically, these decreases are observed within genera associated with GIT mucosal protection such as *Lactobacillus, Bifidobacterium,* and *Faecalibacterium*. In contrast, family *Enterobacteriaceae* within phylum *Proteobacteria* is greatly increased. Interestingly, there is discrepancy among IBD studies regarding changes within phyla *Bacteroidetes*. Some studies suggest a decrease in relative abundance of *Bacteroidetes* in clinical cases of IBD while other studies paradoxically report an increase in this taxa (79, 80). These differences have been suggested to be due to differential spatial colonization of *Bacteroides* spp. comprising large mucosal biofilms in IBD patients vs. healthy controls (85, 86). It should be noted that IBD is a segmental disease preferentially occurring in the distal ileum and colon, with a waxing and waning

disease severity presentation which may also contribute to discrepancies in GM composition among patients (9, 85, 87). GM samples are predominantly of GIT biopsy or fecal origin, and are obtained as part of retrospective studies in patients with either active or remittent disease presentation. Therefore, GM sequencing results should be interpreted in the context of GIT anatomic location, sample source, and disease status.

IL-10$^{-/-}$ Mouse Model

Despite considerable progress in the study of IBD it still remains to be shown whether alterations in GM diversity and composition are a cause or consequence of disease. To date no single agent has been identified that fulfills Koch's postulates. Numerous studies in IBD patients have been performed suggesting increased prevalence of specific bacteria or groups of bacteria (85), however these studies remain largely correlative. One such group of bacteria is Enterohepatic *Helicobacter* spp. including *H. hepaticus*, *H. bilis*, *H. cinaedi*, *H. pullorum*, *H. muridarum* and *H. trongontum* (88-90). *Helicobacter* spp. are a group of gram negative, microaerophilic, helical-shaped bacteria that belong to the order *Campylobacterales* shown to persistently colonize the intestinal tracts and/or liver of both humans and mice (88). In addition, several *Helicobacter* spp. have been associated with chronic intestinal disease (88, 89). However, to date no causal association has been established.

A significant problem in the association of IBD to bacterial factors is that patient studies are largely retrospective and performed after disease onset and diagnosis. Longitudinal studies in animal models can be a method to overcome these challenges. There are approximately 66 different kinds of animal models used for IBD studies (91). These models are classified into several categories depending on method of disease

induction and include chemical, cell-transfer, congenital mutant, and genetically engineered models. One of the earliest and most widely used rodent models is the IL-10$^{-/-}$ mouse (92) and will be the focus of this dissertation.

IL-10 is a well-known regulatory anti-inflammatory cytokine with genetic polymorphisms in the IL-10 locus increasing the risk of both ulcerative colitis and Crohn's disease (93, 94). Mice with a targeted deletion of the *IL-10* gene develop IBD that is characterized by segmental, transmural inflammation that is typically most severe in the cecum and proximal colon. Early studies suggested that mice with altered immune function, such as IL-10$^{-/-}$ mice, develop a spontaneous chronic GIT disease similar to human IBD (92, 95, 96). However subsequent studies of these mice found that they were endemically colonized with *Helicobacter* spp. and are resistant to disease when kept free of infection by *Helicobacter* spp. (97). Additional research showed that *Helicobacter* spp. such as *Helicobacter hepaticus* do not induce disease in monocolonized mice alone, suggesting that other bacterial factors, presumably normal commensal bacteria, play a role in disease pathogenesis (75, 76).

The exact mechanism of how *H. hepaticus* induces disease in the IL-10$^{-/-}$ mouse model remains unclear. However, it is thought that *H. hepaticus* acts as a pro-inflammatory provocateur inducing an inappropriate T cell driven immune response toward the commensal GM resulting in chronic intestinal inflammation and dysbiosis (98, 99). As such, *H. hepaticus* is commonly used as a method to induce the onset of intestinal disease in the IL-10$^{-/-}$ model.

Anecdotally, there have been reports suggesting that the IL-10$^{-/-}$ mouse model may inadvertently be altered by external factors such as rederivation by embryo transfer,

changes in institution, or source of animals which result in an attenuation or loss of disease phenotype. These observations suggest that the influence of environmental factors such as the GM on rodent models is an important experimental variable that warrants further investigation. To evaluate the effect of the GM on disease phenotype we used CMTR to rederive, by surgical embryo transfer, B6.129P2-*Il10*^{tm1Cgn}/J (B6 IL-10$^{-/-}$) and C3Bir.129P2(B6)-Il10^{tm1Cgn}/J (C3H IL-10$^{-/-}$) mice into Crl:CD1 surrogate dams with vendor specific microbiota that varied in complexity and composition (Chapter 4). Our findings suggest that variations in GM play a role in *H. hepaticus* infection and disease phenotype.

CHAPTER 2:

Comparative Evaluation of DNA Extraction Methods From Feces of Multiple Host Species For Downstream Next-Generation Sequencing

Overview

The gastrointestinal tract (GIT) contains a vast community of microbes that greatly outnumber host cells (100) and play an important role in gastrointestinal (GI) physiology (45, 101), immunity of the host (61, 102), and susceptibility to both local and systemic disease (103-105). However, to date only a small percentage of these microbes can be cultured from GI biopsy tissue or fecal samples (106). The development of culture-independent methods such as next generation sequencing (NGS) has made genomic characterization of these microbial communities increasingly feasible and affordable.

Several procedures for extraction of DNA from fecal samples have been described. Most of these studies focus on DNA extraction from human samples, with only a few of these methods reported for use on other species (107-109). Furthermore, several studies have demonstrated that the method of DNA extraction can have an adverse impact on sequencing output and may over- or under-represent specific microbial populations in samples from different habitats (58, 107, 110-113). Moreover, feces contain various PCR inhibitors, some of which may significantly inhibit the PCR reaction used to generate 16S rRNA amplicons prior to sequencing. The nature of these inhibitory substances in fecal samples is variable and kit-based DNA extraction methods may or may not obviate their presence. Considering the increased application of NGS to samples obtained from host species other than human and mouse, there is the need for a

comparative assessment of extraction methods applied to fecal samples collected from multiple species, with 16S rRNA amplicon sequencing as the downstream application.

In this study, fresh fecal samples were collected from eight individuals within five species groups (zebrafish, mouse, cat, dog, and horse) and DNA was extracted using five different DNA extraction methods (Qiagen DNeasy kit, MoBio PowerFecal kit, Qiagen QIAamp Cador Pathogen mini kit, Qiagen QIAamp DNA Stool mini kit, and an isopropanol manual extraction method). The present study evaluates DNA extraction performance of these methods with a focus on DNA yield, purity, NGS output, and cost. Our results demonstrate that certain extraction methods, when performed according to the manufacturer's instructions, perform preferably in samples from specific host species. Additionally, spectrophotometric assessment of DNA elutions prior to PCR had poor predictive value with regard to successful amplification and sequencing. Lastly, comparison of sequencing results from the same sample subjected to different extraction methods show that, while the detection of a limited number of rare taxa may vary, overall community profiles agreed fairly well in the majority of samples. These findings will enable investigators to choose the optimal DNA extraction method to suit current study needs.

Materials and Methods

All studies were performed in accordance with the recommendations put forth in the Guide for the Care and Use of Laboratory Animals and were approved by the University of Missouri Institutional Animal Care and Use Committee. For public owned animals (dog and cat) prior consent of the owner was obtained before fecal samples were obtained.

Sample Collection

Zebrafish samples: Zebrafish (*Danio rerio*) were subjected to euthanasia with 0.1% clove oil in aquarium water, and the entire GI tract was removed and placed in a sterile 2 mL cryovial. The tissue and fecal contents were promptly frozen and stored in a -80°C freezer for two weeks prior to DNA extraction. Mouse (*Mus musculus*) samples: five freshly evacuated fecal pellets per mouse were placed in a 1.5 mL sterile Eppendorf tube. Samples were promptly frozen and stored in a -80°C freezer for two weeks. Prior to each extraction method, one fecal pellet per mouse was removed from the freezer and extraction was performed as described below. Cat (*Felis domesticus*), dog (*Canis familiaris*), and horse (*Equus caballus*) samples: freshly evacuated fecal samples were collected from privately owned cats and dogs. Freshly evacuated equine fecal samples were obtained from horses present in the University of Missouri Veterinary Medical Teaching Hospital for reasons unrelated to gastrointestinal conditions. Upon collection, samples were placed in 50 mL conical tubes and stored in a -80°C freezer for two weeks prior to DNA extraction. A small piece of fecal material was promptly removed from the frozen sample immediately prior to performance of each extraction method; the remaining sample was returned to the freezer.

DNA Extraction

All DNA was extracted and quantified at the University of Missouri Metagenomics Center (MUMC).

Qiagen DNeasy kit

DNA extraction was performed following the manufacturer's recommendations with slight modifications to allow for mechanical disruption. Briefly, for cat, dog, and

horse samples, 25 mg of feces was placed into a sterile 2 mL round-bottom tube containing 500 µL sterile PBS and a 0.5 cm diameter stainless steel bead. Samples were mechanically disrupted using a TissueLyser II (Qiagen, Venlo, Netherlands) for 3 minutes at 30 Hz, followed by centrifugation at 200 × g for 5 min. A 200 µL volume of supernatant was removed and placed in a sterile 1.5 mL Eppendorf tube. An equal volume of buffer AL was added and the samples were processed thereafter following the manufacturer's protocol. For mouse samples, one fecal pellet was placed into a 2 mL sterile round bottom tube containing 500 µL sterile PBS and a 0.5 cm diameter stainless steel bead and processed as described above. For fish samples, the entire GI tract was placed into an autoclaved 2 mL round-bottom tube containing 500 µL sterile PBS and a 0.5 cm diameter stainless steel bead and processed as described above. All samples were eluted in 200 µL AE buffer.

MoBio PowerFecal kit

DNA extraction was performed following the manufacturer's recommendations with small adaptions due to equipment availability. Briefly, for cat, dog, and horse samples, 0.25 mg of fecal sample was added to the dry bead tube containing 750 µL of bead solution and gently vortexed. C1 solution was added, the sample briefly vortexed, and incubated at 65ºC for 10 minutes following the recommended protocol. Samples were shaken for 10 min. in a TissueLyser II (Qiagen, Venlo, Netherlands) at 30Hz. Samples were centrifuged at 13,000 × g for 1 min., the supernatant transferred to the provided 2 mL collection tube, and the remainder of the protocol was followed as recommended by the manufacturer. For mouse samples, one fecal pellet was added to the dry bead tube containing 750 µL of bead solution and processed as described above. For

fish samples, the entire GI tract was placed in the dry bead tube containing 750 µL of bead solution and processed as described above. All samples were eluted in 100 µL solution C6.

Qiagen QIAamp Cador Pathogen Mini kit

DNA extraction was performed following the manufacturer's recommendations with small adaptions due to equipment availability. Briefly, for cat, dog, and horse samples 25 mg of feces was placed into a 2 mL sterile round-bottom tube containing 500 µL of sterile PBS and a 0.5 cm diameter stainless steel bead. Samples were mechanically disrupted using a TissueLyser II (Qiagen, Venlo, Netherlands) for 2 minutes at 25 Hz, followed by centrifugation at 14,000 × g for 2 minutes. A 400 µL volume of supernatant was removed and placed in a sterile 2 mL screw cap tube containing 2 mg of sterile glass beads and 100 µL of lysis buffer ATL. Samples were processed on a TissueLyser II (Qiagen, Venlo, Netherlands) for 10 min. at 50 Hz and the remainder of the protocol was followed as recommended by the manufacturer. For mouse samples, one fecal pellet was placed into a 2 mL sterile round-bottom tube containing 500 µL of sterile PBS and a 0.5 cm diameter stainless steel bead and the sample was processed as described above. For fish samples, the entire GI tract was placed in a 2 mL sterile round-bottom tube containing 500 µL of sterile PBS and a 0.5 cm diameter stainless steel bead and the sample was processed as described above. All samples were eluted in 150 µL AE buffer.

Qiagen QIAamp DNA Stool Mini Kit

DNA extraction was performed following the manufacturer's recommendations. Briefly, for cat, dog, and horse samples, 200 mg of feces was placed in a sterile, round-bottom 2 mL tube containing 1.4 mL ASL lysis buffer and the remainder of the protocol

was followed as described by the manufacturer. For mouse samples, one fecal pellet was placed into a sterile, round-bottom 2 mL tube containing 1.4 mL lysis buffer and the sample was processed as described above. For fish samples, the entire GI tract was placed in a sterile, round bottom 2 mL tube containing 1.4 mL lysis buffer and the sample was processed as described above. All samples were eluted in 200 µL AE buffer.

Isopropanol DNA extraction

DNA extraction was performed as previously described (114). Briefly, for cat, dog, and horse samples, 25 mg of feces was placed into a sterile 2 mL round-bottom tube containing 800 µL lysis buffer and a 0.5 cm diameter stainless steel bead. Samples were mechanically disrupted using a TissueLyser II (Qiagen, Venlo, Netherlands) for 3 minutes at 30 Hz, followed by incubation at 70ºC for 20 minutes with periodic vortexing. Samples were centrifuged at 5000 × g for 5 min., and the supernatant was then transferred to a sterile 1.5 mL Eppendorf tube containing 200 µL of 10 mM ammonium acetate. Lysates were vortexed, incubated on ice for 5 min., and then centrifuged. Supernatant was transferred to a sterile 1.5 mL Eppendorf tube and one volume of chilled isopropanol was added. Samples were incubated on ice for 30 min. and then centrifuged at 16,000 × g, at 4º C, for 15 min. The resulting DNA pellet was washed with 70% ethanol and resuspended in 150 µL Tris-EDTA (10 mM Tris and 1 mM EDTA), followed by addition of 15 µL of proteinase K and 200 µL of AL Buffer. Samples were incubated at 70ºC for 10 min. and 200 µL of 100% ethanol was added to the tubes. Samples were mixed by gentle pipetting and the contents transferred to a spin column from the DNeasy kit. The DNA was purified following the manufacturer's instructions and eluted in 200 µL EB buffer. For mouse samples, one fecal pellet was placed into a sterile 2 mL, round-

bottom tube containing lysis buffer and a 0.5 cm diameter stainless steel bead and the sample was processed as described above. For fish samples, the entire GI tract was placed into a sterile 2 mL round-bottom tube containing lysis buffer and a 0.5 cm diameter stainless steel bead and the sample was processed as described above. All samples were eluted in 200 µl EB buffer.

Quantification and assessment of purity

For all extraction methods, DNA concentrations were determined fluorometrically (Qubit dsDNA BR assay, Life Technologies, Carlsbad CA) and purity was assessed via 260/280 and 260/230 absorbance ratios, as determined via spectrophotometry (Nanodrop 1000 Spectrophotometer, Thermo Fisher Scientific, Waltham, MA). Samples were stored at -20ºC until sequencing.

Library construction and 16S rRNA sequencing

Library construction and sequencing was performed at the University of Missouri DNA Core facility. DNA concentration of samples was determined fluorometrically and all samples were normalized to 3.51 ng/µL for PCR amplification. Bacterial 16S rRNA amplicons were generated using amplification of the V4 hypervariable region of the 16S rRNA gene using universal primers (U515F/806R) flanked by Illumina standard adapter sequences and amplified and pooled for sequencing using the Illumina MiSeq platform as previously described (114). Samples returning greater than 10,000 reads were deemed to have successful amplification.

Informatics analysis

Assembly, binning, and annotation of DNA sequences was performed at the MU Informatics Research Core Facility. Briefly, contiguous DNA sequences were assembled

using FLASH software (115), and culled if found to be short after trimming for a base quality less than 31. Qiime v1.8 (116) software was used to perform *de novo* and reference-based chimera detection and removal, and remaining contiguous sequences were assigned to operational taxonomic units (OTUs) using a criterion of 97% nucleotide identity. Taxonomy was assigned to selected OTUs using BLAST (117) against the Greengenes database (118) of 16S rRNA sequences and taxonomy. Principal component analyses were performed using ¼ root-transformed OTU relative abundance data via a non-linear iterative partial least squares (NIPALS) algorithm, using an open access Excel macro available from the Riken Institute (http://prime.psc.riken.jp/Metabolomics_Software/StatisticalAnalysisOnMicrosoftExcel/index.html).

Statistical analysis

Statistical analysis was performed using Sigma Plot 12.3 (Systat Software Inc., Carlsbad, CA). Differences between DNA extraction methods in total DNA concentration were determined using ANOVA with Student Newman-Keuls post hoc test. Differences in phylum relative abundance following successful NGS amplification, i.e., achieving 10,000 sequences, were determined using either ANOVA with Student Newman-Keuls post hoc test or a t-test with Mann-Whitney post hoc test. Receiver operating characteristic (ROC) curves were generated from 260/280 and 260/230 absorbance ratios obtained from samples of each host species using success of amplification as the binary classifier. Statistical differences in microbial diversity determined using ANOVA with Student Newman-Keuls post hoc test. Results were considered statistically significant for p values ≤ 0.05.

Results

DNA extraction method impacts DNA yield.

In addition to traditional "bench-top" techniques for DNA extraction, there are many commercially available kit-based methods. To assess the suitability of several of these methods for extraction of fecal DNA from multiple host species with the intended downstream use of next-generation sequencing, samples were collected from eight individual mice, cats, dogs, horses, or forty zebrafish, and processed according to the manufacturer's protocol or published methods. For cat, dog, and horse samples, the same fecal bolus was used for all extraction methods. For mice, five fecal samples were collected at the same time and one pellet was used for each method. For zebrafish, forty age-matched fish from the same tank were used, eight per extraction method. Regarding overall DNA yield from a standard mass of starting material, the amount of DNA extracted was dependent on the DNA extraction technique and the host species from which the fecal sample was collected. For all species examined, except the dog, the isopropanol extraction method produced the greatest total DNA yields, and in horse samples, the isopropanol method resulted in significantly higher yields when compared to all other extraction methods (Figure 2.1 A-E). In the dog, no statistically significant difference between extraction methods was identified (Figure 2.1 D). For zebrafish and mouse samples, the isopropanol extraction method resulted in significantly greater yields of total DNA relative to several other methods, with the Cador Pathogen kit also performing well (Figure 2.11A-B). For cat samples, elutions from the isopropanol extraction method were significantly higher than both the Cador Pathogen and DNeasy kit, with comparable yields from the PowerFecal and QIAamp Stool kits (Figure 2.1C).

While a greater DNA yield may suggest, among other things, more efficient bacterial lysis, DNA is normalized to a standard volume and concentration for 16S rRNA amplification. With that in mind, most methods examined in this study provided a sufficient quantity of DNA for normalization and attempted sequencing with the exceptions of DNeasy and PowerFecal extractions from equine samples, DNeasy and Cador Pathogen extractions from feline samples, and QIAamp stool extractions from zebrafish samples.

DNA extraction method influences successful amplification and next generation sequencing (NGS).

A more practical measure of performance is the quality of the DNA elutions generated from each method. The presence of myriad undesirable substances in feces is often blamed for samples that result in low coverage (i.e., sequences per sample) due to PCR inhibition. To assess the quality of the DNA extracted via the methods under evaluation, samples were sequenced on the Illumina MiSeq platform in a 96-well multiplex format. Based on rarefaction analysis of previously published sequencing data (114), we defined successful amplification as a minimal coverage of 10,000 reads per sample. Notably, the method of DNA extraction had a strong impact on the number of samples that successfully amplified, but performance varied between host species. For example, with zebrafish samples, the isopropanol extraction method was most efficient at overcoming PCR inhibition; 8/8 isopropanol-extracted zebrafish samples amplified successfully, compared to between 0/8 and 4/8 samples using DNA extracted via the other methods tested (Table 2.1). Similarly, the PowerFecal kit appeared to be optimal for extraction of DNA from equine feces (7/8 samples amplified); 5/8 samples extracted with

the QIAamp Stool kit amplified successfully. For mouse samples, the PowerFecal-, QIAamp stool-, and isopropanol-extracted samples all performed well with all 8/8 samples amplifying above 10,000 reads. For cat and dog samples, the PowerFecal kit was most able to overcome PCR inhibition, resulting in successful amplification in 7/8 and 8/8 samples, respectively. Isopropanol-extracted dog samples performed well in 7/8 samples. Overall, the PowerFecal kit and the traditional isopropanol extraction method provided the most consistently successful PCR amplification prior to sequencing bacterial DNA from diverse host species, when samples were handled according to the manufacturer's recommendations. While murine feces seemed the least problematic with regard to PCR inhibition, zebrafish, cat, and horse fecal samples each required a specific extraction method for optimal results.

DNA purity does not predict successful amplification and sequencing.

NGS quality control practices require preparation of DNA containing little to no protein, RNA, or polysaccharides, and purity is often assessed via 260/280 and 260/230 absorbance ratios, determined by spectrophotometry. To compare the predictive power for successful amplification of each absorbance ratio, and also to establish cut-off values for one or both of the ratios, receiver-operating characteristic (ROC) curves were generated for each species, with successful amplification as the binary classifier. ROC curves are frequently used in the development of diagnostic assays to compare positive and negative predictive values of test results, and to determine a threshold value with acceptable sensitivity and specificity based on test results of a group of "known" samples. The area under the curve (AUC) can be used as a measure of overall diagnostic (or in this case, predictive) accuracy; an AUC of 1 denotes 100% sensitivity and specificity while

an AUC of 0.5 suggests completely random performance. Unexpectedly, neither high 260/280 or 260/230 absorbance ratios accurately predicted the success of NGS amplification (Figure 2.2 and Table 2.1). For example, DNA from fish samples produced excellent absorbance ratios suggesting relatively pure DNA, but four of five extraction methods either failed to have any successful amplification or had few samples amplify. Conversely, in cat, dog, and horse samples, several DNA extraction methods resulted in extremely low 260/230 absorbance ratios yet produced samples that amplified and sequenced well.

Effect of DNA extraction method on microbial diversity is dependent on host species.

In human studies, it has been shown that variation in DNA extraction can influence the bacterial communities detected during sequencing (Kennedy et al. 2014; Wesolowska-Anderson et al. 2014; Wu et al. 2010). To determine whether the extraction chemistries tested resulted in differential lysis and subsequent skewing of the microbial profile, results of 16S rRNA amplicon sequencing were compared. Annotated to the taxonomic level of phylum, those samples that reached the threshold of 10,000 sequences generally showed good agreement with some exceptions. For example, sequencing of zebrafish samples extracted using the PowerFecal kit or manual isopropanol method detected a higher relative abundance of microbial families within the phylum *Fusobacteria* (Figures 2.3 and 2.4) when compared to samples processed with the DNeasy kit. Specifically, three of the four zebrafish samples processed with the DNeasy kit were dominated by greater than 80% *Proteobacteria*, while the predicted relative abundance of that phylum was less than 40% in the isopropanol extracted samples. The

fact that zebrafish samples represented 40 individual fish, as opposed to 8 samples divided into 5 subsamples precluded statistical comparisons. Sequencing of samples from the other species demonstrated relatively lesser differences at the phylum level, although certain samples yielded disparate results. However, when annotated to the level of family, the microbial profile detected in cat and dog samples demonstrated clear differences between extraction methods in samples that amplified (Figure 2.4). In the mouse and horse, all DNA extraction methods resulted in subjectively similar relative abundance detected at the family levels. Based on the likelihood of success of amplification, the PowerFecal kit appears optimal for extraction of cat and horse samples, while the manual isopropanol extraction method performed best for zebrafish samples. With dog and mouse samples however, there were two or three methods, respectively, that successfully overcame PCR inhibition in seven or more of the eight samples tested, allowing for statistical comparisons of the output. Accordingly, a t-test performed on the relative abundance of all phyla detected in the seven dog samples extracted with the PowerFecal kit or isopropanol method revealed no significant differences. Similarly, an ANOVA was performed to test for differences in the relative abundance of all phyla detected in the eight mouse samples extracted with the PowerFecal kit, QIAamp kit, or isopropanol method. A significant difference ($p = 0.035$) was detected in the relative abundance of the rare phylum Cyanobacteria, with QIAamp-processed samples showing greater abundance when compared to isopropanol-extracted samples. No differences were detected in the relative abundance of any other phylum in the mouse samples extracted with those three methods.

To further evaluate the effect of DNA extraction method on NGS output, principle component analysis (PCA) was performed including only data from methods that resulted in successful amplification in half or more samples for each host species (Figure 2.5). Data from methods that resulted in successful amplification in less than half of the samples were omitted from PCA to avoid skewing of comparisons between the other methods. In PCA, samples that are similar in composition cluster together, based on the presence or absence and relative abundance of all operational taxonomic units (OTUs), i.e., taxa annotated to the finest resolution possible with the primer set being used. As expected based on the bar charts (Figure 2.4), the variation among zebrafish samples extracted using the isopropanol method was much lower than samples isolated using the DNeasy kit (Figure 2.5A). In the mouse and horse, individual animal samples tended to cluster together regardless of which DNA extraction method was used (Figure 2.5B, E). In the dog and cat, individual animal samples clustered along the PC1 axis. However, dependent on which DNA extraction method was used, several samples separated along PC2. As a means of comparing the ability of tested extraction methods to lyse rare or hard-to-lyse taxa, α-diversity of samples that amplified was determined using the Chao1 Index (Figure 2.6). Despite the paucity of significant differences detected between methods, a few trends were noted. In mouse samples, microbial diversity was highly concordant across all extraction methods capable of overcoming PCR inhibition. In the dog samples, there was considerable variability in the Chao1 indices of samples generated via most extraction methods, perhaps reflecting an increased exposure to environmental microbes, or differences between portions of the same fecal sample. Interestingly, equine samples had statistically greater microbial diversity in

samples extracted using the PowerFecal kit, relative to those QIAamp Stool-extracted samples that amplified successfully. Collectively, these data illustrate that successful amplification and sequencing, as well as the microbial profile detected via NGS, can be influenced by DNA extraction method and, depending on host species and the output of interest, these changes may be dramatic or subtle.

Discussion

With the decrease in costs associated with NGS, characterization of GI microbial communities is becoming increasingly feasible. However, to date, the majority of studies have focused on human fecal samples with far less optimization of techniques for use with samples from other species. In the current study, the performance of five DNA extraction methods was evaluated using samples collected from five diverse host species. Taken as a whole, the data suggest that samples from a particular host species may be amenable to DNA extraction using only certain methods.

This phenomenon was first noticed when comparing the concentration of DNA in elutions from each method. While the manual isopropanol precipitation yielded consistently high levels of DNA, the PowerFecal kit resulted in comparable yields from zebrafish and mouse samples, and the DNeasy kit produced comparable yields in feline and canine samples. One possible explanation for the greater yields generated via isopropanol extraction is the fact that the other kit-based methods rely solely on retention of DNA in a column-based matrix. In the isopropanol method, DNA is precipitated via addition of a chaotropic salt and isopropanol on ice, followed by subsequent elution over a column. That said, other differences in the extraction chemistry may also influence efficiency of lysis and removal of PCR inhibitors.

We also noted considerable variability in the amount of DNA extracted within several samples, dependent on extraction method used, as evidenced by the large standard deviation among sample groups. This variation could be due to the efficiency of the DNA extraction methods tested. However, this could also be due to variability in the diet that these animals consume or the amount of true microbial biomass loaded with each sample as cat and dog samples were found to contain a large amount of particulate matter such as hair and bone fragments. Similarly, horse fecal samples contained substantial amounts of large particulate fiber matter. Although care was taken during measurement of starting sample mass, these particulates could have an effect on the amount of fecal biomass that was available for DNA extraction.

More importantly, the method of DNA extraction was found to strongly influence the number of samples that successfully amplified, but in a species-dependent fashion. For example, the isopropanol method was uniquely well-suited for use with zebrafish samples, resulting in successful amplification in 8/8 samples, while successful amplification and sequencing of equine samples necessitated use of the PowerFecal kits. Taken together, these data suggest that the substances present in the feces responsible for PCR inhibition likely differ between host species. Furthermore, all zebrafish samples had high A260/A280 and A260/A230 absorbance ratios, suggesting relatively "clean" elutions, but three out of the five extraction methods tested completely failed NGS amplification. This may be an artifact of processing as the entire zebrafish GI tract was processed along with fecal contents. Extracted samples likely contained a large amount of host DNA which may have resulted in dilution of bacterial DNA when performing PCR with a standard DNA concentration. However, yields from isopropanol-extracted samples

were noted to be the highest and performed well. Conversely, in the cat, dog and horse samples, both high and low A260/A280 and A260/A230 absorbance values were detected, possibly indicating contamination from guanidine residue during DNA extraction or dietary carbohydrate carryover. These samples were thus expected to have variable to unsuccessful amplification, however several such samples successfully amplified. Taken together, these results indicate that DNA purity, as determined via 260/280 or 260/230 absorbance ratio, cannot reliably predict successful amplification.

Several studies have shown that variation in DNA extraction can impact NGS-based characterizations of bacterial communities. In the present study, only small differences in NGS output were observed for most samples at the phylum level, with the aforementioned exception of zebrafish samples. In zebrafish however, use of the PowerFecal kit or the isopropanol method resulted in detection of a higher relative abundance of the phylum *Fusobacteria*, while samples extracted via the DNeasy kit showed predominantly *Proteobacteria*. When overall microbial profiles were compared at the level of OTU via PCA, we noted substantial variation among the samples extracted with the DNeasy kits. Due to the scant amount of digesta present in zebrafish, DNA was extracted from individual fish as compared to serial or identical fecal samples from other species evaluated in this study. Even though all fish used for this study were specific pathogen free and housed in the same aquarium, differences in OTU variation could be due to true differences between individual fish. That said, it is worth noting that the community profiles generated using the isopropanol extraction method are not in agreement with other published reports of zebrafish microbiota (119). While Roeselers *et al*. and other groups have identified *Proteobacteria* as the predominant phylum in the gut

of zebrafish, *Fusobacteria* was the primary phylum detected in the current study. Whether this is a function of extraction method or due to a difference in the populations tested is unclear.

Collectively, these data highlight the need to match appropriate fecal DNA extraction methods to the host species in question. As the feasibility of NGS increases and with rising pressure from funding agencies to enhance experimental reproducibility (120), it is paramount that standardized methods of sample processing be performed. This study illustrates the importance of careful consideration of DNA extraction method when designing experiments and interpreting data from studies performed in multiple species.

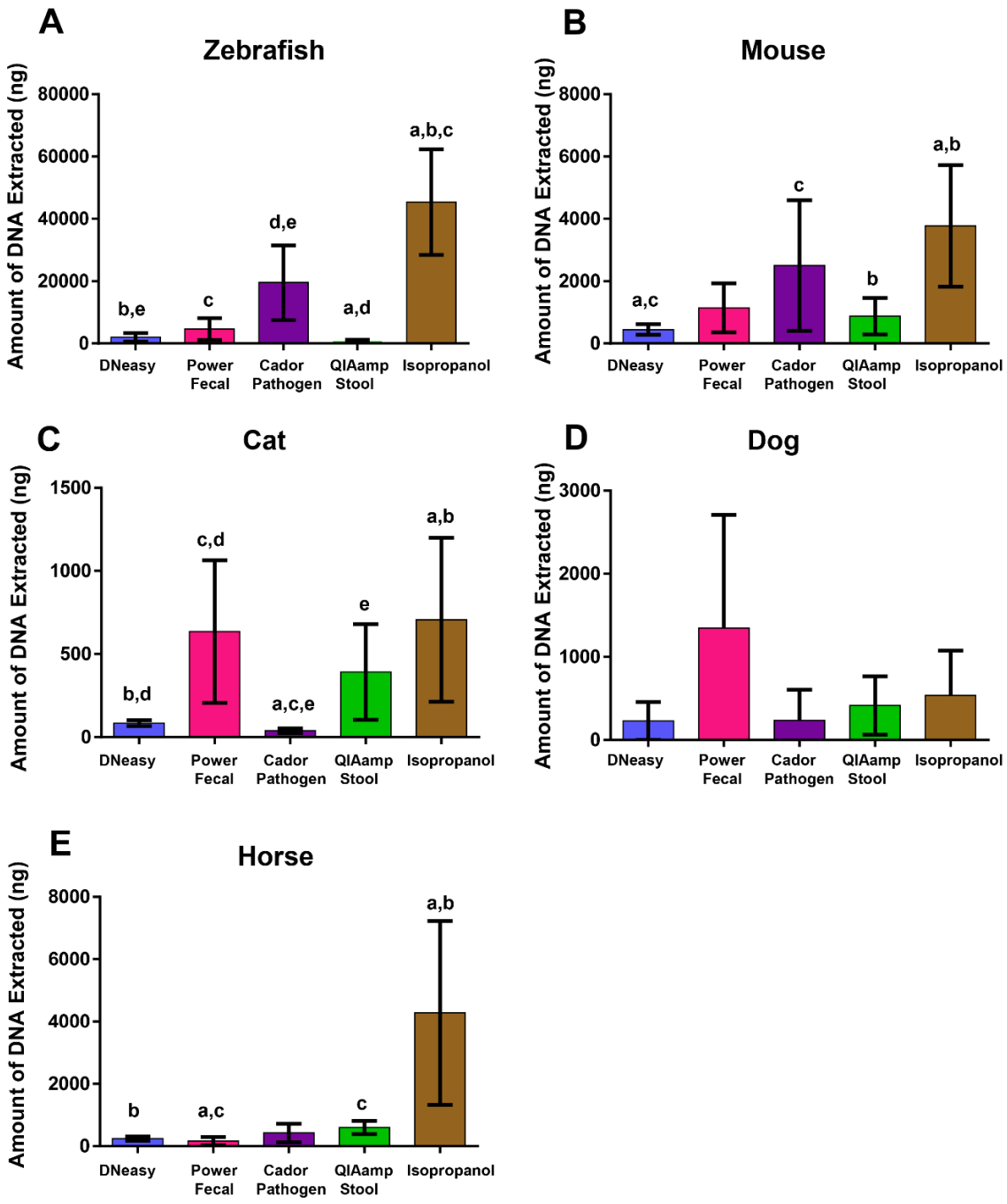

Figure 2.1. Fecal DNA extraction efficiency varies dependent on extraction method and host species. Mean total amount (± standard deviation) of DNA extracted from zebrafish gastrointestinal tract (A) or a standardized mass of feces from mice (B), cats (C), dogs (D), or horses (E), using four commercially available DNA extraction kits and one manual extraction procedure (isopropanol). n = 40 individual zebra fish, and 8 individuals for mouse, cat, dog, and horse with 8 samples used for all extraction methods. Samples were extracted and total DNA was measured by fluorometry. Statistical significance determined using one-way ANOVA with Student Newman-Keuls post hoc test. Significance defined by $p \leq 0.05$ and denoted by lower case letters.

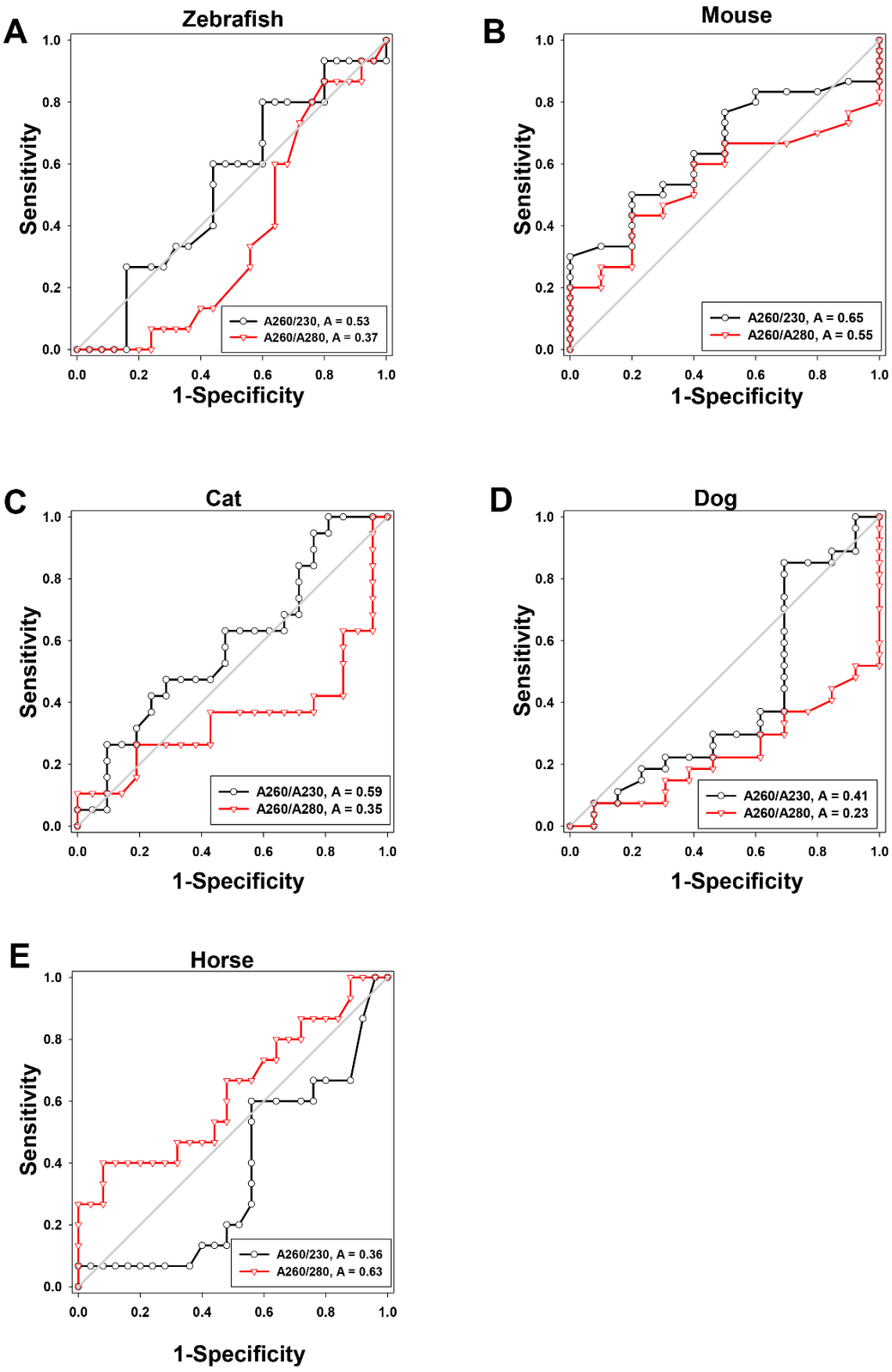

Figure 2.2. Receiver operator curves of 260/280 and 260/230 nm absorbance for all DNA extraction methods for each animal species. Absorbance values of all DNA samples from each species (n = 40) were plotted in an ROC generated by Sigma-Plot.

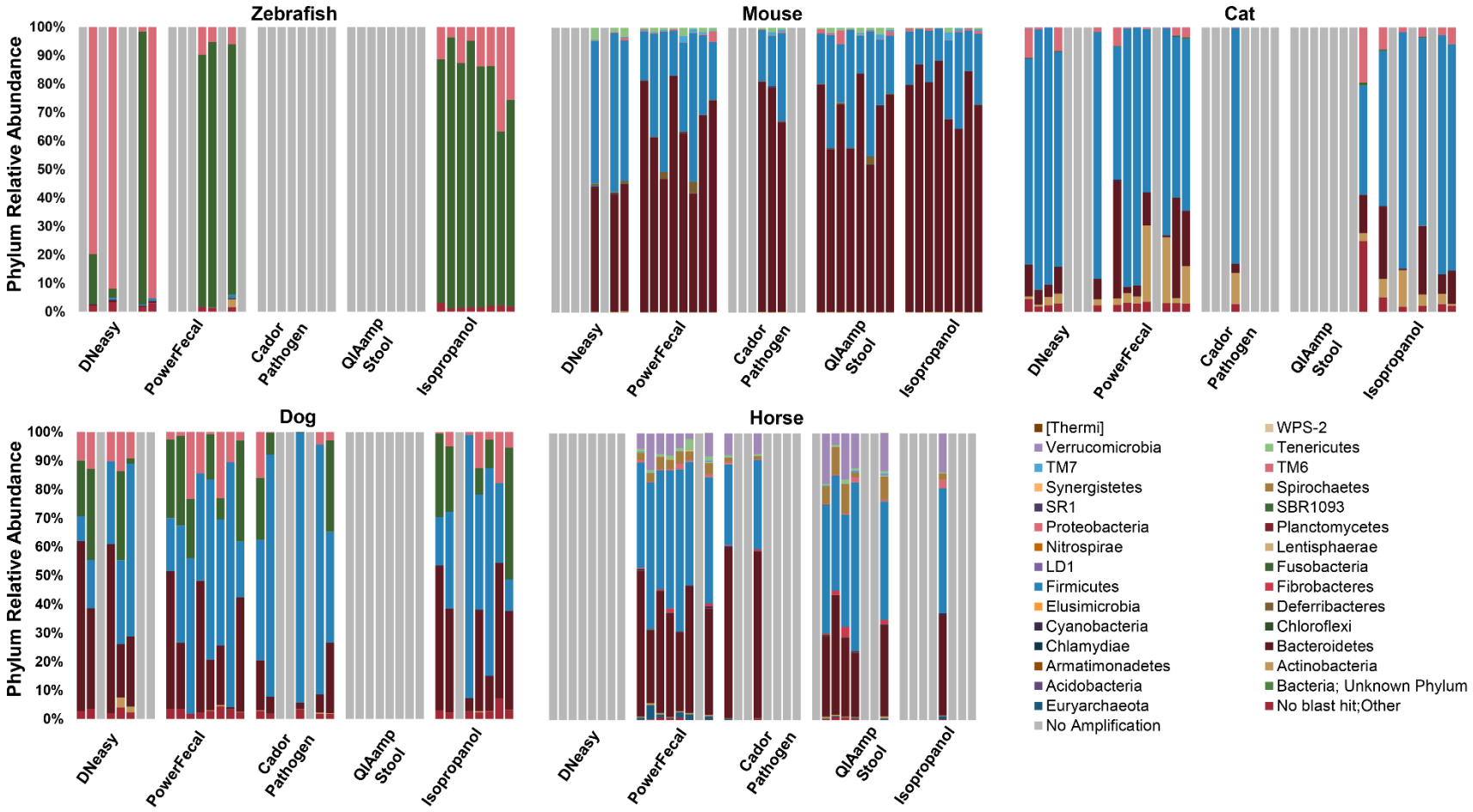

Figure 2.3. Comparison of DNA extraction method on next generation sequencing (NGS) relative abundance at the phylum level. Gray bars represent samples that resulted in sequencing below 10,000 reads. *n* = 8 samples per extraction method.

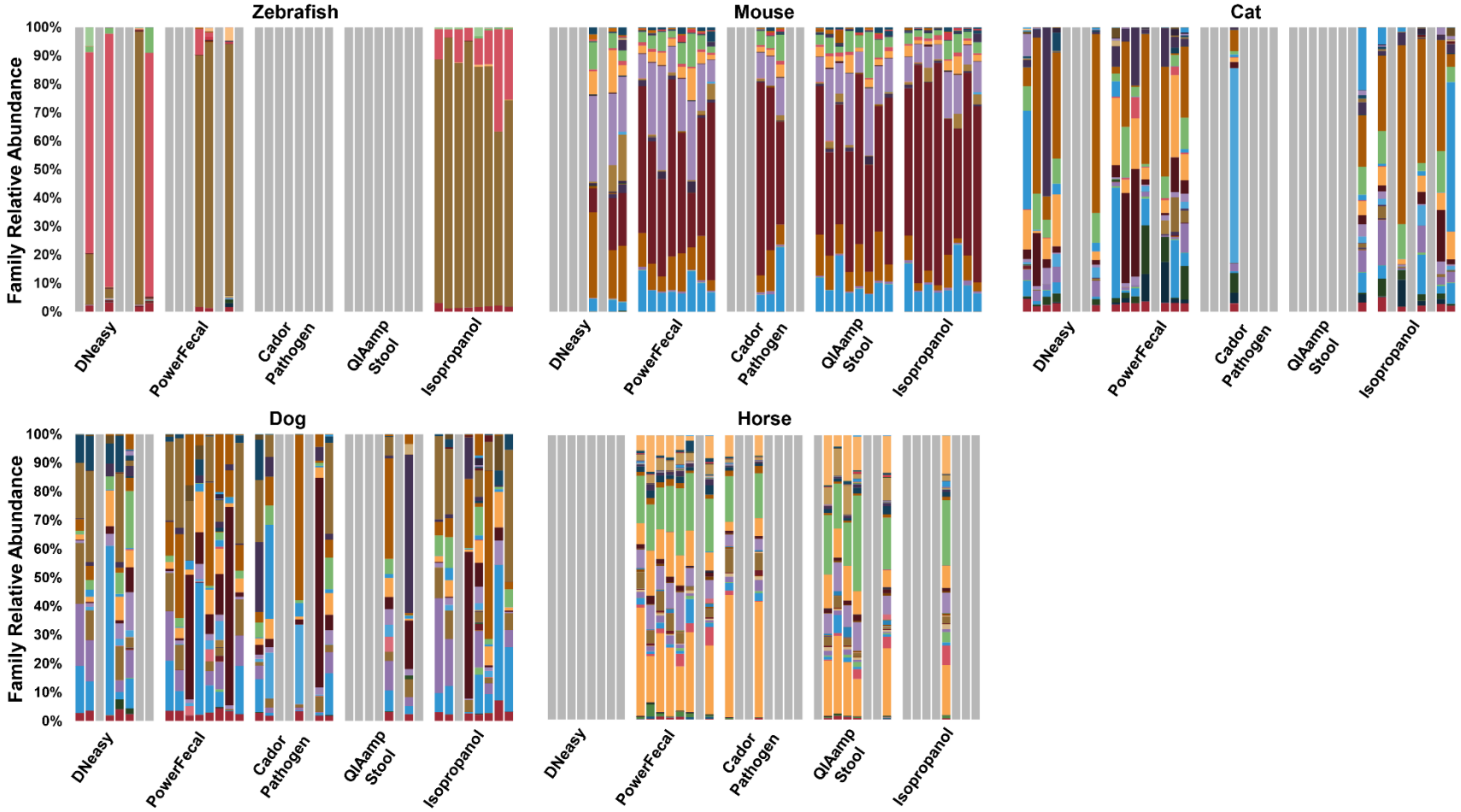

Figure 2.4. Comparison of DNA extraction method on next generation sequencing (NGS) relative abundance at the phylum level. Gray bars represent samples that resulted in sequencing below 10,000 reads. *n* = 8 samples per extraction method.

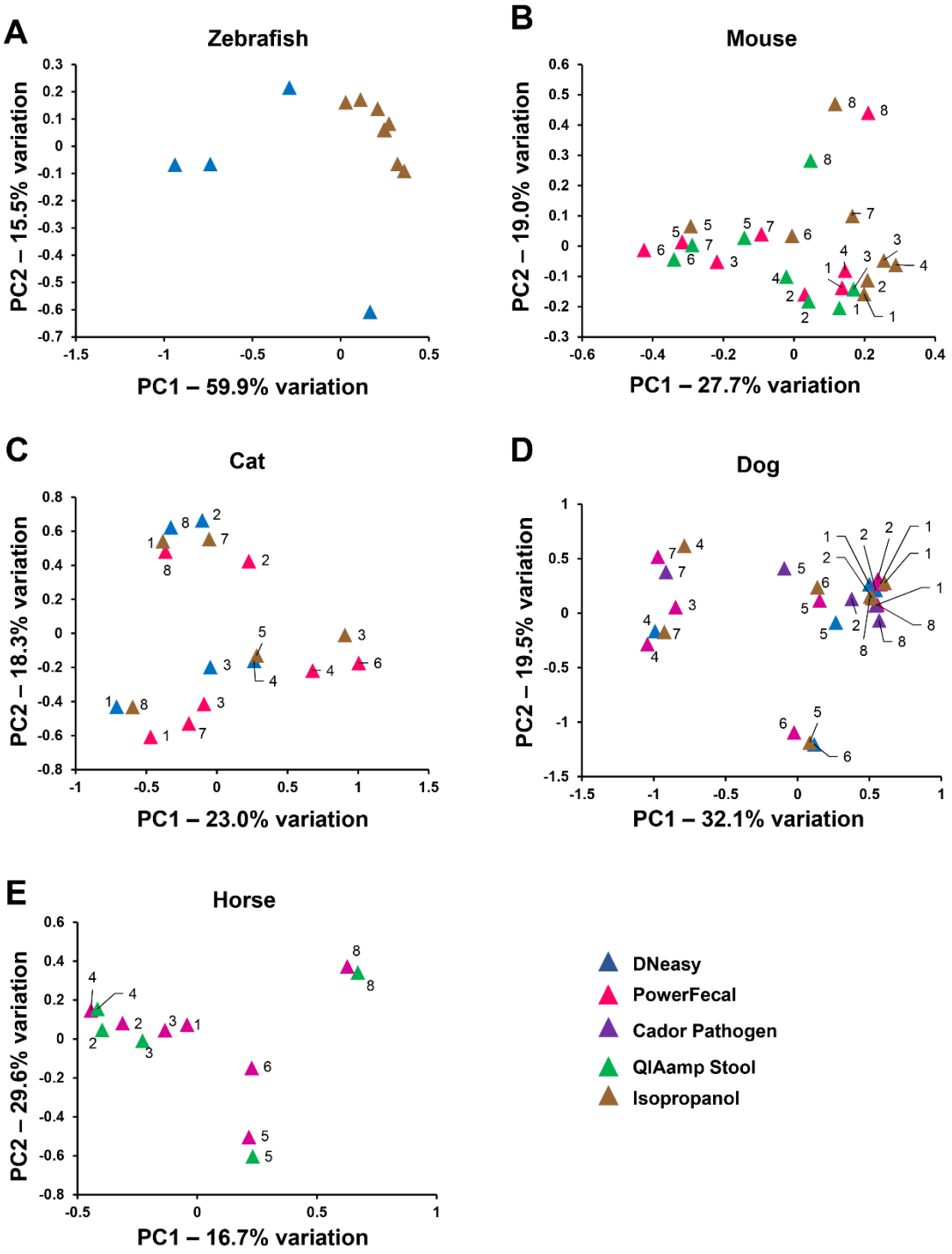

Figure 2.5. Principal Component Analysis (PCA) of samples with successful amplification and sequencing in at least half (4/8) samples. Colors denote extraction method: DNeasy (blue), PowerFecal (pink), CadorPathogen (purple), QIAmp Stool (green), and Isopropanol (brown). Numbers denote individual animal samples tracked across all kits tested for that species.

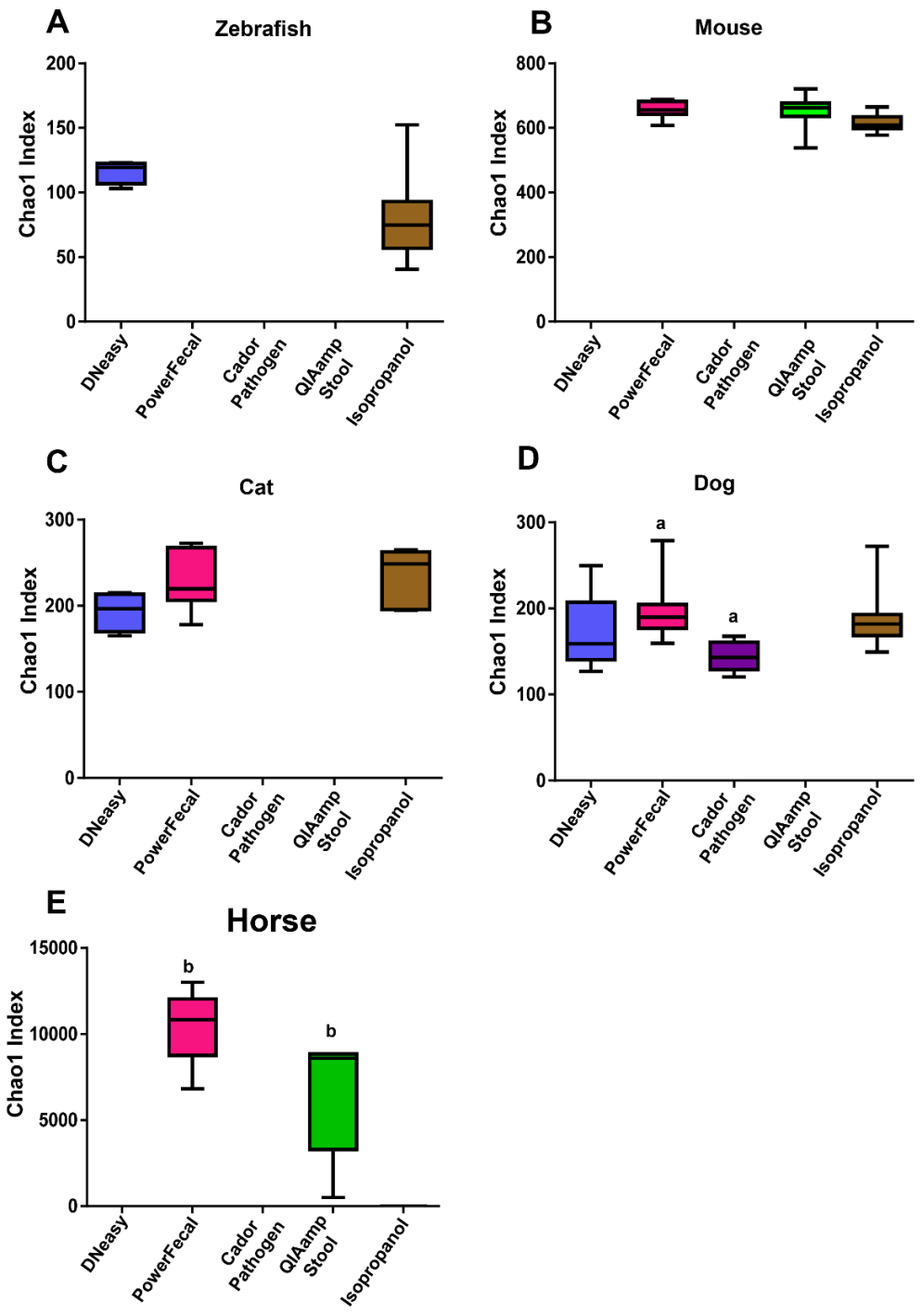

Figure 2.6. Diversity of fecal microbiota. Chao1 estimate of microbial diversity plotted by Tukey box and whisker graph. For zebrafish and horse samples, statistical significance was determined using student's t-test. For mouse, cat, and dog samples, statistical significance was determined using ANOVA with Student Newman Keuls post hoc test. Statistical significance defined by $p \leq 0.05$ and denoted in the figure by lower case letters.

Extraction Method	Cost ($)	Time (hr)	Mean A260/A280 ± s.d. Mean A260/A230 ± s.d.					Amplification				
			Fish	Mouse	Cat	Dog	Horse	Fish	Mouse	Cat	Dog	Horse
DNeasy	3.16	1 - 1.5	2.0 ±0.02 2.06 ±0.13	2.0 ±0.23 0.95 ±0.29	1.83 ±0.15 0.26 ±0.04	2.13 ±0.49 0.39 ±0.18	1.56 ±0.19 0.53 ±0.06	4/8	3/8	5/8	5/8	0/8
PowerFecal	5.26	1.5 - 2	1.85 ±0.09 2.02 ±0.40	1.9 ±0.23 1.14 ±0.36	1.57 ±0.19 1.0 ±0.27	1.65 ±0.18 1.31 ±0.60	1.66 ±0.21 0.38 ±0.04	3/8	8/8	7/8	8/8	7/8
Cador Pathogen	4.06	1.5 - 2	2.0 ±0.04 1.78 ±0.32	1.9 ±0.23 1.7 ±0.38	3.11 ±2.22 0.50 ±0.31	2.19 ±0.19 0.64 ±0.49	2.46 ±0.94 0.34 ±0.1	0/8	3/8	1/8	5/8	2/8
QIAamp Stool	4.32	1.5 - 2	2.1 ±0.05 2.19 ±1.06	2.2 ±0.62 2.03 ±1.06	2.07 ±0.07 0.82 ±0.48	2.13 ±0.13 1.67 ±0.41	3.32 ±0.72 0.07 ±0.01	0/8	8/8	1/8	2/8	5/8
Isopropanol	3.51	3.5 - 4	1.98 ±0.04 2.18 ±0.12	1.9 ±0.06 1.9 ±0.23	2.38 ±0.62 0.82 ±0.48	2.2 ±0.31 0.85 ±0.32	1.84 ±0.45 0.72 ±0.57	8/8	8/8	5/8	7/8	1/8

Table 2.1. Comparison of DNA extraction methods. Cost of DNA extraction methods calculated on per sample basis to include cost of kits, Eppendorf tubes, stainless steel beads, and pipette tips. Time of extraction method determined from start of fecal processing to DNA elution. Mean 260/280 and 260/230 nm absorbance (as determined by spectrophotometry) and standard deviation for all DNA extraction methods for each animal species. Number of amplified samples determined based on the total number of samples resulting in greater than 10,000 reads. n = 8 per extraction method.

CHAPTER 3:

Development of Outbred CD1 Mouse Colonies with Distinct Gut Microbiota Profiles for Use in Complex Microbiota Targeted Rederivation (CMTR)

Overview

The gastrointestinal (GI) tract harbors a complex and dynamic microbial community which has been suggested to have many local and systemic physiological effects on both health and disease conditions (13, 15, 121). With increased advances in high throughput sequencing technologies, studying the gut microbiota (GM) is becoming easier and there has been a notable explosion in recent GM publications. Despite these advances in technology, several challenges for studying the GM remain to be overcome. Human clinical GM studies have contributed significantly to the scientific understanding of a variety of diseases. However, these studies remain largely correlative with confounding experimental variables such as genetics, diet, environment, and patient compliance. For these reasons the use of animal models, particularly rodents, has been invaluable to understanding the role of the GM in health and disease. Nevertheless, animal models are not without challenges. Most animal models used to study the effects of the GM in health and disease are focused on the use of germfree, monocolonized, or defined microbiota animals. Although useful, these models have an overly simplified GM complexity and may not adequately reflect the true physiologic effect of the complex nature of human GM in health and disease. An alternative strategy, is the use of humanized mouse models. Humanized mice are rederived by surgical embryo transfer into germ free surrogate dams and then colonized with human microbiota samples.

While highly useful, studies indicate not all human GM species can colonize mice, suggesting that these animal models also have limitations (63, 64) .

A common practice in the generation of rodent models is the rederivation of desired mouse strains by surgical implantation of embryos or morulae into conventionally housed surrogate dams with strong maternal care instincts and high reproduction indices. This technique can be used to eliminate unwanted disease from mouse colonies as well as to recover cryopreserved mouse strains. While useful for these reasons, rederivation should also be considered as one possible method to study the GM composition by generation of isogenic mice with varying GM profiles. However, the desired GM profile is often associated with inbred mouse strains that have low maternal care instincts and thusly low reproduction indices. In addition, inbred mice oftentimes have decreased success rates for embryo transfer making them suboptimal as surrogate dams. In order to overcome this, we proposed that outbred colonies of CD1 mice could be generated with pre-defined vendor specific GM profiles. We demonstrate that CD1 colonies can indeed be generated with specific GM profiles and in our hands, these GM profiles are stable and can be maintained for at least six generations. Due to the strong maternal care instincts of these mice and the stability of the established GM profiles, these mice are invaluable tools for complex microbiota targeted rederivation (CMTR) of any mouse model warranting GM study.

Materials and Methods

Mice

The current study was conducted in accordance with the guidelines set forth by the Guide for the Use and Care of Laboratory Animals, the Public Health Service Policy

on Humane Care and Use of Laboratory Animals, and were approved by the University of Missouri Institutional Animal Care and Use Committee.

For embryo transfer (ET) recipients, eight to ten week old female C57BL/6J (The Jackson Laboratory, Bar Harbor, ME), C57BL/6NTac (Taconic Biosciences, Inc., Cambridge City, IN facilities), and Crl:CD1 (Charles River Laboratories, Wilmington, MA) mice were purchased and allowed to acclimate for one week prior to use. Embryos from eight week old female Crl:CD1 (Charles River Laboratories) mice were harvested from colonies maintained on site. Vasectomized, seven to eight week old Crl:CD1 male mice (Charles River Laboratories) were co-housed to induce pseudopregnancy and intrauterine embryo transfer was performed. All mice were housed in microisolator cages on ventilated racks (Thoren, Hazelton, PA) on a 14:10 light dark cycle, and provided *ad libitum* access to 5058 irradiated breeder chow (LabDiet, St. Louis, MO) and acidified autoclaved water.

Embryo collection and transfer

On day 1, embryo donors received IP injection of 5 IU of pregnant mare serum gonadotropin (PMSG) (Calbiochem, San Diego, CA) in 0.2 ml Dulbecco's phosphate-buffered saline (DPBS) with no calcium or magnesium (Life Technologies, Carlsbad, CA) at 2.5 hours post-light induction to induce superovulation. On day 3, at 5 hours post-light induction, embryo donors received an IP injection of 5 IU human chorionic gonadotropin (hCG) in 0.2 ml DPBS and were mated to intact males of the same genotype. Surrogate embryo recipient females demonstrating uninduced signs of estrus were mated with a sterile, vasectomized Crl:CD1 male (Charles River Laboratories). Post-mating, CD1:CRL embryo donors were euthanized and embryos were collected

aseptically. Briefly, the peritoneal cavity was opened and the reproductive tract visualized. Oviducts were excised and placed in 50µl of pre-warmed type IV-S hyaluronidase (Sigma, St. Louis) reconstituted at 1mg/ml in HEPES media (Sigma) supplemented with 4 mg/ml bovine serum (Sigma) for five to ten minutes. Clutches of embryos were released from oviducts with gentle manipulation under a dissecting microscope, and collected with a sterile glass hand-pipette. Surrogate females (Crl:CD1, Charles River Laboratories; C57BL/6J, The Jackson Laboratory; C57BL/6NTac, Taconic Biosciences, Inc., Cambridge, IN facilities) were inspected for copulatory plugs and plug-positive mice were used for embryo transfer. Briefly, surrogate females were anesthetized via IM injection of ketamine/xylazine cocktail at 5.5 mg and 1 mg per 100 g body weight respectively, and placed in sternal recumbency. A dorsal midline incision was made and the uterine oviducts located by dissecting through the retroperitoneal muscle. Embryos in 3 to 5 µl of media were injected into the oviducts using a glass hand-pipette. Skin incisions were closed with sterile surgical staples and mice received a subcutaneous injection of 2.5 mg/kg of body weight flunixin meglumine (Banamine®) prior to recovery on a warming pad.

Maintenance of Breeding Colonies

Male and female 8-10 week old CD1 mice are mated according to GM profile following an outbred mating scheme and housed in microisolator cages on ventilated racks (Thoren, Hazelton, PA) on a 14:10 light dark cycle, and provided *ad libitum* access to 5058 irradiated breeder chow (LabDiet, St. Louis, MO) and acidified autoclaved water.

Isopropanol DNA extraction of fecal samples

DNA extraction was performed as previously described (114). Briefly, cecal contents were thawed at room temperature and a sterile 0.5 cm diameter stainless steel bead and 800 µl of lysis buffer were added to the 2 ml round-bottom tube. Samples were mechanically disrupted using a TissueLyser II (Qiagen, Venlo, Netherlands) for 3 minutes at 30 Hz, followed by incubation at 70ºC for 20 minutes with periodic vortexing. Samples were centrifuged at 5000 × g for 5 minutes, and the supernatant was transferred to a sterile 1.5 ml Eppendorf tube containing 200 µl of 10mM ammonium acetate. Lysates were vortexed, incubated on ice for 5 minutes, and then centrifuged. Supernatant was transferred to a sterile 1.5 ml Eppendorf tube and one volume of chilled isopropanol was added. Samples were incubated on ice for 30 minutes and centrifuged at 16000 × g at 4ºC for 15 minutes. The DNA pellet was washed with 70% ethanol and resuspended in 150 µl Tris-EDTA, followed by addition of 15 µl of proteinase K and 200 µl AL buffer (DNeasy Blood and Tissue kit, Qiagen). Samples were incubated at 70ºC for 10 minutes and 200 µl of 100% ethanol was added to the tubes. Samples were mixed by gentle pipetting and the contents transferred to a spin column from the DNeasy kit (Qiagen). The DNA was further purified following the manufacturer's instructions and eluted in 200 µl EB buffer (Qiagen). DNA concentrations were determined fluorometrically (Qubit dsDNA BR assay, Life Technologies, Carlsbad CA) and samples were stored at 20ºC until sequencing.

Library Construction and 16S rRNA sequencing

Library construction and sequencing was performed at the University of Missouri DNA Core. Bacterial 16SrRNA amplicons were generated in a multiplexed (96-well) format using amplification of the V4 hypervariable region of the 16S rRNA gene, and

then sequenced on the Illumina MiSeq platform as previously described (114). Samples returning greater than 10,000 reads were deemed to have successful amplification.

Informatics analysis

Assembly, binning, and annotation of DNA sequences was performed at the University of Missouri Informatics Research Core Facility. Briefly, contiguous DNA sequences were assembled using FLASH software (115), and culled if found to be short after trimming for a base quality less than 31. Qiime v1.8 (116) software was used to perform *de novo* and reference-based chimera detection and removal, and remaining contiguous sequences were assigned to operational taxonomic units (OTUs) using a criterion of 97% nucleotide identity. Taxonomy was assigned to selected OTUs using BLAST (117) against the Greengenes database (118) of 16SrRNA sequences and taxonomy.

Statistical Analysis

For gut microbiota analysis, OTUs with less than 10,000 reads were excluded from the data set. Bar graphs were generated with Microsoft Excel (Microsoft, Redmond WA) and principal component analysis (PCA) was generated using Paleontological Statistics Software Package (PAST) 3.12 (122). All groups were visually inspected for descriptive analysis of consistency between animals (bar graphs) or clustering of animals within groups (PCAs). Statistical testing for differences in beta-diversity was performed via PERMANOVA, implemented using PAST 3.12. Statistical analysis of differences in phyla and OTU relative abundance was performed using Sigma Plot 13.0 (Systat Software Inc., Carlsbad CA) using one-way ANOVA with GM profile (i.e., GMJAX, GMTAC, GMCRL) as the independent variables, followed by Student Newman-Keuls

post hoc test. To account for multiple testing, OTUs with a p value of <0.001 were considered statistically significant.

Results

First and second generation CD1 offspring have GM profiles similar to embryo transfer surrogate dams.

The gastrointestinal tract of pups is colonized by the gut microbiota (GM) of the dam during and shortly following the birthing process. We chose to capitalize on this phenomenon to generate outbred CD1 colonies with distinct GM profiles. CD1 embryos were surgically transferred to surrogate dams purchased from three different vendors (Figure 3.1). Following birth pups remained with the surrogate dam, removed at weaning, and raised to adulthood in ventilated micro-isolator racks following barrier husbandry practices to minimize GM cross contamination. Fecal samples from 8-10 week old first and second generation offspring were characterized via sequencing of the V4 hypervariable region of the 16S rRNA gene.

To evaluate the GM composition of first and second generation offspring as compared to ET surrogate dams, we examined the relative abundance annotated to the level of phyla and OTU. We found that first and second generation offspring maintained an overall GM profile pattern at both the phyla and OTU level similar to surrogate dams (Figure 3.2A and 3.2B). To further evaluate the similarities between dam and offspring, we performed principal component analysis (PCA). In unweighted PCA, samples that are similar in microbial composition cluster together, whereas samples that are dissimilar are farther apart. Surrogate dams and first and second generation offspring clustered tightly along PC1 indicating similar β-diversity within GM profile group (Figure 3.3). In

addition, differential clustering along PC2 into three distinct groups illustrates the presence and maintenance of three distinct CD1 GM profiles in both the first and second generation offspring similar to surrogate dams. One-Way PERMANOVA analysis of GM profiles indicates the maintenance of three separate profiles with $p = 0.001$

Sixth generation CD1 colonies maintain three distinct GM profiles varying in composition and complexity.

To evaluate the longevity of maintaining three distinct GM profiles, we monitored GM composition and complexity of 8-10 week old sixth generation females. Similar to our previous findings in unweighted PCA, female mice demonstrated tight intra-group clustering along PC1 and differential clustering along PC2 indicating three distinct GM profiles (Figure 3.4). These data suggest that the tested GM profiles are stable and can be maintained under the current animal housing and husbandry conditions.

Outbred CD1 colonies with varying GM colonization can be an important research method to evaluate effects of the GM on health and disease or when controlling for the GM as an experimental variable. To investigate the potential use of the established colonies as surrogate dams and thus GM donors for future CMTR, we examined the microbial composition and diversity of fecal samples from sixth generation 8-10 week old females. We found significant differences between GM profiles in the relative abundance at both the phylum and OTU level. Specifically, we found that sixth generation females with GMJAX profiles had a higher relative abundance of phylum *Actinobacteria* than either the GMCRL or GMTAC (Figure 3.5A and Table 3.1). In addition, both the GMCRL and GMTAC females had a higher relative abundance of the

phyla *Defferibacteres* and TM7 than GMJAX females. GMJAX and GMCRL had significantly higher levels of the phylum *Tenericutes*.

Several OTUs were notably different between the three GM profiles. For GMJAX females we found an increased relative abundance in Genus *Bacteroides*, Genus *Parabacteroides*, Family *Peptostreptococcaceae*, Genus *Anaeroplasma*, and *Akkermansia muciniphila*, and Genus *Prevotella* as compared to the other GM profiles (Figure 3.5B and Table 3.2). GMCRL females were enriched in relative abundance of Genus *Aldercreutzia*, Order *Bacteroidales*, Genus *Prevotella*, and *Family Rikenellacea*. Whereas GMTAC females had relatively more *Mucispirillum schaedleri*, Genus *Anaerostipes* and Genus *Blautia*. In contrast, decreased relative abundance of Genus *Odoribacter* and *Sutterella* were noted in GMCRL females when compared to other groups. Interestingly, *Allistipes massiliensis*, Order YS2, Genus *Lactococcus*, Genus *Candidatus Arhtromitus*, Genus *Anaerostipes*, and Genus *Blautia* were below detectable levels in GMJAX females. Comparison of bacterial richness between GM profiles revealed decreased richness in GMJAX females compared to GMCRL and GMTAC profiles. No differences in richness were noted between GMCRL and GMTAC profiles (Figure 3.6A). Bacterial diversity between groups was evaluated using Chao1 analysis. Females with the GMJAX and GMTAC profiles had significantly decreased bacterial diversity compared to both GMCRL females. No difference was observed between mice with GMJAX and GMTAC profiles (Figure 3.6B).

Discussion

As interest in the study of the gut microbiota continues to rise, there is an increasing need for methods to fully study microbial composition and function. Current

methods include the use of germ-free mice or mono-colonized mice. While these methods can be useful, they do not fully take into account interactions between microbes in naturally occurring complex GI populations. Human studies, while useful for studying complex microbe interactions are often confounded by uncontrollable experimental variables and have limited longitudinal utility due to focus on microbiota changes after disease onset. To overcome these limitations, we investigated the use of embryo transfer as a method to develop outbred mouse colonies colonized with distinct vendor-specific gut microbiota (GM) profiles. We surgically implanted embryos from the same outbred stock into surrogate dams harboring different GM communities varying in complexity and composition. We found that first and second generation offspring were similar in β diversity to surrogate dams with no differences in observed GM phylum and OTU profiles between dam and offspring indicating successful transfer of GM profile from dam to pup.

Complex microbiota targeted rederivation (CMTR) can be a valuable resource for the targeted study of the effects of complex gut microbiota on health and disease. In order to use these colonies as surrogate dams for CMTR, they must exhibit longevity and stability of GM composition in a breeding colony. We found that by using barrier husbandry techniques, breeding colonies with distinct GM profiles can be maintained with minimal GM drift for at least six generations. These data underscore the stability of the GM in outbred, healthy, adult females.

To further evaluate the utility of these colonies as GM donors for CMTR, we examined the composition and complexity of the GM profiles of each colony. We found several differences among the groups at both the phyla and OTU level. Specifically, in

the GMJAX females we found an increased relative abundance of Genus *Bacteroides*, Genus *Parabacteroides*, Family *Peptostreptococcaceae*, Genus *Anaeroplasma*, *Akkermansia muciniphila*, and Genus *Prevotella* when compared to the other GM profiles. In GMCRL females we observed enrichment in the relative abundance of Genus *Aldercreutzia*, Order *Bacteroidales*, *Family Rikenellacea*, and Genus *Prevotella*. We also noted relatively more *Mucispirillum schaedleri*, Genus *Anaerostipes* and Genus *Blautia* in GMTAC females.

CMTR provides an alternative strategy to evaluate the contribution of complex GM in health and disease. The outbred CD1 colonies we generated have stable GM with demonstrable differences in both composition and complexity. These mice provide an opportunity to study the effect of the GM composition on disease phenotype of isogenic mouse models. For example, in inflammatory bowel disease (IBD), $CD1_{GMJAX}$ surrogate dams might be chosen for CMTR of these mouse models due to the absence of Genus *Candidatus Arthromitus* (an important modulator of T cell development). In neurodevelopment models, such as models of autism where decreased relative abundance of Genus *Prevotella* was shown to be associated with disease severity(123), $CD1_{GMCRL}$ surrogate dams may be chosen to investigate the contribution of increased Genus *Prevotella* on disease severity. In addition to evaluation of composition, CMTR offers the ability to examine the effect of GM complexity on disease phenotype. Several recent studies have suggested that alterations in GM complexity is associated with disease severity in a variety of diseases including IBD, obesity, and type 2 diabetes (31, 124-127) . Taken as a whole, these studies illustrate the utility of CMTR as a method to further evaluate the role of complex, naturally occurring GM on host health and disease.

In addition to use as a tool to address specific GM targeted research questions, CMTR should also be considered as a possible means to help alleviate research concerns over model reproducibility. The National Institutes of Health (NIH) recently raised concerns over the reproducibility of studies within biomedical research (120, 128). To address these concerns over reproducibility, CMTR may be used as a method to ensure that specific models begin with optimized complex GM profiles to ensure that all mice of the same genotype have similar GM composition at the start of experimentation enabling direct comparison of experimental results between institutions. In addition to isogenic studies, CMTR can also be used to study the effect of a single GM profile on mouse models with differing genetics.

Collectively, the data in this study provide proof of concept that surgical embryo transfer to establish outbred mice with differing vendor-specific gut microbiota is possible. We have demonstrated that these GM profiles are stable for at least six generations, underscoring the stability of the GM in apparently healthy mice. As the GM composition of these mice is a naturally occurring complex GM, they provide a unique alternative strategy to study the effect of complex GM on mouse models and provide a method to help ensure model reproducibility.

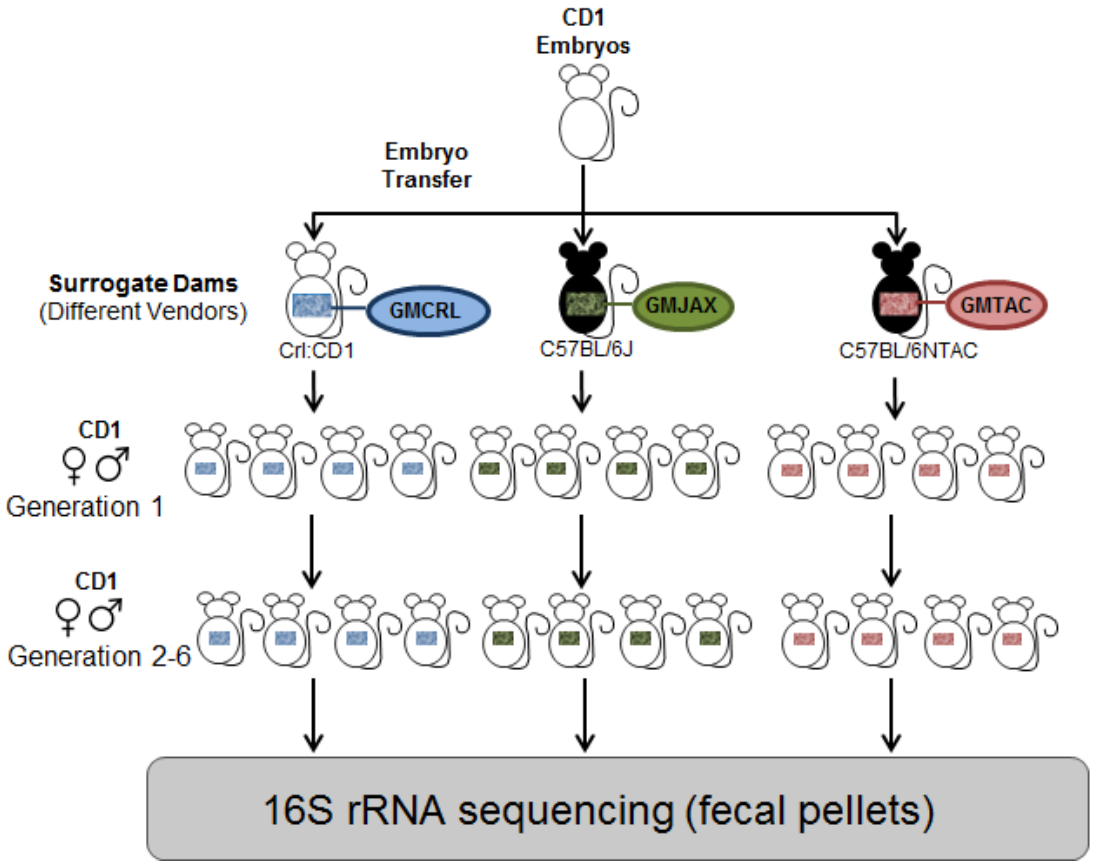

Figure 3.1. Experimental design used to generate CD1 mice with different gut microbiota (GM). Schematic diagram showing embryo transfer scheme used to rederive CD1 mice to Crl:CD1$_{GMCRL}$, C57BL/6J$_{GMJAX}$, C57BL/6NTac$_{GMTAC}$ surrogate dams. 8-10 week old offspring were mated using an outbred mating scheme and maintained as three separate breeding colonies for six generations.

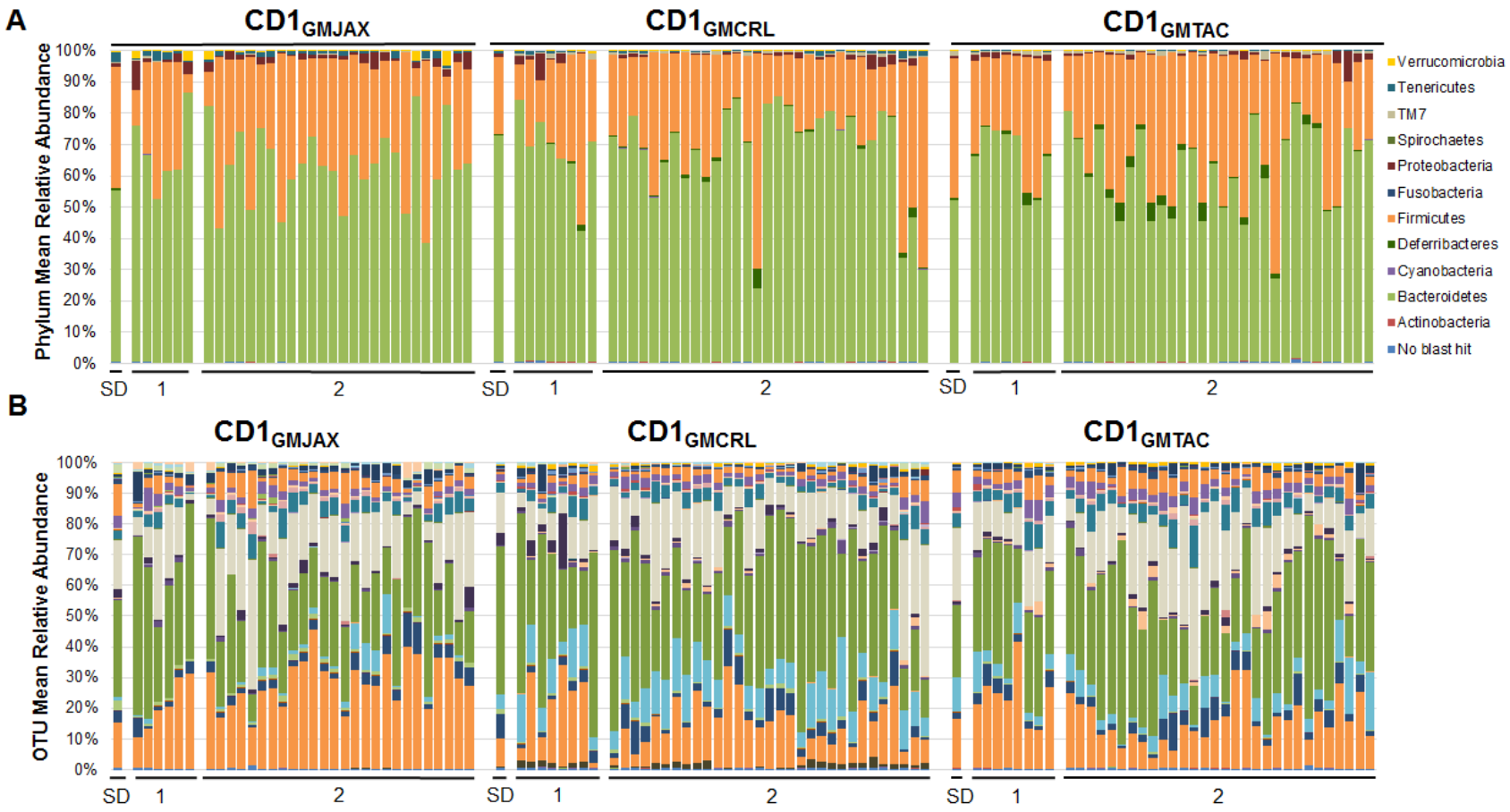

Figure 3.2. Comparison of the relative abundance of taxa in fecal samples from surrogate dam and 1st and 2nd generation offspring. SD = Surrogate Dam; 1 = First generation females; 2 = 2nd generation females. Representative samples of embryo transfer dams (n = 5-6 per GM profile), 1st generation female offspring (n = 5-6 per embryo transfer dam), and second generation offspring (n = 8-12 per first generation dam). A) Bar charts of relative abundance of taxa at phyla level. Legend of phyla at right. B) Bar charts of relative abundance of taxa at OTU level.

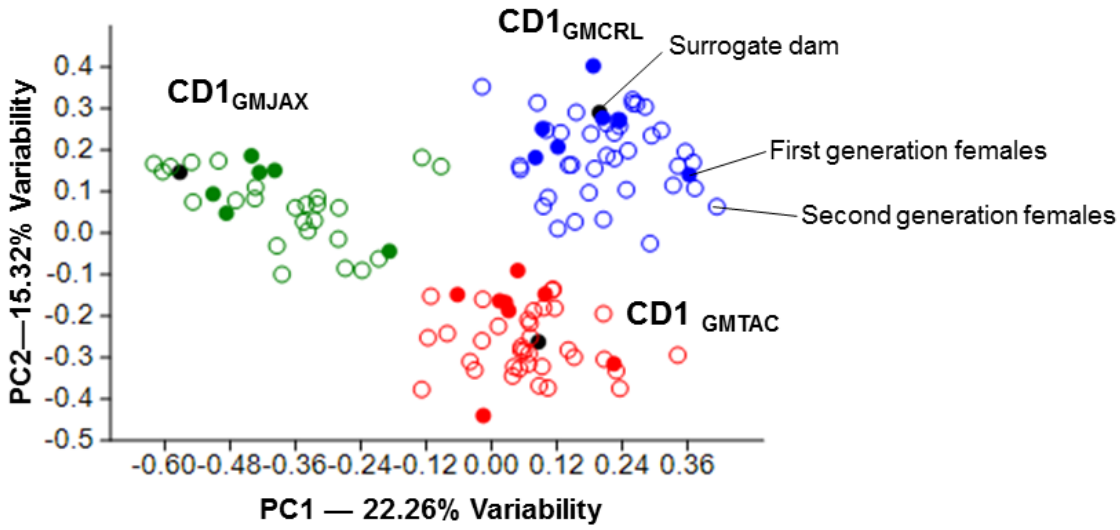

Figure 3.3. First and second generation females maintain three distinct gut microbiota (GM) communities with similar microbial composition. Unweighted principal component analysis (PCA) of representative fecal samples from 8-10 week old CD1 females, first generation (n = 5-6 per embryo transfer dam) and second generation (n = 8-12 per first generation dam).

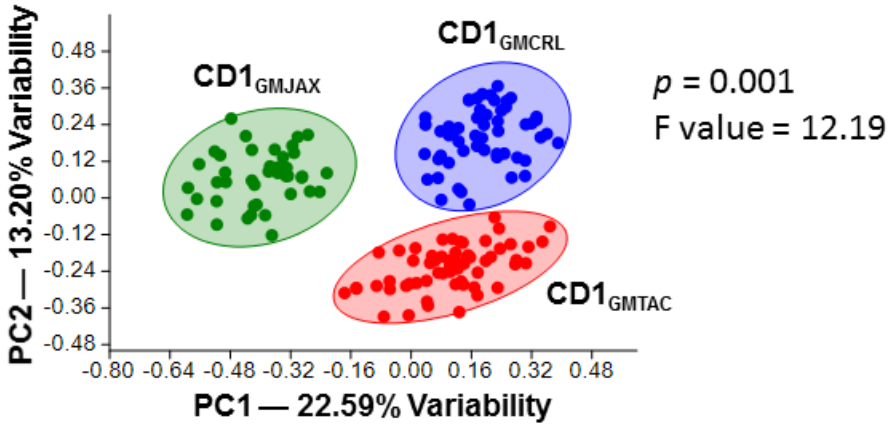

Figure 3.4. Distinct GM profiles of rederived CD1 colonies can be maintained for six generations. Unweighted principal component analysis (PCA) of representative fecal samples from sixth generation 8-10 week old female CD1 mice (n = 35-40 per GM profile).

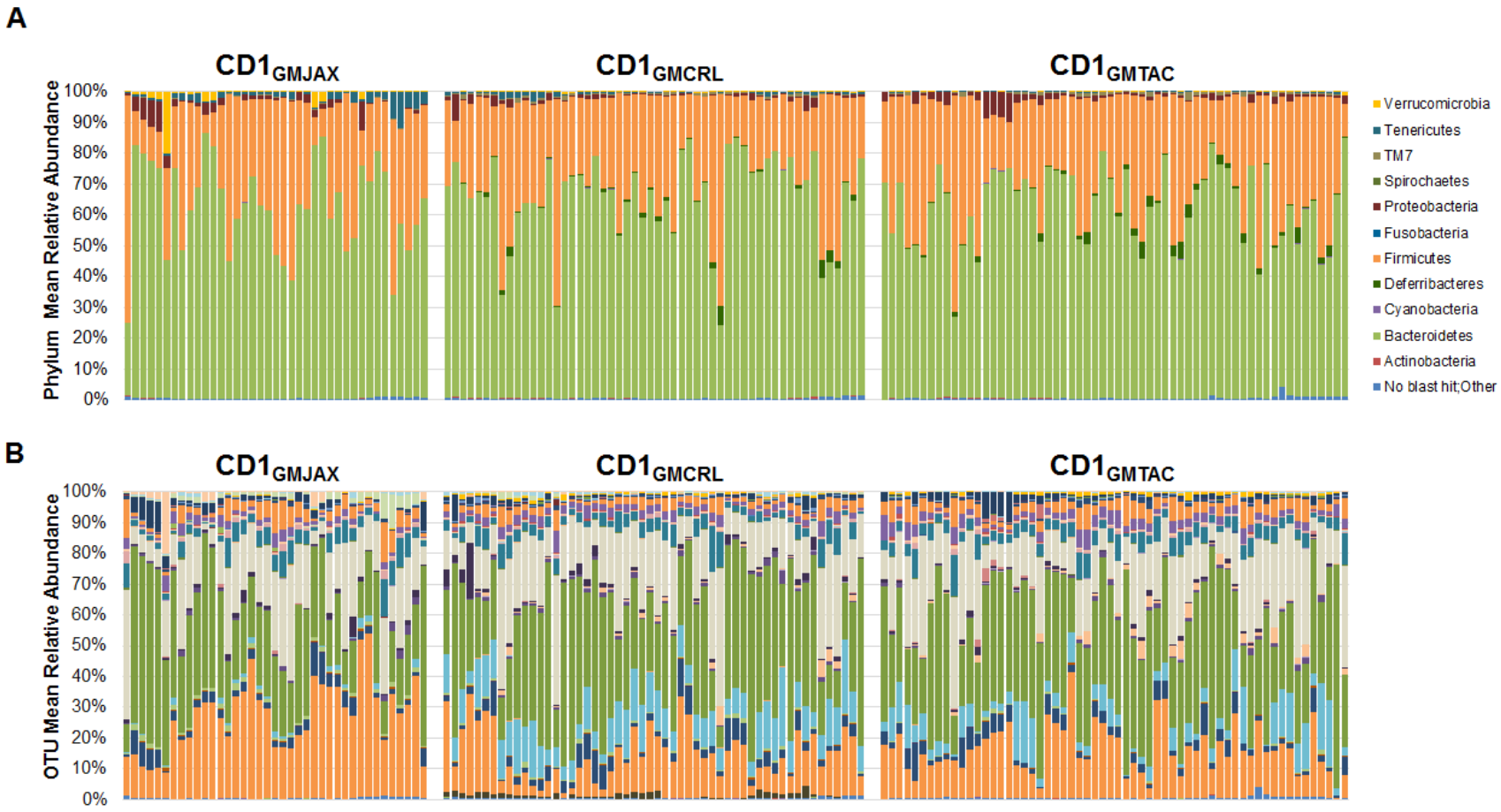

Figure 3.5. Comparison of relative abundance of taxa of rederived sixth generation GM groups. Representative samples for sixth generation 6-8 week old CD1 female mice (n = 35-40 per GM profile). A) Bar charts of relative abundance of taxa at phyla level. Legend of phyla at right. B) Bar charts of relative abundance of taxa at OTU level.

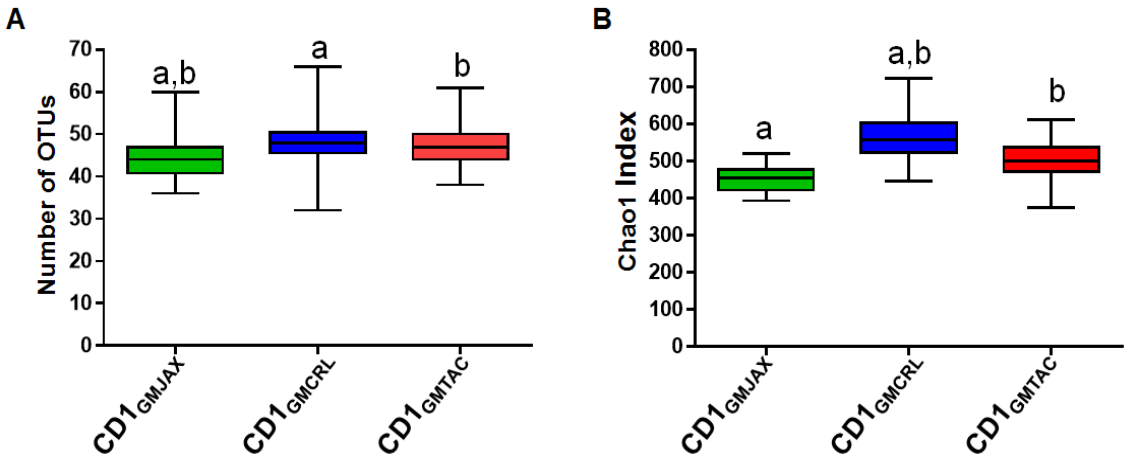

Figure 3.6. Comparison of gut microbiome (GM) richness and complexity of rederived sixth generation GM groups. Tukey box and whisker graph of sixth generation 6-8 week old CD1 female mice (n = 35-40 per GM profile). Statistical significance comparisons determined by One-way ANOVA with Student Newman Keuls post hoc test. Statistical significance defined by $p \leq 0.05$ and denoted in the figure by lower case letters.

Significant Phyla	GMJAX relative to GMCRL		GMJAX relative to GMTAC		GMTAC relative to GMCRL		GMJAX	GMCRL	GMTAC
OTU	P value	Mean Fold Change	P value	Mean Fold Change	P value	Mean Fold Change	Mean Relative Abundance (±SEM)	Mean Relative Abundance (± SEM)	Mean Relative Abundance (± SEM)
Actinobacteria	**0.001**	0.35	0.120	0.25	0.027	0.67	0.002±3.1E-05	0.0007±0.0001	0.0004 ±7.26E-05
Defferibacteres	**0.001**	0.001	<**0.001**	0.0007	0.070	1.49	9.62E-06 ±2.75E-06	0.008±0.001	0.012±0.001
TM7	<**0.001**	0.21	<**0.001**	0.09	0.534	1.06	0.001±0.0001	0.005±0.0005	0.006±0.0006
Tenericutes	<**0.001**	3.04	<**0.001**	8.05	0.023	1.18	0.02±0.0003	0.007±0.0008	0.001±0.0002

Table 3.1. Statistical comparison of the relative abundance of Phyla between GM profiles. *p*-value, mean fold change, and mean relative abundance are shown. Statistical significance determined using One-way ANOVA with Student Newman-Keuls post hoc test. Bold face values indicate statistical significance ($p \leq 0.001$).

Significant Operational Taxonomic Unit (OTU)		GMJAX relative to GMCRL		GMJAX relative to GMTAC		GMTAC relative to GMCRL		GMJAX	GMCRL	GMTAC
Phylum	**OTU**	**P value**	**Mean Fold Change**	**P value**	**Mean Fold Change**	**P value**	**Mean Fold Change**	**Mean Relative Abundance (±SEM)**	**Mean Relative Abundance (± SEM)**	**Mean Relative Abundance (± SEM)**
Actinobacteria	Family *Coriobacteriaceae*	0.001	0.69	**<0.001**	1.49	0.57	0.34	9.7E-05±2.0E-06	0.001±5.6E-05	5.1E-05±1.2E-05
	Genus *Aldercreutzia*	**<0.001**	0.33	0.274	0.66	**<0.001**	0.49	1.5E-04±1.7E-05	4.6E-04±6.2E-05	0.0002±2.8E-05
Bacteroidetes	Order *Bacteroidales*	**<0.001**	3.71E-05	0.122	0.04	**<0.001**	0.001	3.7E-05±1.6E-06	0.01±0.001	8.4E-06±4.1E-06
	Genus *Bacteroides*	**<0.001**	2.03	**<0.001**	1.70	0.03	1.19	0.3±0.72	0.13±0.01	0.16±0.01
	Genus *Parabacteroides*	0.03	1.40	**<0.001**	1.89	**<0.001**	0.74	0.003±0.0002	0.002±0.0001	0.001±0.0001
	Genus *Prevotella*	**<0.001**	1.88	**<0.001**	1.48	**<0.001**	0.42	0.01±0.0007	0.006±0.0005	0.003±0.0004
	Family *Rikenellaceae*	**<0.001**	0.07	**<0.001**	0.11	**<0.001**	0.62	0.008±0.001	0.108±0.0006	0.07±0.0007
	Alistipes massiliensis	*	0.000	**<0.001**	0.000	**<0.001**	0.29	0.00±0.00	0.0005±6.19E-05	0.0002±3.7E-05
	Genus *Odoribacter*	**<0.001**	0.85	0.358	1.07	0.004	0.79	0.008±0.001	0.001±0.0008	0.008±0.0007
Cyanobacteria	Order YS2	*	0.000	0.014	0.000	**<0.001**	1.28	0.00±0.00	0.001±0.0001	0.006±1.0E-04
	Order *Streptophyta*	0.90	1.23	**<0.001**	3.91	**<0.001**	0.31	7.5E-05±1.9E-05	6.1E-05±1.2E-05	1.9E-05±5.8E-06
Deferribacteres	*Mucispirillum schaedleri*	**<0.001**	0.001	**<0.001**	0.001	0.004	1.48	9.9E-06±2.8E-06	0.008±0.001	0.01±0.002
Firmicutes	Genus *Lactococcus*	*	0.000	1.00	0.000	**<0.001**	0.005	0.00±0.00	0.0001±4.01E-05	6.8E-06±6.6-E07
	Genus *Candidatus Arthromitus*	*	0.000	0.163	0.000	**<0.001**	0.36	0.00±0.00	0.0004±7.68E-05	0.002±0.0001
	Genus *Clostridium*	0.42	1.38	**<0.001**	60.32	**<0.001**	0.02	0.002±2.9E-05	0.0001±2.18E-05	3.1E-06±8.1E-07
	Genus *Anaerostipes*	*	0.000	**<0.001**	0.000	**<0.001**	6.07	0.00±0.00	3.5E-05±2.7E-05	0.002±3.48E-05
	Genus *Blautia*	*	0.000	0.024	0.000	0.15	0.51	0.00±0.00	1.2E-05±3.4E-06	7.6E-06±2.49E-06

	Genus *Dorea*	**<0.001**	2.91	**<0.001**	6.26	0.06	0.46	0.0001±1.0E-05	0.0003±8.8E-05	0.0003±2.1E-05
	Family *Peptococcaceae*	0.33	0.90	**<0.001**	23.136	**<0.001**	0.039	0.0003±3.5E-05	0.0003±2.51E-05	1.03E-05±9.0E-06
	Genus rc4-4	**<0.001**	0.40	0.890	0.52	**<0.001**	0.77	0.001±1.6E-04	0.003±0.0002	0.002±0.0001
	Family *Peptostreptococcaceae*	**<0.001**	5142.66	**<0.001**	26.88	0.55	191.27	0.002±7.4E-04	3.3E-05±1.3E-06	6.4E-05±4.0E-05
	Family *Ruminococcaceae*	0.50	0.83	**<0.001**	0.66	**<0.001**	1.24	0.02±0.002	0.023±0.002	0.03±0.002
	Genus *Oscillospira*	0.003	1.57	0.182	0.99	**<0.001**	1.57	0.04±0.005	0.026±0.002	0.04±0.002
	Genus *Ruminococcus*	0.80	1.06	0.001	0.68	**<0.001**	1.55	0.004±6.0E-04	0.004±0.0004	0.007±0.002
	Family *Erysipelotrichaceae*	0.008	0.45	**<0.001**	0.99	0.09	0.45	0.001±1.6E-04	0.003±0.0004	0.002±0.0001
Proteobacteria	Class *Alphaproteobacteria*	0.002	2.47	**<0.001**	2.80	0.31	0.88	6.2E-05±1.7E-05	2.5E-05±1.4E-05	2.2E-05±7.4E-06
	Zea luxurians	0.21	1.19	0.004	3.57	**<0.001**	0.33	0.0002±6.0E-05	0.0002±3.9E-05	6.7E-05±2.7E-05
	Genus *Sutterella*	**<0.001**	1.98	0.024	1.07	0.03	1.84	0.02±0.004	0.009±0.001	0.02±0.003
	Oxalobacter formigenes	0.14	0.81	**<0.001**	3.72	**<0.001**	0.22	3.2E-05±6.9E-06	3.9E-05±7.4E-06	8.5E-06±6.1E-07
	Family *Enterobacteriaceae*	**<0.001**	0.01	**<0.001**	0.02	0.02	0.42	5.5E-06±1.6E-06	0.0005±0.0001	0.0002±5.6E-05
TM7	Family F16	**<0.001**	0.21	**<0.001**	0.19	0.41	1.05	0.001±1.2E-04	0.005±0.0005	0.0006±6.0E-05
Tenericutes	Genus *Anaeroplasma*	**<0.001**	5.37	**<0.001**	1097.61	**<0.001**	0.005	0.02±0.003	0.003±0.0006	1.5E-05±5.8E-06
	Order F39	0.42	1.04	**<0.001**	3.17	**<0.001**	0.33	0.004±6.3E-04	0.003±0.0005	0.001±0.0001
Verrucomicrobia	*Akkermansia muciniphila*	**<0.001**	20.98	**<0.001**	33.55	0.00	0.625	0.01±0.005	0.0005±0.0001	0.0003±0.0001

Table 3.2. Statistical comparison of the relative abundance of OTU between GM profiles. *p*-value, mean fold change, and mean relative abundance are shown. Statistical significance determined using One-way ANOVA with Student Newman-Keuls post hoc test. Bold face values indicate statistical significance ($p \leq 0.001$). *Statistical comparison not applicable due to 0.000 OTU relative abundance.

CHAPTER 4:

Impact of Complex Microbiota Targeted Rederivation (CMTR) on the IL-10-/- Mouse Model of Inflammatory Bowel Disease

Overview

Inflammatory bowel disease (IBD) is a multifactorial disease thought to involve a complex interaction between genetic and environmental factors, leading to aberrant immune responses to normally innocuous microbes. Two known primary forms of disease exist, ulcerative colitis and Crohn's disease (CD), which share many clinical symptoms and are characterized by chronic, relapsing inflammation affecting the gastrointestinal (GI) tract. Both forms of IBD are associated with substantial morbidity and long-term costs to patient, health care, and society (70, 129, 130). CD preferentially occurs in the distal ileum and colon, areas that contain the highest density of bacteria, suggesting that alterations in bacterial communities (dysbiosis) within these regions may influence disease outcome. Although the exact etiology of IBD remains unknown, recent advances in sequencing technology have shown that patients with IBD have an abnormal composition and function of GI microbiota (79, 131). Further demonstrating the role of the gut microbiota (GM) in disease is the positive clinical response of some IBD patients when antimicrobials and probiotics are prescribed (9, 81). However, the mechanism of how these changes in microbial diversity and composition induce disease or alter disease outcome remains largely unknown.

Studies in human IBD patients have contributed greatly to the understanding of IBD. However, these studies are largely retrospective and can be confounded by experimental variables such as variation in genetics, environment, and patient

compliance. Mouse models that mimic human IBD have also contributed extensively to our understanding of disease pathogenesis as they allow experimentation with tightly controlled variables. A number of widely used models utilize chemical induction of inflammation via administration of epitheliotoxic compounds such as dextran sulfate sodium (DSS), or genetic modification that lead to the development of chronic inflammation (74). Using mouse models to study the role of the microbiota in IBD can be challenging, with most options focused on the use of germfree, monocolonized, or defined microbiota animals. While these models are largely useful for the study of specific GM populations, they are by definition restricted in GM complexity and do not recapitulate the complexity of the human GM. An alternative is the use of humanized mouse models. Traditionally, humanized mice are rederived as germ free animals and then colonized with human microbiota samples. While these animals can provide useful information on alterations in GM, not all human bacterial species colonize mice (63, 64), which may impact disease outcome. Moreover, mice colonized with xenomicrobiota such as human GM have significantly diminished numbers of mucosal T cells, suggesting the need for appropriate cognate host:microbiota interations in immune system development (61).

A common practice in rodent model generation is rederivation of mouse strains by surgical transfer of embryos or morulae from the desired research model to surrogate dams that are chosen for their strong maternal capabilities. This is done for a variety of reasons such as to render mouse colonies free of unwanted infectious disease or to recover mouse strains previously cryopreserved as germplasm. While rederivation may

be useful for these reasons, it can also be considered as both a source of unanticipated phenotypic variation, or as a means to evaluate the role of the GM in a model phenotype. In the current study, we used a technique we refer to as complex microbiota targeted rederivation (CMTR) to study naturally-occurring complex GM profiles in isogenic animals, thus allowing controlled study of the impact of these microbial communities on disease severity. Specifically, genetically identical C57BL/6 IL-10$^{-/-}$ and C3H/HeJBir IL-10$^{-/-}$ embryos were transferred into surrogate CD-1 or C57BL/6 dams harboring distinct complex gut microbial communities. To induce disease, pups were inoculated with *Helicobacter hepaticus* at 24 and 26 days of age. Colonic and cecal lesion scores as well as changes in microbiota were evaluated at 111 days of age using histopathology and microbial 16S rRNA amplicon sequencing respectively. Disease severity was significantly decreased in mice colonized with the GM derived from mice from Charles River Laboratories (GMCRL) as compared to mice colonized with the GM from The Jackson Laboratory mice (GMJAX) or Taconic Bioscience (GMTAC). Furthermore, several physiologically relevant bacterial species were found to be altered in all groups dependent on which surrogate dam was used for rederivation.

Materials and Methods

Mice

The current study was conducted in accordance with the guidelines set forth by the Guide for the Care and Use of Laboratory Animals and the Public Health Service Policy on Humane Care and Use of Laboratory Animals. All studies and protocols were approved by the University of Missouri Institutional Animal Care and Use Committee.

For embryo transfer (ET) recipients, eight to ten week old female C57BL/6J (The Jackson Laboratory, Bar Harbor, ME), C57BL/6NTac (Taconic Biosciences, Inc., Cambridge, IN facilities), and Crl:CD1 (Charles River Laboratories, Wilmington, MA) mice were purchased and allowed to acclimate for one week prior to use. Embryos from 8 week-old female B6.129P2-*Il10*^{tm1Cgn}/J (B6 IL-10$^{-/-}$) and C3Bir.129P2(B6)-Il10^{tm1Cgn}/J (C3H IL-10$^{-/-}$) (The Jackson Laboratory) mice were harvested from colonies maintained on site. Vasectomized, eight to ten week old Crl:CD1 male mice (Charles River Laboratories) were co-housed to induce pseudopregnancy and intrauterine embryo transfer was performed. All mice were housed in microisolator cages on ventilated racks (Thoren, Hazelton, PA) on a 14:10 light dark cycle, and provided *ad libitum* access to 5058 irradiated breeder chow (LabDiet, St. Louis, MO) and acidified autoclaved water.

Embryo collection and transfer

On day 1, embryo donors received IP injection of 5 IU of pregnant mare serum gonadotropin (PMSG) (Calbiochem, San Diego, CA) in 0.2 ml Dulbecco's phosphate-buffered saline (DPBS) with no calcium or magnesium (Life Technologies, Carlsbad, CA) at 2.5 hours post-light induction to induce superovulation. On day 3, at 5 hours post-light induction, embryo donors received an IP injection of 5 IU human gonadotropin (hCG) in 0.2 ml DPBS and were mated to intact males of the same genotype. Surrogate embryo recipient females demonstrating uninduced signs of estrus were mated with a sterile, vasectomized Crl:CD1 male (Charles River Laboratories). Post-mating, B6.129P2-*Il10*^{tm1Cgn}/J, C3Bir.129P2(B6)-Il10^{tm1Cgn}/J, or Crl:CD1 embryo donors were euthanized and embryos were collected aseptically. Briefly, the peritoneal cavity was

opened and the reproductive tract visualized. Oviducts were excised and placed in 50µl of pre-warmed type IV-S hyaluronidase (Sigma, St. Louis) reconstituted at 1mg/ml in HEPES media (Sigma) supplemented with 4 mg/ml bovine serum (Sigma) for five to ten minutes. Clutches of embryos were released from oviducts with gentle manipulation under a dissecting microscope, and collected with a sterile glass hand-pipette. Surrogate females (Crl:CD1, Charles River Laboratories; C57BL/6J, The Jackson Laboratory; C57BL/6NTac, Taconic Biosciences, Inc., Cambridge, IN facilities) were inspected for copulatory plugs and plug-positive mice were used for embryo transfer. For the latter, surrogate females were anesthetized via IM injection of ketamine/xylazine cocktail at 5.5 mg and 1 mg per 100 g body weight respectively, and placed in sternal recumbency. A dorsal midline incision was made and the uterine oviducts located by dissecting through the retroperitoneal muscle. Embryos in 3 to 5 µl of media were injected into the oviducts using a glass hand-pipette. Skin incisions were closed with sterile surgical staples and mice received a subcutaneous injection of 2.5 mg/kg of body weight flunixin meglumine (Banamine®) prior to recovery on a warming pad.

Generation of CD1 GMCRL, GMJAX, and GMTAC colonies

We also sought to establish colonies of outbred mice harboring distinct complex microbiota that is naturally occurring gin contemporary rodent producers. Doing so would facilitate future CMTR studies as outbred mice have greatly improved reproductive indices. To this end, eight to ten week old female C57BL/6J (The Jackson Laboratory), C57BL/6NTac (Taconic Biosciences, Inc.), and Crl:CD1 (Charles River Laboratories) mice were purchased and allowed to acclimate for one week prior to use.

Embryos from eight week old Crl:CD1 (Charles River Laboratories) mice were harvested from colonies maintained on site. Vasectomized, eight to ten week old Crl:CD1 male mice (Charles River Laboratories) were co-housed to induce pseudopregnancy and intrauterine embryo transfer was performed. Offspring from surrogate dams were mated using an outbred mating scheme and individual colonies with targeted GM were maintained for two generations. Second generation eight to ten week old females were used for rederivation of B6.129P2-*Il10*^{tm1Cgn}/J (B6 IL-10$^{-/-}$) mice.

Bacterial cultivation and inoculation

Helicobacter hepaticus (MU94) was grown on 5% sheep blood agar plates (Becton Dickinson, Franklin Lakes, NJ) overlaid with 5 ml *Brucella* broth (Becton Dickinson) supplemented with 5% fetal bovine serum (Sigma-Aldrich, St. Louis, MO) and incubated for 24 hours at 37ºC in a microaerobic chamber with 90%N_2, 5%H_2, and 5%CO_2 gas mixture. Twenty-four hours later, cultures were transferred to 250 ml Erlenmeyer flasks containing *Brucella* broth supplemented with 5% fetal bovine serum and incubated for an additional 48 hours. Immediately prior to use, cultures were observed microscopically for viability. Experimental mice were intra-gastrically gavaged at 23 and 25 days of age with 10^8 bacteria suspended in 0.5 ml *Brucella* broth.

qPCR of *Helicobacter hepaticus*

DNA was extracted from cecal contents to determine the relative abundance of *H. hepaticus* in rederived mice using qPCR analysis and previously described *Helicobacter hepaticus* primers (132). Briefly, samples were assayed in triplicate in 10 µL reactions that each contained 0.25 µL of each primer, 5 µL QuantiTect SYBR Green PCR Master

Mix (BioRad, Hercules, CA), 2.75 µL nuclease-free water, and 2 µL sample DNA. Reactions were amplified in a real-time thermocycler (C1000 Touch Thermal Cycler CFX384 Real Time system, BioRad) using the following parameters: incubation at 95ºC for 15 min, 15 s of denaturation at 94ºC (40 cycles), 20 s of annealing at 58ºC, and 30 s of extension at 72ºC. Fluorescence was monitored at the end of each extension phase (BioRAD CFX Manageer 3.1, Biorad). Technical replicates were averaged and fold change of each GM group was compared to *H. hepaticus* expression in the GMCRL group.

Evaluation of Cecal and Colonic Disease

At 111±2 days of age, experimental mice were euthanized by CO_2 asphyxiation, and necropsy was performed. The entire gastrointestinal tract was removed and the colon length from cecal attachment to anus was measured. The cecum was incised longitudinally, and cecal contents were removed and placed in a sterile 2 ml round bottom tube. Samples were flash frozen in liquid nitrogen and stored at -80ºC until processed for DNA extraction. Cecal tissue was rinsed with sterile saline and laid flat, serosal surface down, on a small section of white note card. The colon was removed and rinsed with sterile saline. Tissues were immersed in 10% buffered formalin for 48 hours and processed for hematoxylin and eosin staining. Histological evaluation was performed by a rodent pathologist, blinded to the identity of the animal's experimental group.

Scoring of cecal and colonic lesions

Tissues were evaluated for disease using a scoring system previously adapted by our lab (133). Detailed evaluation of the severity of epithelial hyperplasia (0, none; 1,

mild; 2, moderate, 3, severe with crypt branching and/or herniation; 4, dysplasia) and inflammatory changes (0, no inflammation 1, mild inflammation limited to the mucosa; 2, moderate inflammation limited to the mucosa and submucosa; 3, severe inflammation with obliteration of normal architecture, erosions, crypt abscesses; and 4, severe inflammatory changes with ulceration). In addition, a separate score for the longitudinal extent of epithelial hyperplasia and inflammation was assigned (0, no significant changes; 1, one or two foci occupying less than 10% of the mucosa; 2, multifocal lesions occupying 10-60% of the mucosa; 3, diffuse lesions occupying greater than 60% of the mucosa). The final lesion score was calculated as (hyperplasia score × longitudinal extent of hyperplasia score) + (inflammation score × longitudinal extent of inflammation score). Total disease scores ranged from 0 (no disease) to 24 (severe disease).

Isopropanol DNA extraction of cecal contents

DNA extraction was performed as previously described (114). Briefly, cecal contents were thawed at room temperature and a sterile 0.5 cm diameter stainless steel bead and 800 µl of lysis buffer were added to the 2 ml round-bottom tube. Samples were mechanically disrupted using a TissueLyser II (Qiagen, Venlo, Netherlands) for 3 minutes at 30 Hz, followed by incubation at 70ºC for 20 minutes with periodic vortexing. Samples were centrifuged at 5000 × g for 5 minutes, and the supernatant was transferred to a sterile 1.5 ml Eppendorf tube containing 200 µl of 10mM ammonium acetate. Lysates were vortexed, incubated on ice for 5 minutes, and then centrifuged. Supernatant was transferred to a sterile 1.5 ml Eppendorf tube and one volume of chilled isopropanol was added. Samples were incubated on ice for 30 minutes and centrifuged at 16000 × g

at 4ºC for 15 minutes. The DNA pellet was washed with 70% ethanol and resuspended in 150 µl Tris-EDTA, followed by addition of 15 µl of proteinase K and 200 µl AL buffer (DNeasy Blood and Tissue kit, Qiagen). Samples were incubated at 70ºC for 10 minutes and 200 µl of 100% ethanol was added to the tubes. Samples were mixed by gentle pipetting and the contents transferred to a spin column from the DNeasy kit (Qiagen). The DNA was further purified following the manufacturer's instructions and eluted in 200 µl EB buffer (Qiagen). DNA concentrations were determined fluorometrically (Qubit dsDNA BR assay, Life Technologies, Carlsbad CA) and samples were stored at 20ºC until sequencing.

Library Construction and 16S rRNA sequencing

Library construction and sequencing was performed at the University of Missouri DNA Core. Bacterial 16SrRNA amplicons were generated in a multiplexed (96-well) format using amplification of the V4 hypervariable region of the 16S rRNA gene, and then sequenced on the Illumina MiSeq platform as previously described (114). Samples returning greater than 10,000 reads were deemed to have successful amplification.

Informatics analysis

Assembly, binning, and annotation of DNA sequences were performed at the University of Missouri Informatics Research Core Facility. Briefly, contiguous DNA sequences were assembled using FLASH software (115), and culled if found to be short after trimming for a base quality less than 31. Qiime v1.8 (116) software was used to perform *de novo* and reference-based chimera detection and removal, and remaining contiguous sequences were assigned to operational taxonomic units (OTUs) using a

criterion of 97% nucleotide identity. Taxonomy was assigned to selected OTUs using BLAST (117) against the Greengenes database (118) of 16SrRNA sequences and taxonomy.

Statistical Analysis

Statistical analysis was performed using Sigma Plot 13.0 (Systat Software Inc., Carlsbad CA). Differences in lesion score, phylum, and OTU relative abundance were determined using two-way ANOVA with sex and GM profile (i.e., GMJAX, GMTAC, GMCRL) as the independent variables, followed by Student Newman-Keuls post hoc test. To account for multiple testing, OTUs with a p value <0.01 were considered statistically significant. Statistical differences in Chao1 index, colon length, and relative abundance of *H. hepaticus* following quantitative PCR were first evaluated using two-way ANOVA to assess main effects and interactions between sex and GM profile. No main effects were detected between male and female mice in any of those values, thus data from male and female mice were pooled and all subsequent analyses was performed using one-way ANOVA with Student Newman-Keuls post hoc test. Tests with a p value <0.05 were considered statistically significant. For gut microbiota analysis, OTUs with less than 10,000 reads were excluded from the data set. Bar graphs were generated with Microsoft Excel (Microsoft, Redmond WA) and principal component analysis (PCA) was generated using Paleontological Statistics Software Package (PAST) 3.12 (122). All groups were visually inspected for descriptive analysis of consistency between animals (bar graphs) or clustering of animals within groups (PCAs). Statistical testing for

differences in beta-diversity was performed via PERMANOVA, implemented using PAST 3.12.

Results

IL-10$^{-/-}$ mice with GMCRL have decreased typhlocolitis severity

In order to determine the impact of differing complex GM communities on disease severity, B6 IL-10$^{-/-}$ embryos were transferred to surrogate dams purchased from three different vendors (Figure 4.1). Surrogate dams were allowed to naturally deliver and raise pups. To induce disease, weanling pups were inoculated with *Helicobacter hepaticus* at 24 and 26 days of age. Experimental mice were euthanized at 111 days of age and the cecum and colon were removed for gross evaluation of colon length and histopathologic assessment of disease severity. Grossly, mice rederived in surrogate dams harboring Taconic GM (hereafter referred to as GMTAC) had significantly decreased colon length when compared to mice rederived in surrogate dams with either GMCRL (Charles River Laboratories) or GMJAX (The Jackson Laboratory) microbiota profiles (Figure 4.2A). To further evaluate disease severity, histopathologic scoring of lesions in the colon and cecum was performed. Rederived B6 IL-10$^{-/-}$ mice harboring GMCRL had significantly lower mean lesion scores in both the colon (Figure 4.2C) and cecum (Figure 4.2E) as compared to mice colonized with GMJAX and GMTAC. In addition, mice rederived to surrogate dams with GMJAX had lower cecal lesion scores than mice rederived to surrogate dams with GMTAC. No differences in lesion severity were detected between male and female mice in any of the GM groups examined.

To determine if these findings were unique to the IL-10$^{-/-}$ model on a C57BL/6 genetic background, C3H IL-10$^{-/-}$embryos were implanted in surrogate dams from the same vendors as used in the B6 IL-10$^{-/-}$experiment. In the C3H IL-10$^{-/-}$ model, mice rederived in surrogate dams with either GMJAX or GMTAC had significantly shorter colon length than mice rederived in surrogate dams with GMCRL (Figure 4.2B), while no statistical difference in colon length was found between the GMJAX and GMTAC groups. As in the B6 genetic background, mice rederived in surrogate dams with GMCRL had significantly lower mean lesion scores in both the colon (Figure 4.2D) and cecum (Figure 4.2F) than either the GMJAX or GMTAC groups, with differences in mean lesion score also detected between mice harboring GMJAX and GMTAC. Again, no differences were found in lesion severity between males and females in the GM groups examined.

Diversity and composition of GM profiles differ following disease onset.

To evaluate the contribution of the GM in the differential disease severity observed between mice, cecal contents were characterized via sequencing of the V4 hypervariable region of the 16S rRNA gene. Decreases in microbial diversity have been associated with susceptibility to inflammation and may be indicative of IBD disease severity. In the B6 IL-10$^{-/-}$ model, mice rederived in surrogate dams with GMCRL had a statistically higher mean Chao1 index, indicating a more diverse cecal microbial composition, than either the GMJAX or GMTAC groups (Figure 4.3A). In addition, the GMTAC group had a greater mean Chao1 index than the GMJAX group. However, in the C3H IL10$^{-/-}$ model, the GMCRL group had a lower mean Chao1 index than either the

GMJAX or GMTAC groups respectively (Figure 4.3B). As pups of either genetic background were exposed to similar maternal microbes at birth, these differences in microbial diversity following disease induction suggest that there is an interaction between host genetic background and GM profile in shaping microbial diversity.

To evaluate β-diversity among rederivation groups, principal component analysis (PCA) was performed. In PCA, samples that are similar in microbial composition cluster together. In the B6 IL-$10^{-/-}$ model, PCA demonstrated that mice harboring GMCRL and GMJAX clustered independently, indicating that these are distinct microbial populations (Figure 4.3C and Table 4.1). In addition, these two groups demonstrate tight within group clustering indicating that animals within individual groups were highly similar. In contrast, the GMTAC group demonstrated greater inter- and intra- group variability along PC1 and PC2 as compared to GMCRL and GMJAX groups, indicating a less uniform microbial composition in those mice. PCAs were also examined in the context of lesion scores and no differences in clustering patterns of high or low lesions scores were noted within any of the GM profile groups (data not shown). In the C3H IL-$10^{-/-}$ model, independent clustering of GMCRL was noted while GMTAC and GMJAX clustered closely together indicating greater compositional similarity between the latter two groups (Figure 4.3D and Table 4.1). The GMCRL and GMTAC groups demonstrated tight intra-group clustering along PC2, with GMJAX mice having increased intra-group variability along PC2.

Differences in phylum and OTU relative abundance between GM profiles.

To identify specific microbial taxa that correlate with resistance or susceptibility to disease, relative abundance of the microbiota at both the phylum and OTU level was compared between GM profiles. In the B6 IL-$10^{-/-}$ model, the phyla *Deferribacteres* and TM7 were enriched in mice of the GMCRL group as compared to mice in GMJAX and GMTAC groups (Figure 4.4A and Table 4.2). In the GMJAX and GMTAC groups, bacteria in the phylum *Proteobacteria* were present in greater relative abundance in mice rederived in GMTAC surrogate dams. Conversely, in the C3H IL-$10^{-/-}$ model, a greater relative abundance of the phylum *Proteobacteria* was detected in mice of the GMCRL group (Figure 4.4B and Table 4.2) as compared to mice in the GMJAX and GMTAC groups. Moreover, the phylum *Deferribacteres* was detected at greater relative abundance in the GMTAC group as compared to GMCRL and GMJAX groups.

Resolved to the level of OTU, differences were detected in the relative abundance of several OTUs detected in all GM profiles (Figure 4.5A and Table 4.3). In the B6 IL$10^{-/-}$ model, several differences were found between GMCRL and the GMJAX and GMTAC groups; specifically, greater relative abundances of family *Rikenellaceae*, order *Bacteroidales, Mucispirillum schaedleri*, family *Clostridiaceae*, family *Peptostreptococcaceae*, family *Ruminococcaceae*, genus *Sutterella*, order RF39, and family F16 were detected (Table 4.3). Mice with the GMJAX profile had a higher relative abundance of *Bacteroides acidifaciens* and genus *Clostridium*. Similarly, in the C3H IL$10^{-/-}$ model, the GMCRL profile had significantly higher levels of family *Mogibacteriaceae*, family *Christensenellaceae*, family *Clostridiaceae*, and genus *Sutterella* relative to the other GM profiles (Figure 4.5B and Table 4.4). In contrast, the

GMJAX group had higher relative abundance of family *Ruminococcaceae* than either the GMCRL or GMTAC groups. Additionally, the GMTAC group both had higher relative abundance of *Mucispirillum schaedleri*, relative to GMJAX. As embryos from both IL-$10^{-/-}$ mouse strains were rederived in the same pools of surrogate dams, the fact that differences between the GM profiles in the relative abundance of certain OTUs was not consistent in both the B6 and C3H strains suggests a differential effect on colonization influenced by genetic background.

While differential disease susceptibility may be a function of differential abundance of specific taxa, it may also be explained by the presence or absence of select taxa unique to each GM profile. Interestingly, in B6 IL$10^{-/-}$ mice, *Alistipes massiliensis*, *Roseburia faecis*, *Clostridium saccharogumia*, and genus *Megamonas* were found in mice rederived in GMCRL dams, whereas *Eubacterium dolichum* was detected only in the GMTAC rederived group. *Aggregatibacter pneumotropica* was only found in GMJAX and GMTAC groups with *Propionibacterium acnes* and genus *Phascolarctobacterium* detected in only GMCRL and GMJAX groups; *Candidatus Arthromitus* (segmented filamentous bacterium), genus *Anaerotruncus* and *Oxalobacter formigenes* were detected in both the GMTAC and GMCRL groups.

In contrast, in the C3H IL$10^{-/-}$ mice, the GMCRL group harbored several unique OTUs including *Prevotella copri*, *Alistipes massiliensis*, family *Paraprevotellaceae*, *Enterococcus casseliflavus*, *Faecalibacterium prausnitzii*, genus *Phascolarctobacterium*, genus *Fusobacterium*, genus *Anaerobiospirillum*, genus *Prevotella*, and genus *Anaerotruncus*. *Parabacteroides distasonis*, family *Porphyromonadaceae*, genus

Enterococcus, genus *Roseburia*, family *Desulfovibrionaceae*, and *Flexispira rappini* were found to overlap between the GMJAX and GMTAC groups; genus *Turicibacter* and family *Peptostreptococcaceae* were detected in both the GMJAX and GMCRL groups; genus *Anaerotruncus* and *Candidatus Arthromitus* were specific to the GMTAC and GMCRL groups. Differences in the presence of these OTUs and their interaction with other OTUs present at significantly different levels may account for observed differences in disease severity.

GM profile affects *Helicobacter hepaticus* colonization.

Helicobacter spp. are thought to be a provocateur of intestinal inflammation and dysbiosis (134, 135) and as such are necessary for the induction of disease in the IL-$10^{-/-}$ model. To determine if the observed differences in lesion score among GM groups could be due to differences in *H. hepaticus* colonization, we performed semi-quantitative real time PCR on cecal bacterial contents. In both B6 IL-$10^{-/-}$ (Figure 4.6A) and C3H IL-$10^{-/-}$ (Figure 4.6B) mice, mice colonized with GMCRL had significantly lower relative abundance of *H. hepaticus* than mic colonized with GMJAX or GMTAC. All mice received the same *H. hepaticus* inoculum post-weaning and are genetically identical, suggesting differences between GM profiles resulted in differing colonization resistance against *H. hepaticus*.

Alterations in disease severity and GM composition independent of surrogate dam genetics and maternal care.

Because the initial complex microbiota targeted rederivation (CMTR) was performed using surrogate dams with varying genetic backgrounds, it is possible that

differences in maternal care, *in* utero environment, or epigenetic factors contributed to the observed differential disease severity. To address this consideration, we established breeding colonies of CD1 dams harboring either the GMCRL, GMJAX, or GMTAC profiles. To do so, CMTR was used to transfer CD1 embryos to three surrogate dams (Crl:CD1, C57BL/6J, and C57BL/6NTac), and thus generate pups with the previously studied GM profiles (Figure 4.7). Offspring were then used to establish three separate breeding colonies using an outbred mating scheme. Colonies were monitored for two generations using next generation sequencing to confirm expected differences in GM composition and complexity. PCA of first and second generation females at 8-10 weeks of age confirmed three distinct GM profiles (Figure 4.8). Second generation females were used as surrogate dams for CMTR of the B6 IL-$10^{-/-}$ strain. As in the previous studies, pups were inoculated with *H. hepaticus* at 24 and 26 days of age and disease severity was assessed at 111 days of age. Grossly, B6 IL-$10^{-/-}$ pups harboring GMCRL had a significantly greater colon length than the GMJAX or GMTAC groups (Figure 4.9A). In addition, GMCRL-colonized pups had lower cecal and colonic histopathologic lesion scores compared to GMJAX and GMTAC groups, in agreement with findings from studies using inbred surrogate dams (Figure 4.9B and Figure 4.9C).

Again confirming the previous findings in the B6 IL-$10^{-/-}$ model, sequencing of cecal contents revealed that the GMCRL group had increased diversity when compared to the GMJAX and GMTAC groups (Figure 4.10A). Moreover, the GMTAC group was more diverse than the GMJAX group. PCA demonstrated that each group maintained three distinct microbial profiles (Figure 4.10B). To further investigate GM composition,

relative abundance at the phylum and OTU level were examined. As in our initial experiments using the B6 IL-10$^{-/-}$ model, there was increased relative abundance of phylum *Proteobacteria* in both the GMJAX and GMTAC groups (Figure 4.11A and Table 4.2). In contrast to our previous findings, there was lower relative abundance of *Deferribacteres* in GMJAXmice, with increased relative abundance observed in GMTAC males. At the OTU level, we found several OTUs which differed between groups and had similar relative abundance patterns as seen in the previous study including *Bacteroides acidifaciens*, family *Rikenellaceae*, order *Bacteroidales*, *Mucispirillum schaedleri*, family *Clostridiaceae*, genus *Clostridium*, and family F16 (Figure 4.11B and Table 4.5). In addition, we found several species within the phyla *Bacteroidetes*, *Firmicutes*, and *Proteobacteria* that differed between groups including genus *Bacteroides*, family *Mogibacteriaceae*, family *Christensenellaceae*, genus rc4-4, order *Clostridiales*, family *Enterobacteriaceae*, and genus *Helicobacter*.

To determine if the observed differences in lesion score among GM groups could be explained by differences in *H. hepaticus* colonization, we performed semi-quantitative real time PCR on cecal contents. As observed in our previous experiments, we found that B6 IL-10$^{-/-}$ mice with GMCRL were colonized with *H. hepaticus* to a lesser degree than mice colonized with either GMJAX or GMTAC profiles (Figure 4.12).

Discussion

With increasing availability of culture-independent technologies, there are abundant studies providing evidence of the importance of the GM in both GI and systemic disease. However, research using human subjects remains confounded by

genetic and environmental variables. The use of mouse models allows longitudinal studies to characterize the GM with careful control of both genetic and environmental variables. Manipulation of individual microbes, or use of GF mice, while useful in certain contexts, is somewhat reductionist and does not take into account the interactions between naturally occurring complex GI populations.

In this study, we demonstrate that complex microbiota targeted rederivation (CMTR) by embryo transfer can be used as a method to study the influence of complex microbial communities in rodent models of disease. We surgically implanted genetically identical embryos, collected from IL-10$^{-/-}$ mice, into surrogate dams harboring different GM varying in composition and complexity to produce IL-10$^{-/-}$ pups colonized with the desired maternal GM profiles. Using these methods, we show that the GM of surrogate dam greatly influences colonic and cecal disease phenotype in both the B6 IL-10$^{-/-}$ and C3H IL-10$^{-/-}$ mouse models. In both genetic backgrounds, IL-10$^{-/-}$ mice born to surrogate dams colonized with GMCRL had longer colon length and lower mean colonic and cecal lesion scores indicating a lower disease phenotype in these animals. In addition, we found that on the B6 background, mice born to GMTAC-colonized surrogate dams had the most severe disease phenotype while mice rederived to GMJAX-colonized surrogate dams had intermediate disease severity. On the C3H background, IL-10$^{-/-}$ mice born to surrogate dams harboring either GMJAX or GMTAC had significantly higher colon and cecal lesion scores relative to mice born to dams colonized with GMCRL. Interestingly, we found that in both IL-10$^{-/-}$ strains tested, the GMCRL group had the lowest relative abundance of *H. hepaticus* in cecal samples. This suggests that the composition of the

bacterial species present in the GMCRL profile may be interfering with *Helicobacter* colonization.

Previous IBD studies have suggested that decreased GI microbial diversity correlates with increased inflammation and disease severity (79, 124, 125). We show that differences in microbial diversity were present between GM groups dependent on surrogate dam used for rederivation and the host genetic background. In the B6 IL-10$^{-/-}$ model, we found increased microbial diversity in the GMCRL group which had the lowest disease score. In contrast, C3H IL-10$^{-/-}$ mice had a decreased diversity in the GMCRL group. This unexpected interaction between genetic background and GM profile may be a reflection of an abnormal innate immune response, as C3H IL-10$^{-/-}$ mice carry a mutation in the TLR4 gene rendering innate immune cells such as macrophages unable to respond to LPS (136, 137).

In both genetic backgrounds tested, we found differences in several physiological bacteria associated with the strain and vendor of the surrogate dams chosen for rederivation which likely contribute to the differences in observed disease severity between groups. In the B6 background, genus *Clostridium,* family *Ruminococcaceae*, and family *Rikenellaceae* were present at significantly lower relative abundance in the GMJAX- and GMTAC-colonized mice, the groups that developed more severe inflammation. In addition, in both genetic backgrounds, we detected lower relative abundance of family *Clostridiaceae*. These data are consistent with previous findings in human patients with confirmed IBD (79, 138-140) suggesting that increased relative abundance of these taxa may contribute to the protection from disease observed in the

GMCRL group. In addition, we found that, in both B6 and C3H mice, there was a greater relative abundance of phylum *Proteobacteria* in the GMJAX and GMTAC profiles, and greater relative abundance of genus *Sutterella*, genus *Bilophila*, and family *Enterobacteriaceae* in the B6 IL-10$^{-/-}$ mice and genus *Sutterella* in the C3H IL-10$^{-/-}$ mice. Increased abundance of these OTUs has also been suggested to play a role in IBD severity in humans (79, 141, 142).

Previous studies have suggested that normal enteric bacteria are essential for the development of chronic intestinal colitis in IL-10$^{-/-}$ mice (76). These mice exhibit varying degrees of disease severity dependent on housing conditions used. Specifically, when housed under germ-free conditions these mice fail to develop colitis whereas specific pathogen-free (SPF) or conventionally housed mice develop chronic colitis. When gnotobiotic IL-10$^{-/-}$ mice are monocolonized with *H. hepaticus* they fail to develop intestinal disease, implicating the role of the normal GM in disease pathogenesis (75). Moreover, differential effects of institutional housing and associated variation in GM composition influences disease severity (143). Taken as a whole, these data underscore the importance of the GM in IBD pathogenesis. However, the mechanism of these bacterial interactions and their role in inducing disease severity remains to be fully explored. CMTR provides a platform to further examine these complex host:GM interactions.

With recent concerns of ensuring animal models of disease are consistent and reproducible it becomes paramount that a clear understanding of the contribution of the GM is clearly defined (120, 128). Along with the inclusion of both sexes, randomization,

and better powered studies, we believe that differences in the GM may also explain some of this poor reproducibility. CMTR allows generation of isogenic mice harboring distinct, well-characterized GM or, alternatively, could be used to generate genetically disparate colonies of mice seeded with the same GM. As such, we feel that CMTR will have a significant impact on the methods used to study the GM contribution to health and disease. While we used this technique in a model of IBD and have also used it successfully in a rat model of colorectal cancer (144), it could be used in any model in which the GM is hypothesized to have an influence.

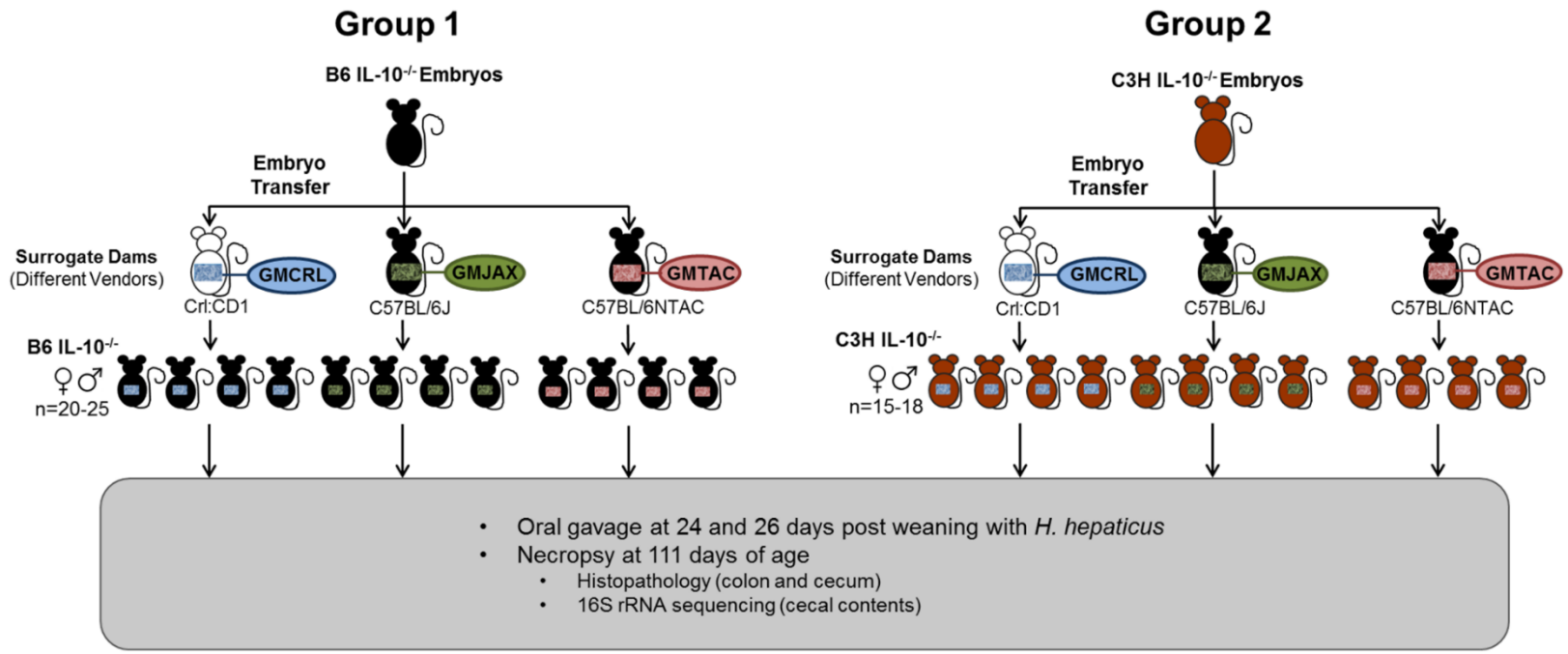

Figure 4.1. Experimental design used to generate IL-10-/- pups with different GI microbiota (GM). Schematic diagram showing embryo transfer scheme used to generate B6.129P2-*Il10*^{tm1Cgn}/J (B6 IL-10$^{-/-}$) and C3Bir.129P2(B6)-Il10^{tm1Cgn}/J (C3H IL-10$^{-/-}$) pups to Crl:CD1$_{gmCRL}$, C57BL/6J$_{gmJAX}$, C57BL/6NTac$_{gmTAC}$ surrogate dams. Pups were inoculated with *H. hepaticus* at 24 and 26 days of age and necropsied at 111 days of age. Cecal contents were submitted for sequencing and cecal and colonic disease evaluated.

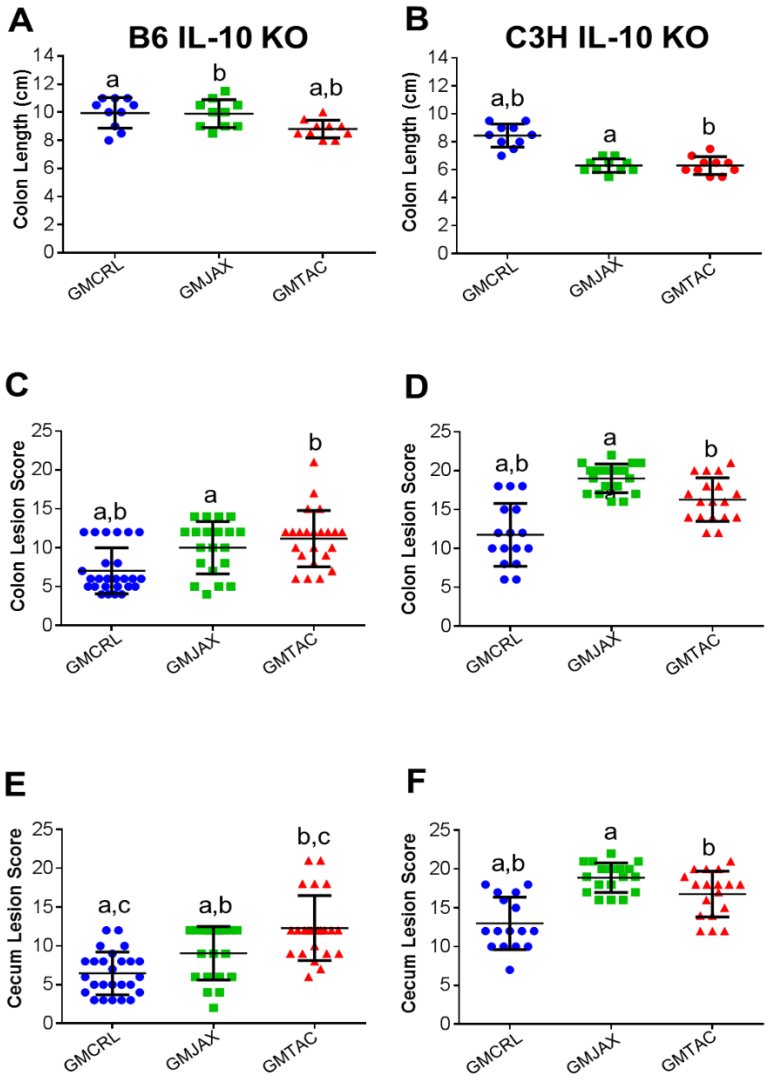

Figure 4.2. Colonic and cecal disease is decreased in male and female mice rederived to GMCRL surrogate dams. Colon length of B6 (A) and C3H (B) IL-10$^{-/-}$ mice with differing gut microbiota profiles: GMCRL (Charles River Laboratories), GMJAX (The Jackson Laboratory), and GMTAC (Taconic); (n = 10 per group). Colon lesion score of B6 (C) and C3H (D) IL-10$^{-/-}$ mice with differing GM profiles (n = 15-25 per group). Cecal lesion score of B6 (E) and C3H (F) IL-10$^{-/-}$ mice with differing GM profiles (n = 15-25 per group). Colon length measured at time of necropsy from cecum to anus. Statistical significance determined by one way-ANOVA with Student Newman-Keuls post hoc test. $p \leq 0.05$ is significant. Colonic and cecal lesion scores based on severity and longitudinal extent of epithelial hyperplasia and inflammation (0 = no disease and 24 = most severe disease). Statistical significance of lesion scores and sex determined using two way-ANOVA with Student Newman-Keuls post hoc test. Bars indicate mean and SEM. $p \leq 0.05$ is significant. Statistical significance between groups annotated by same lower case letters above dot plots.

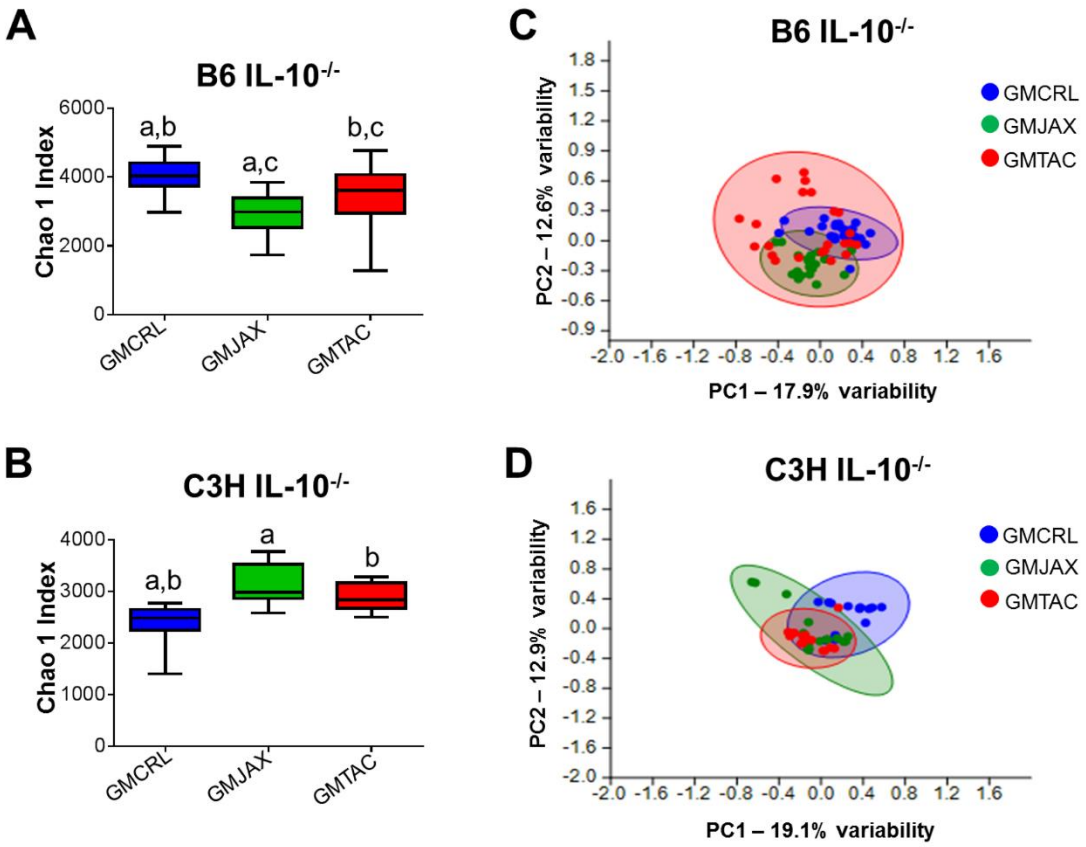

Figure 4.3. Alterations in gut microbiota (GM) diversity and colonization of rederived B6 IL-10-/- and C3H IL-10-/- mice following disease onset. Chao1 estimate of microbial diversity plotted by Tukey box and whisker graph of B6 (A) and C3H (B) IL-10$^{-/-}$ rederived mice (n = 15-25 mice per group). Statistical significance determined by one-way ANOVA with Student Newman-Keuls post hoc test. $p \leq 0.05$ is significant. Statistical significance between groups annotated by same lower case letters above box plots. Unweighted principal component analysis (PCA) of B6 (C) and C3H (D) IL-10$^{-/-}$ rederived mice (n = 15-25 mice per group). Blue circles = GMCRL; green circles = GMJAX; and red circles = GMTAC. Statistical significance determined by one-way PERMANOVA. p <0.001 is significant.

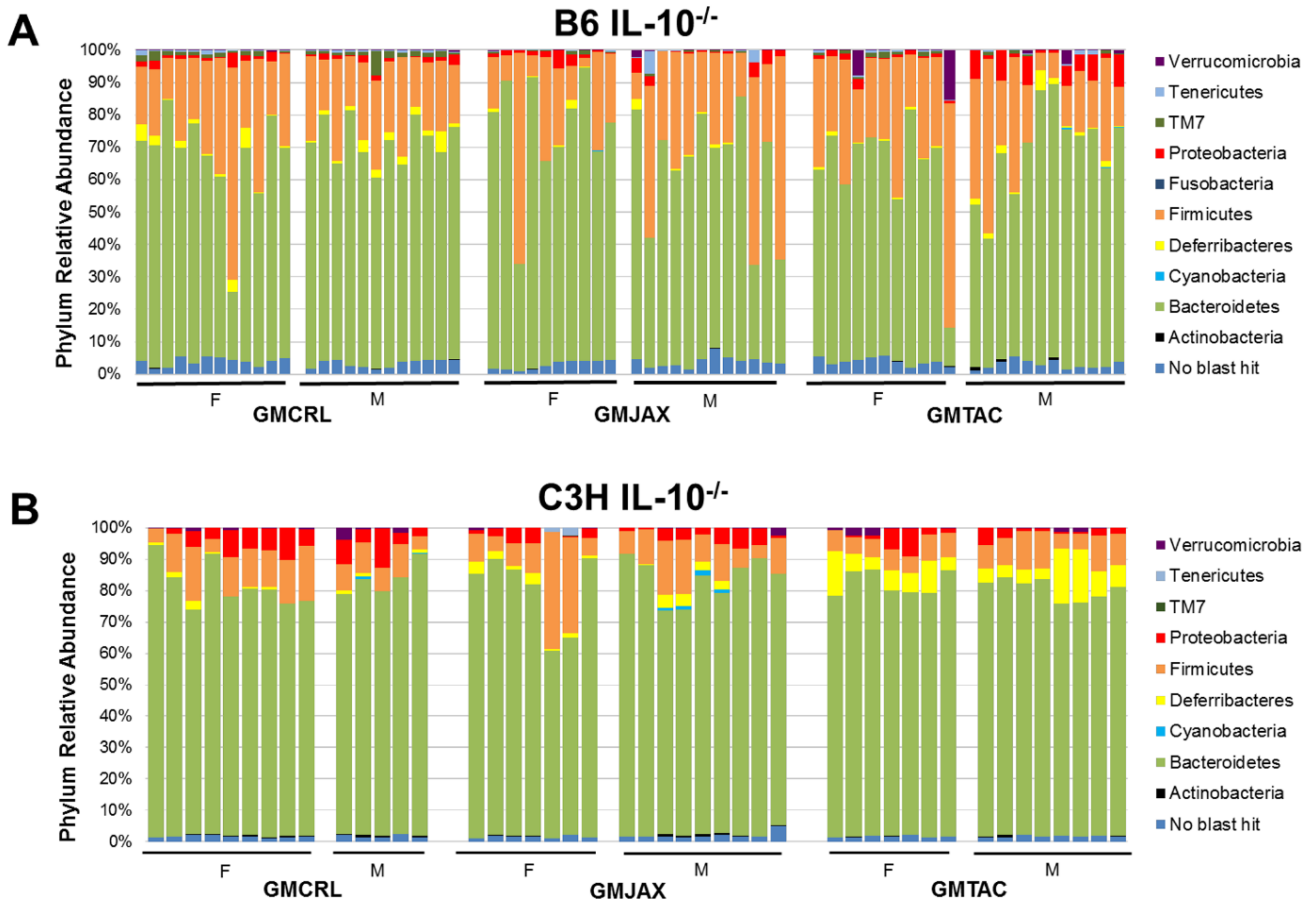

Figure 4.4. Relative abundance of rederived groups at taxonomic level of phylum. B6 (A) and C3H (B) IL-10$^{-/-}$ mice (n = 15-25 mice per group). Legend of each phyla group is shown at the right.

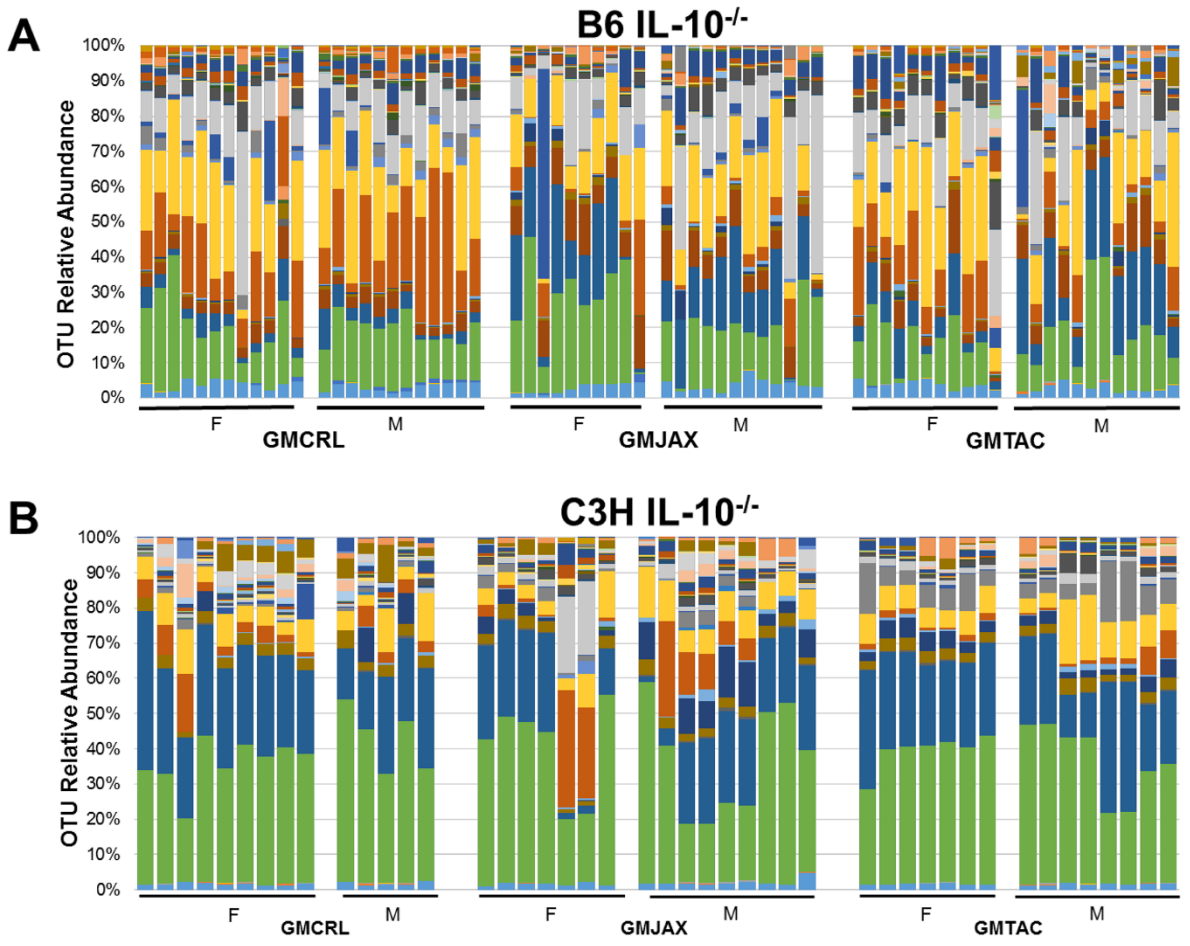

Figure 4.5. Relative abundance of rederived groups at taxonomic level of operational taxonomic unit (OTU). B6 (A) and C3H (B) IL-10$^{-/-}$ mice (n = 15-25 mice per group).

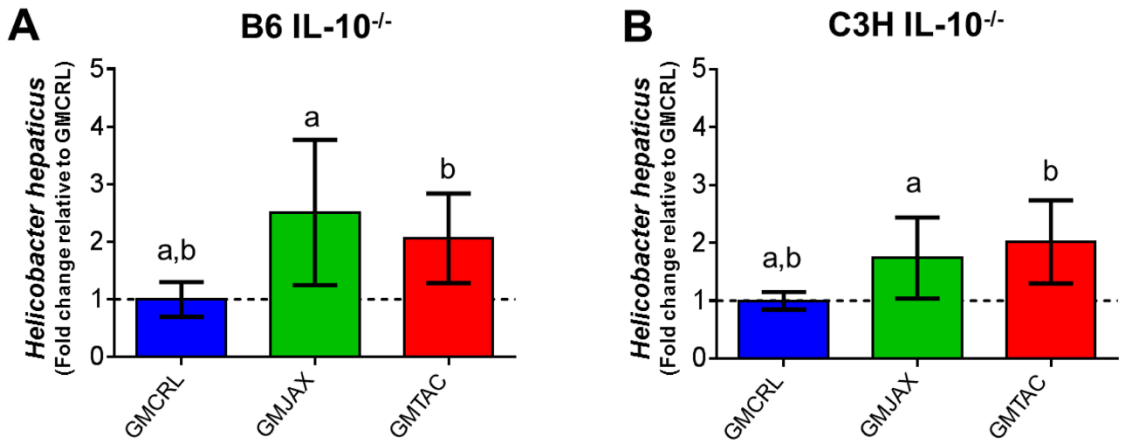

Figure 4.6. Relative abundance of *Helicobacter hepaticus* within rederived groups in B6 IL-10-/- and C3H IL-10-/- mice. B6 (A) and C3H (B) IL-$10^{-/-}$ rederived mice (n = 15-25 mice per group). Statistical significance determined by one-way ANOVA with Student Newman-Keuls post test. Bars represent SEM. $p \leq 0.05$ is significant. Statistical significance between groups annotated by same lower case letters above bar charts.

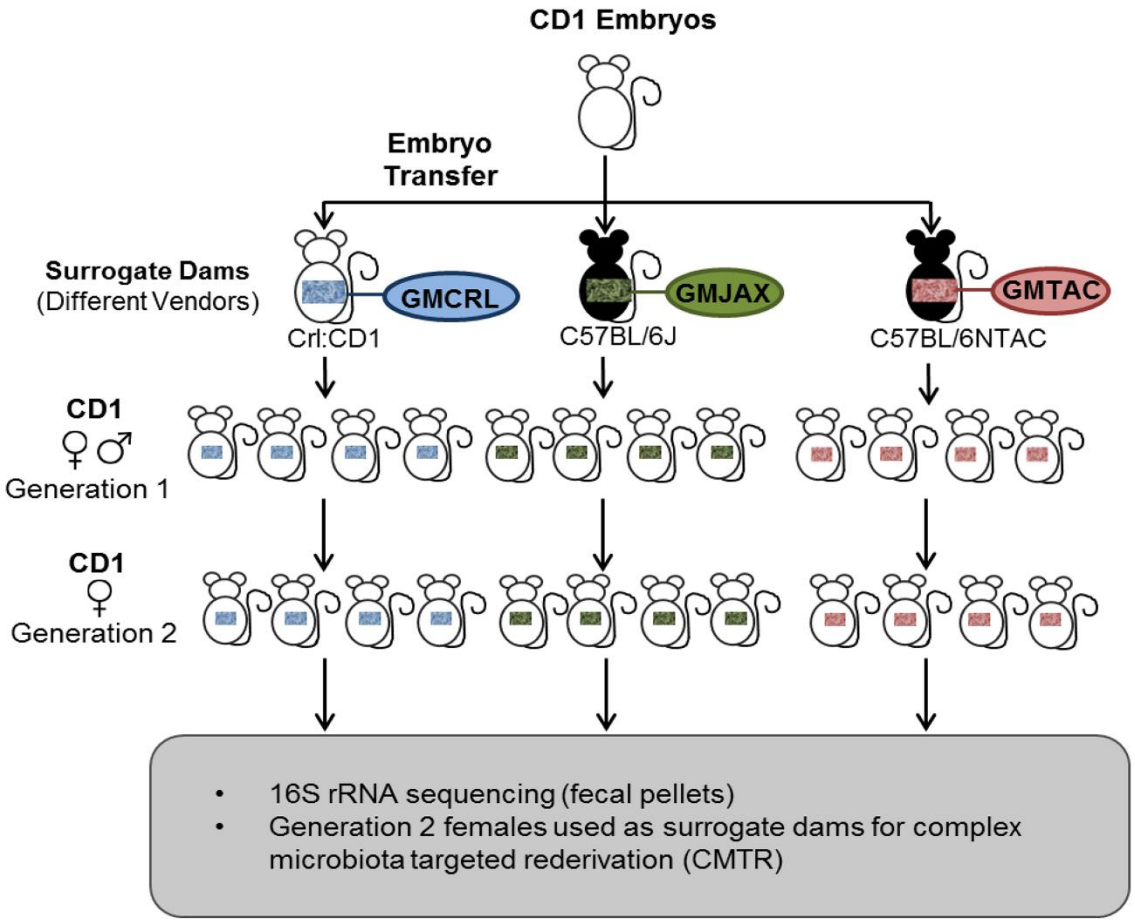

Figure 4.7. Experimental design used to generate CD1 mice with different gut microbiota (GM). Schematic diagram showing embryo transfer scheme use to rederived CD1 mice to Crl:CD1$_{GMCRL}$, C57BL/6J$_{GMJAX}$, C57BL/6NTac$_{GMTAC}$ surrogate dams. At maturity pups were mated using an outbred mating scheme and maintained as a breeding colony for two generations. Second generation 8-10 week old females were used for subsequent complex microbiota targeted rederivation (CMTR) of B6 IL-10$^{-/-}$ mice.

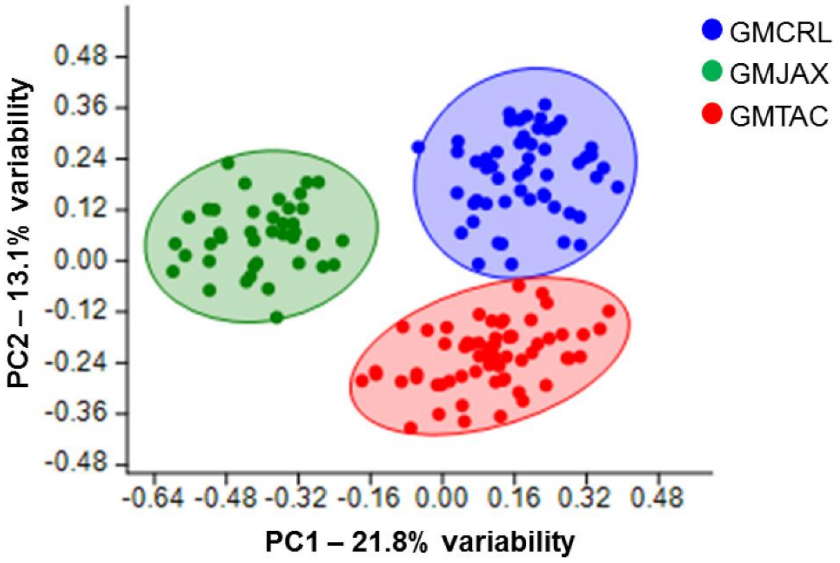

Figure 4.8. Principal component analysis of the gut microbiota (GM) of rederived CD1 mice. Representative samples from 1st and 2nd generation females at 8-10 weeks of age. n = 45-50. Blue circles = GMCRL; green circles = GMJAX; and red circles = GMTAC.

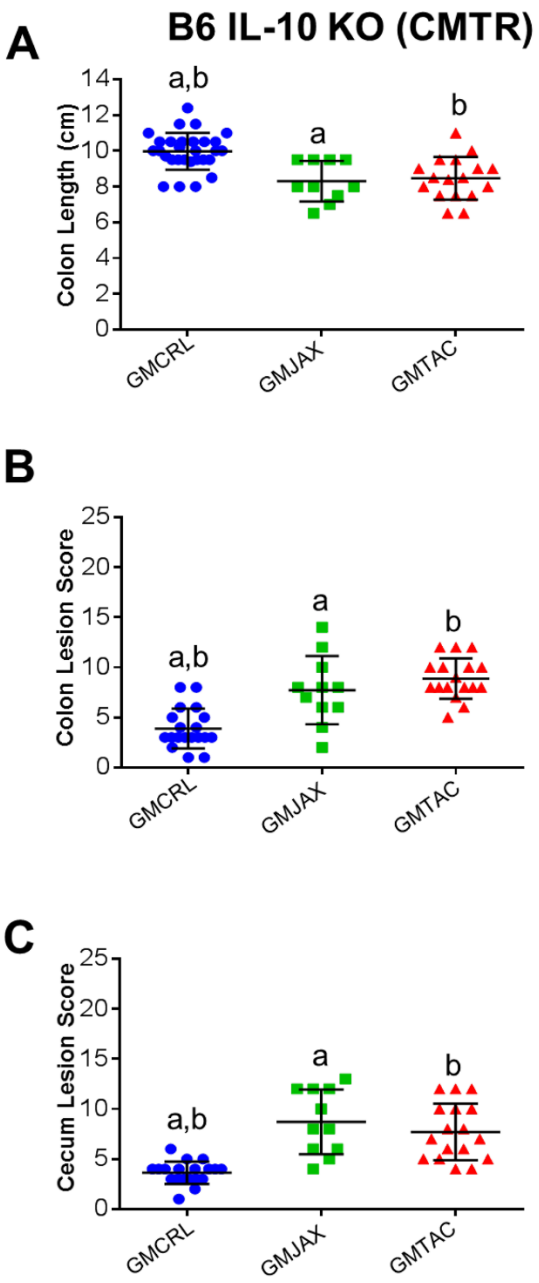

Figure 4.9. Colonic and cecal disease is decreased in B6 IL-10-/- mice following CMTR to CD1GMCRL surrogate dams. Colon length (A), colon lesion score (B), and cecal lesion score (C) of B6 IL-10$^{-/-}$ mice with different gut microbiota (GM). Statistical significance determined by one-way ANOVA with Student Newman-Keuls post test. Bars indicate mean and SEM. $p \leq 0.05$ is significant. Statistical significance between groups annotated by same lower case letters above dot plots.

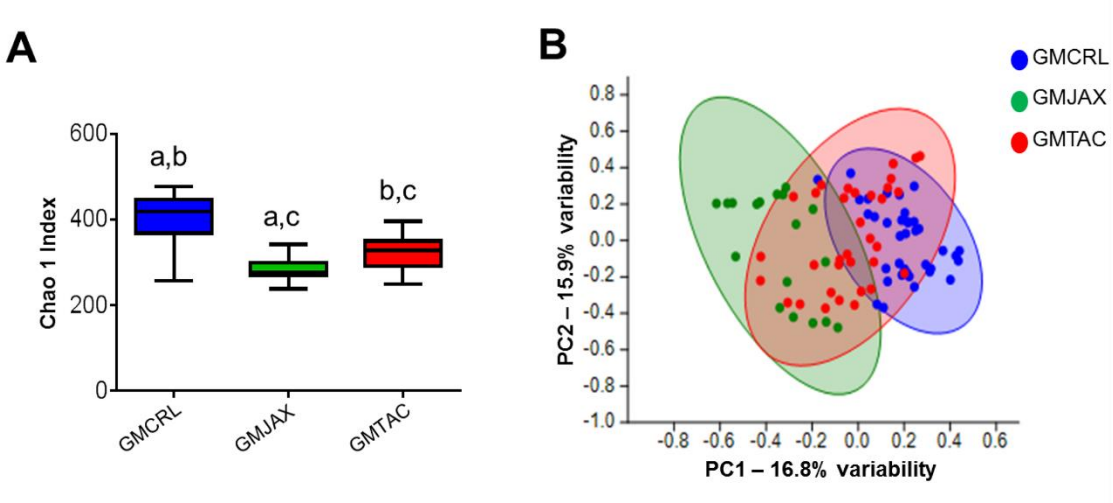

Figure 4.10. Alterations in gut microbiota (GM) diversity and colonization in B6 IL-10-/- mice following CMTR to CD1 surrogate dams. (A) Chao1 estimate of microbial diversity plotted by Tukey box and whisker graph of B6 IL-10$^{-/-}$ rederived mice (n = 15-25 mice per group). Statistical significance determined by one-way ANOVA with Student Newman-Keuls post test. $p \leq 0.05$ is significant. Statistical significance between groups annotated by same lower case letters above bar charts. Unweighted principal component analysis (PCA) of B6 IL-10$^{-/-}$ rederived mice (n = 15-25 mice per group). Blue circles = GMCRL; green circles = GMJAX; and red circles = GMTAC. Statistical significance determined by one-way PERMANOVA. p <0.001 is significant.

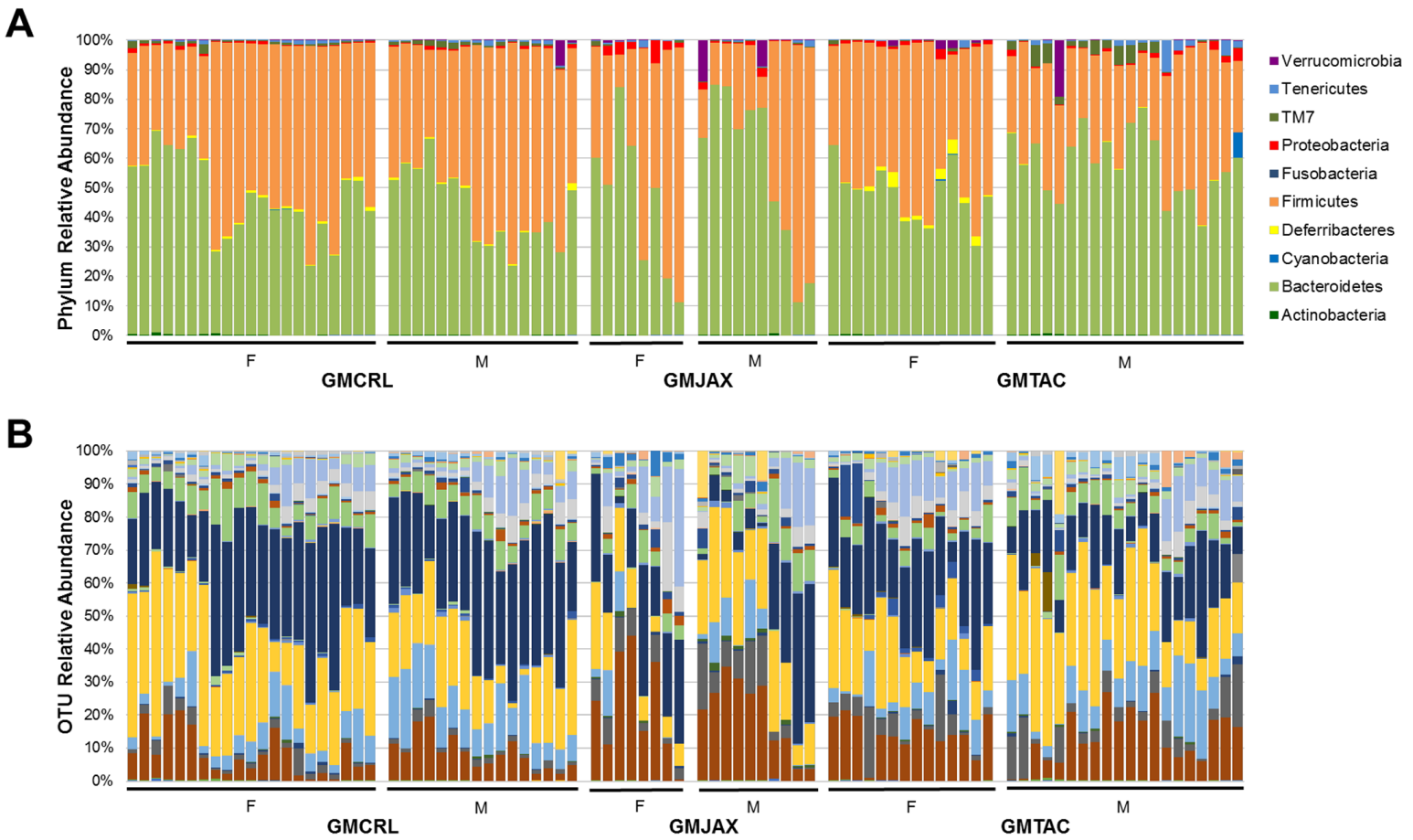

Figure 4.11. Relative abundance of B6 IL-10-/- mice following CMTR to CD1 surrogate dams at taxonomic level of phylum and operational taxonomic unit (OTU). A) Bar charts of relative abundance of phyla. Legend of phyla shown at right. B) Bar charts of relative abundance of OTU. n = 20–35 per group.

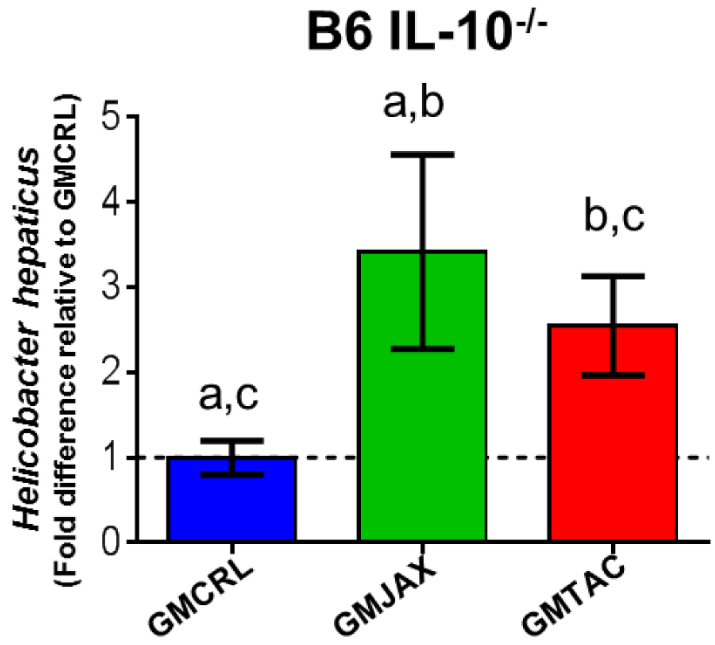

Figure 4.12. Relative abundance of *Helicobacter hepaticus* colonization of B6 IL-10-/- mice following CMTR to CD1 surrogate dams. Statistical significance determined by one-way ANOVA with Student Newman-Keuls post test. $p \leq 0.05$ is significant. Statistical significance between groups annotated by same lower case letters above bar charts. n = 20–35 per group.

Mouse Model	GMJAX relative to GMCRL		GMJAX relative to GMTAC		GMTAC relative to GMCRL	
	p-value	F-value	*p*-value	F-value	*p*-value	F-value
B6 IL-10$^{-/-}$	**0.0001**	7.076	**0.0182**	8.466	**0.0017**	10.517
C3H IL-10$^{-/-}$	**0.0188**	9.97	**0.0176**	6.989	**0.0001**	8.586
B6 IL-10$^{-/-}$ (CMTR)	**0.001**	9.735	**0.0299**	7.728	**0.001**	7.329

Table 4.1. PERMANOVA analysis of Bray-Curtis dissimilarities for bacterial OTU community structure in relation to rederivation GM group. *p*-values are based on 9999 permutations with the lowest possible *p*-value of 0.0001. Bold face values indicate statistical significance ($p \leq 0.05$).

Significant Phylum		GMJAX relative to GMCRL		GMJAX relative to GMTAC		GMTAC relative to GMCRL		GMCRL	GMJAX	GMTAC
Mouse Model	**Phylum**	***p*-value**	**Mean Fold Change**	***p*-value**	**Mean Fold Change**	***p*-value**	**Mean Fold Change**	**Mean Relative Abundance (±SEM)**	**Mean Relative Abundance (± SEM)**	**Mean Relative Abundance (± SEM)**
B6 IL-10$^{-/-}$	*Deferribacteres*	**<0.001**	0.256	0.248	0.509	0.013	0.510	0.021 ±0.003	0.005 ±0.001	0.01 ±0.002
	Proteobacteria	0.580	1.24	**0.01**	0.540	**0.01**	0.764	0.014 ±0.002	0.017 ±0.003	0.032 ±0.007
	TM7	**<0.001**	0.176	**0.003**	0.447	**0.008**	0.379	0.015 ±0.003	0.003 ±0.0001	0.006 ±0.0001
C3H IL-10$^{-/-}$	*Deferribacteres*	0.386	1.923	**<0.001**	0.226	**<0.001**	9.904	0.008 ± 0.002	0.017 ±0.004	0.078 ±0.01
	Proteobacteria	**0.008**	0.477	0.446	1.148	**0.01**	0.437	0.06 ±0.009	0.029 ±0.005	0.025 ±0.007
B6 IL-10$^{-/-}$ (CMTR)	*Deferribacteres*	0.050	**0.001**	**0.004**	0.001	0.104	1.592	0.005 ±.0007	3.36E-06 ±1.85E-06	0.008 ±0.002
	Proteobacteria	**<0.001**	3.195	0.033	1.624	**0.006**	1.967	0.005 ±0.0006	0.018 ±0.004	0.011 ±0.001
	TM7	0.120	0.294	**0.006**	0.163	0.047	1.802	0.009 ±0.001	0.003 ±0.0008	0.016 ±0.003

Table 4.2. Statistical comparison of the relative abundance of phyla between rederivation groups within the B6 IL-10-/- and C3H IL-10-/- models. *p*-value, mean fold change, and mean relative abundance are shown. Statistical significance and interactions of GM profile, sex, and OTU were determined using two-way ANOVA with Student Newman-Keuls post test. Bold face values indicate statistical significance ($p \leq 0.01$).

Significant OTUs in B6 IL-10$^{-/-}$ Model		GMJAX relative to GMCRL		GMJAX relative to GMTAC		GMTAC relative to GMCRL		GMCRL	GMJAX	GMTAC
Phylum	**OTU**	***p*-value**	**Mean Fold Change**	***p*-value**	**Mean Fold Change**	***p*-value**	**Mean Fold Change**	**Mean Relative Abundance (±SEM)**	**Mean Relative Abundance (±SEM)**	**Mean Relative Abundance (±SEM)**
Bacteroidetes	*Bacteroides acidifaciens*	**<0.001**	2.824	0.415	1.121	**<0.001**	2.523	0.053 ±0.009	0.149 ±0.021	0.0002 ±1.0E-05
Bacteroidetes	Family *Rikenellaceae*	**<0.001**	0.224	0.067	0.439	**0.002**	0.510	0.165 ±0.0219	0.037 ±0.014	0.091 ±0.012
Bacteroidetes	Order Bacteroidales	0.127	0.455	0.165	9.056	**0.008**	0.050	0.004 ±0.0009	0.002 ±0.0001	0.0002 ±0.0001
Deferribacteres	*Mucispirillum schaedleri*	**<0.001**	0.179	0.134	0.356	**0.010**	0.502	0.021 ±0.003	0.004 ±0.001	0.0105 ±0.003
Firmicutes	Family *Clostridiaceae*	**<0.001**	0.224	0.506	2.336	**<0.001**	0.096	0.009 ±0.0001	0.002 ±6.1E-05	8.3E-05 ±2.2E-05
Firmicutes	Family *Peptococcaceae*	**0.003**	1.527	**<0.001**	0.000	0.310	1.288	0.0002 ±2.71E-05	0.000 ±0.000	0.0002 ±5.2E-05
Firmicutes	Family *Peptostreptococcaceae*	**0.007**	0.198	0.624	3.07	**0.003**	0.0644	0.0012 ±0.0004	0.002 ±9.5E-05	7.9E-05 ±6.5E-05
Firmicutes	Family *Ruminococcaceae*	**<0.001**	0.473	**0.002**	0.503	0.649	0.941	0.021 ±0.001	0.001 ±0.002	0.019 ±0.003
Firmicutes	Genus *Allobaculum*	0.966	0.790	0.017	0.073	**0.004**	10.778	0.0004 ±0.0001	0.003 ±0.0002	0.004 ±0.001
Firmicutes	Genus *Clostridium*	0.238	1.474	**0.009**	20.55	**0.044**	0.096	0.0007 ±0.0002	0.001 ±0.0003	5.1E-05 ±2.4E-05
Proteobacteria	Genus *Bilophila*	*	0.000	**<0.001**	0.0002	**<0.001**	0.000	0.000 ±0.000	1.0E-05 ±1.0E-06	0.007 ±0.002
Proteobacteria	Genus *Sutterella*	0.446	0.399	**0.007**	0.137	0.013	2.916	0.006 ±0.001	0.002 ±0.0008	0.016 ±0.005
Tenericutes	Order RF39	**<0.001**	0.036	**0.005**	0.066	**0.002**	0.547	0.005 ±0.0007	0.0002 6.9E-05	0.003 ±0.0006
TM7	Family F16	**<0.001**	0.197	0.302	0.474	**0.005**	0.415	0.0137 ±0.002	0.003 ±0.0008	0.006 ±0.001

Table 4.3. Statistical comparison of the relative abundance of OTUs between rederivation groups within the B6 IL-10-/- model. *p*-value, mean fold change, and mean relative abundance are shown. Statistical significance and interactions of GM profile, sex, and OTU were determined using two-way ANOVA with Student Newman-Keuls post test. Bold face values indicate statistical significance ($p \leq 0.01$). *Statistical comparison not applicable due to 0.000 OTU relative abundance.

Significant OTUs in C3H IL-10$^{-/-}$ Model		GMJAX relative to GMCRL		GMJAX relative to GMTAC		GMTAC relative to GMCRL		GMCRL	GMJAX	GMTAC
Phylum	**OTU**	***p*-value**	**Mean Fold Change**	***p*-value**	**Mean Fold Change**	***p*-value**	**Mean Fold Change**	**Mean Relative Abundance (±SEM)**	**Mean Relative Abundance (±SEM)**	**Mean Relative Abundance (±SEM)**
Deferribacteres	*Mucispirillum schaedleri*	0.384	2.235	**<0.001**	0.225	**<0.001**	9.338	0.0078 ±0.002	0.017 ±0.004	0.078 ±0.012
Firmicutes	Family *Mogibacteriaceae*	**<0.001**	0.099	0.671	2.715	**<0.001**	0.038	0.011 ±0.002	0.001 ±0.0004	0.0004 ±6.6E-06
Firmicutes	Family *Christensenellaceae*	0.020	0.312	0.330	4.832	**0.006**	0.064	0.003 ±0.001	0.001 ±0.0004	0.0002 ±8.9E-05
Firmicutes	Family *Clostridiaceae*	**<0.001**	0.242	0.396	3.082	**<0.001**	0.076	0.003 ±0.002	7.0E-05 ±3.0E-05	2.2E-05 ±5.0E-06
Firmicutes	Family *Ruminococcaceae*	0.162	1.627	**0.006**	3.891	0.113	0.430	0.006 ±0.001	0.010 ±0.002	0.003 ±.0004
Proteobacteria	Genus *Sutterella*	**0.004**	0.382	0.448	1.678	**0.002**	0.243	0.039 ±0.008	0.015 ±0.004	0.009 ±0.002

Table 4.4. Statistical comparison of the relative abundance of OTUs between rederivation groups within the C3H IL-10-/- model. *p*-value, mean fold change, and mean relative abundance are shown. Statistical significance and interactions of GM profile, sex, and OTU were determined using two-way ANOVA with Student Newman-Keuls post test. Bold face values indicate statistical significance ($p \leq 0.01$).

Significant OTUs in B6 IL-10$^{-/-}$ (CMTR to CD1 Surrogates)		GMJAX relative to GMCRL		GMJAX relative to GMTAC		GMTAC relative to GMCRL		GMCRL	GMJAX	GMTAC
Phylum	**OTU**	***p*-value**	**Mean Fold Change**	***p*-value**	**Mean Fold Change**	***p*-value**	**Mean Fold Change**	**Mean Relative Abundance (±SEM)**	**Mean Relative Abundance (±SEM)**	**Mean Relative Abundance (±SEM)**
Bacteroidetes	*Bacteroides acidifaciens*	**0.002**	3.260	0.620	1.16	**<0.001**	2.809	0.022 ±0.003	0.072 ±0.013	0.062 ±0.01
Bacteroidetes	Family *Rikenellaceae*	**0.006**	0.458	**0.003**	0.446	0.979	1.027	0.095 ±0.01	0.043 ±0.014	0.100 ±0.01
Bacteroidetes	Genus *Bacteroides*	**<0.001**	2.527	0.036	1.554	**0.005**	1.625	0.0834 ±0.009	0.211 ±0.306	0.136 ±0.012
Bacteroidetes	Order *Bacteroidales*	**0.01**	0.000	0.058	0.000	0.595	0.387	0.0002 ±4.12E-05	0.000 ±0.000	0.0001 ±2.3E-05
Deferribacteres	*Mucispirillum schaedleri*	**0.016**	0.0005	**<0.001**	0.0004	0.012	1.592	0.005 ±0.0007	3.36E-06 ±1.8E-06	0.008 ±0.002
Firmicutes	Family *Mogibacteriaceae*	**<0.001**	0.374	0.032	0.564	**0.005**	0.662	0.0008 ±0.00005	0.0003 ±6.83E-05	0.0005 ±6.9E-05
Firmicutes	Family *Christensenellaceae*	**<0.001**	2.858	**<0.001**	2.332	0.691	1.226	0.0003 ±0.00004	0.001 ±0.0001	0.0003 ±4.5E-05
Firmicutes	Family *Clostridiaceae*	**0.01**	0.288	0.916	0.977	**0.005**	0.294	0.0001 ±0.00024	0.0003 ±6.04E-05	0.0003 ±7.6E-05
Firmicutes	Genus *Clostridium*	**0.01**	0.000	0.688	0.000	**0.004**	0.432	0.0005 ±0.0001	0.000 ±0.000	7.6E-05 ±4.2E-06
Firmicutes	Genus rc4-4	**<0.001**	0.035	0.044	0.088	**<0.001**	0.402	0.0028 ±0.0003	9.74E-05 ±1.02E-06	0.001 ±.0002
Firmicutes	Order *Clostridiales*	**<0.001**	0.611	0.776	0.960	**<0.001**	0.636	0.318 ±0.015	0.19 ±0.035	0.202 ±0.015
Proteobacteria	Family *Enterobacteriaceae*	**0.002**	21.629	**0.006**	24.616	0.974	0.879	8.93E-06 ±3.3E-07	0.002 ±0001	7.84E-06 ±3.0E-06
Proteobacteria	Genus *Helicobacter*	**<0.001**	5.346	**<0.001**	2.301	0.095	2.323	0.003 ±0.0005	0.025 ±0.005	0.007 ±0.001
TM7	Family F16	0.108	0.294	**0.008**	0.163	0.075	1.801	0.009 ±0.001	0.002 ±0.0008	0.016 ±0.003

Table 4.5. Statistical comparison of the relative abundance of OTUs between CMTR groups within the B6 IL-10-/- model. *P* value, mean fold change, and mean relative abundance are shown. Statistical significance and interactions of GM profile, sex, and OTU were determined using two-way ANOVA with Student Newman-Keuls post test. Bold face values indicate statistical significance ($p \leq 0.01$).

CHAPTER 5:

Supporting Projects

Overview

The purpose of this chapter is to briefly outline several smaller projects that were in support of the research performed in chapters 2-4. In this chapter we will describe additional gross and histologic changes we noted in the IL-10$^{-/-}$ mouse model, discuss the generation of inbred FVBN/J colonies with GM profiles that vary in complexity and composition, and evaluate complex GM profile transfer through co-housing.

Gross and Histologic Comparison of B6 and C3H IL-10$^{-/-}$ Mice

During our initial evaluation of gross disease in B6 and C3H IL-10$^{-/-}$ mice used in projects outlined in chapter 4, we noted that there were subjective differences in consistency, color, and odor of cecal and colonic contents as well as the tissue appearance of distal ileum, cecum, and proximal colon at the close of the study (111 days post inoculation). Specifically, we noted that in C3H IL-10$^{-/-}$ mice, cecal and colonic contents were thick in consistency, normal in color with a distinct sulfurous odor as compared to B6 IL-10$^{-/-}$ mice. In addition, the distal ileum, cecum, and proximal colon was markedly thickened with a corrugated appearance on cut surface in all C3H IL-10$^{-/-}$ mice examined. In contrast, the cecal contents of B6 IL-10$^{-/-}$ mice were normal to dark brown in color with a normal to watery consistency. The cecum and proximal colon were moderately thickened with only a few mice having gross lesions visible in the distal ileum. In addition, the cecum appeared grossly larger in B6 IL-10$^{-/-}$ as compared with C3H IL-10$^{-/-}$ mice (Figure 5.1A). However, at the time of necropsy gross images of tissues, cecal and colonic contents, as well as cecal weights were not obtained. C3H IL-10$^{-/-}$ mice had

decreased colonic length, and increased cecal and colonic disease lesion scores as compared to B6 IL-10$^{-/-}$ mice (chapter 4) indicating an increased disease severity in these mice. Additionally, the histologic appearance of marked epithelial ulceration (occasionally with hemorrhage), transmural inflammation, and epithelial dysplasia was frequently observed in sections from the cecum and colon at the cecal-colonic junction of C3H IL-10$^{-/-}$ mice (Figure 5.1B). Furthermore, we frequently observed gross thickening of the distal ileum near the cecum in C3H IL-10$^{-/-}$ mice. However, gross and histopathologic images were note obtained. Interestingly, we also noted differences in the presence of rectal prolapse in male and female mice of both strains with the greater incidence of rectal prolapse occurring in B6 IL-10$^{-/-}$ mice irrespective of GM profile (Table 5.1). This data is intriguing as the incidence of rectal prolapse does not appear to correlate with disease severity indicating that clinical observation of rectal prolapse cannot be used as a prognostic indicator of disease.

Disparate gross and histological results between B6 and C3H IL-10$^{-/-}$ mice, are not surprising as it is well known that the C3H IL-10$^{-/-}$ mice have a mutation in the TLR4 gene which makes innate immune cells such as macrophages unable to respond to LPS. However, a side by side comparison of lesion severity in both mouse strains has not been previously described. In addition, the majority of research studies using IL-10$^{-/-}$ mice focus solely on female mice and as such, disparate results of rectal prolapses between males and females has not been recorded. Based on our observations, we plan to implement a larger study to thoroughly compare and describe differences in lesion severity between the two models using the GMJAX profile which had the highest cecal and colonic lesion scores (chapter 4).

Generation of FVB_{GMHSD} and $CD1_{GMHSD}$ Mouse Colonies

We successfully generated and maintained Crl:CD1 outbred mouse colonies for use as surrogate dams for CMTR (chapter 3). In addition, we demonstrated that these colonies could successfully be used to generate isogenic mice with differential GM colonization that could be used to study the effect of GM on host disease phenotype (chapter 4). However, it should be considered that the Crl:CD1 mouse colonies are an outbred stock and dependent on study design, they may not be suitable for CMTR use in all studies. In order to offer an alternative CMTR strategy for these types of studies, we generated FVBN/J colonies with four different GM profiles varying in complexity and composition similar to our previously described studies in chapter 3. We used embryos harvested from FVBN/J donor females (herein noted as FVB) obtained from The Jackson Laboratories and rederived by surgical transfer to Crl:$CD1_{GMCRL}$, C57BL/6_{GMJAX}, C57BL/6_{GMTAC}, and Hsd:$CD1GM_{HSD}$ surrogate dams obtained from the vendor as previously described in chapter 3. Offspring resulting from embryo transfer were mated using an inbred brother-sister mating scheme and maintained for 2-4 generations. In accordance with our previous results, we found that FVB mice could be rederived using CMTR and maintained as four colonies with distinct GM profiles (one-way PERMANOVA; $F = 8.38$, $p = 0.0001$) (Figures 5.2). Consistent with our previous results in chapter 3, we found that each profile had demonstrable differences in both phylum and OTU relative abundance (Figure 5.3) as well as richness and diversity (Figure 5.4). In addition to the rederivation of FVB mice, we also rederived Crl:CD1 embryos to HSD:$CD1_{GMHSD}$ surrogate dams to produce a colony of CD1 mice with a GM profile

more complex than those previously characterized in chapter 3. As expected these mice maintained the GMHSD profile (data not shown).

As we anticipate using the FVB colonies for CMTR, as an alternative to the use of CD1 mice, we compared the GM profiles of both FVB and CD1 colonies to determine differences between groups. To evaluate β-diversity among rederivation groups, principal component analysis (PCA) was performed (Fig 5.5). Statistical differences between GM ($F = 6.5$, $p = 0.001$) and genotype ($F = 5.9$, $p = 0.001$) were observed with no interactions as determined by two-way PERMANOVA. As anticipated, although maintaining distinct GM profiles, both FVB and CD1 mice with GMJAX, GMTAC, or GMHSD clustered closely together indicating similarity in composition. Interestingly, FVB and CD1 mice with GMCRL profiles clustered differentially along PC1 and PC2, suggesting increased variability in GM composition. To examine differences in taxa between FVB and CD1 mice, relative abundance at the phylum and OTU level was compared (Fig. 5.6). Subjectively, as a whole the FVB colonies appear to have less variability in OTU relative abundance among all GM profiles examined. In addition, FVB_{GMTAC} mice have a lower relative abundance of family *Rikenellaceae* as compared to $CD1_{GMTAC}$ mice. In contrast, $CD1_{GMTAC}$ and $CD1_{GMCRL}$ mice have increased relative abundance of genus *Bacteroides*. Both the $CD1_{GMJAX}$ and $CD1_{GMTAC}$ appear to have a higher level of Order Clostridiales than FVB_{GMJAX} and FVB_{GMTAC} profiles.

It should be noted, that rederivation of the FVB colonies was performed approximately two years following rederivation of the original CD1 colonies. During this time period, it is possible that vendor GM profiles may drift resulting in differing colonization of surrogate dams used for rederivation of the two groups which may

contribute to the observed differences between the FVB_{GMCRL} and $CD1_{GMCRL}$ mice. However, on PCA analysis GMJAX, GMTAC, or GMHSD groups appeared to cluster together suggesting that extreme variability may be vendor dependent. Alternatively, it is also possible that disparate colonization of the FVB and CD1 colonies could be due to differences in host genotype.

In agreement with our previous results (chapter 3) we found that FVB colonies with varying complex GM profiles can be generated and maintained for several generations. In addition, we found that with the exception of the GMCRL profile, the FVB colonies have similar GM profiles to the CD1 colonies we previously created. Taken as a whole, these data suggest that the FVB colonies can provide an alternative CMTR surrogate dam for studies where maternal genetic influence is a valid concern.

Transfer of Complex GM by Co-housing and Natural Mating

We have demonstrated that CMTR can be used as a method to colonize isogenic mice with GM profiles of varying composition and complexity. However, due to the need for knowledge of advanced surgical techniques and cost of embryo transfer this method may not be feasible at all institutions. To address this, our lab investigated the possibility of complex GM transfer by co-housing and natural mating. Our previous studies indicated that the GMTAC profile produced the most robust disease phenotype in B6 IL-$10^{-/-}$ mice (chapter 4). This mouse strain is only available from The Jackson Laboratories and is colonized with a relatively simple GM as compared to the GMTAC profile. As GM profile is passed from dam to pup, we hypothesized that co-housing and subsequent generational mating of offspring could be used to transfer the GMTAC profile to the homozygous F2 generation dependent on dam GM profile. To test this, we used

varying combinations of male and female B6 IL-$10^{-/-}{}_{GMJAX}$ mice co-housed with male or female wild type $B6_{GMTAC}$ mice (Figure 5.7). Male mice were mated to females and remained in the cage for a four-day period. Following mating, females were removed and placed in a new cage until parturition. In keeping with the pattern of maternal GM, heterozygous offspring were brother-sister mated, and fecal pellets were collected for 16S rRNA sequencing from resultant IL-$10^{-/-}$ homozygous male and female pups once they reached 8-10 weeks of age.

To evaluate β-diversity among groups, PCA was performed (Figure 5.8). Interestingly, we found three distinct GM profiles, with F2 generation mice demonstrating an intermediate GM profile irrespective of original founding dam GM profile. In addition, we found clear inter- group separation of the F2 generation along PC2 into male and female groups suggesting sex dependent GM colonization. A two-way PERMANOVA was performed on F2 generation samples that examined the effect of historical maternal GM profile ($F = 6.80$, $p = .0005$) and sex ($F = 16.50$, $p = 0.0001$) on subsequent F2 generation GM profile with a significant interaction between the main effects ($p = 0.0173$). To identify differences in taxa between groups, we examined the relative abundance of taxa within each profile at both the phyla and OTU levels (Figure 5.9). Subjectively, male homozygous F2 mice have a greater relative abundance of phylum *Deferribacteres* than females, with an increase in genus *Oscillospira*. In contrast, female F2 mice had much higher relative abundance of family S24-7 than male mice, subjectively similar levels to that observed in B6 IL-$10^{-/-}{}_{GMJAX}$ breeders. Interestingly, both male and female F2 mice have similar levels of family *Rikenellaceae* to levels observed in $B6_{GMTAC}$ breeders, suggesting successful transfer of this bacterial group to

the F2 generation. We also examined each generation for differences in richness and diversity (Figure 5.10). A two-way ANOVA was performed on F2 generation samples with no statistical differences found between generations.

Our data suggest that co-housing and subsequent mating does not generate F2 homozygous offspring with GMTAC profiles. However, it appears that the F2 generation is a blend of both GM profiles. While we did not generate mice with an exact match for the GMTAC profile, the blended profile may be sufficient to produce IL-$10^{-/-}$ mice that have the desirable increase in disease phenotype observed in chapter 4. This was not examined in the context of this dissertation, but could be addressed in future projects.

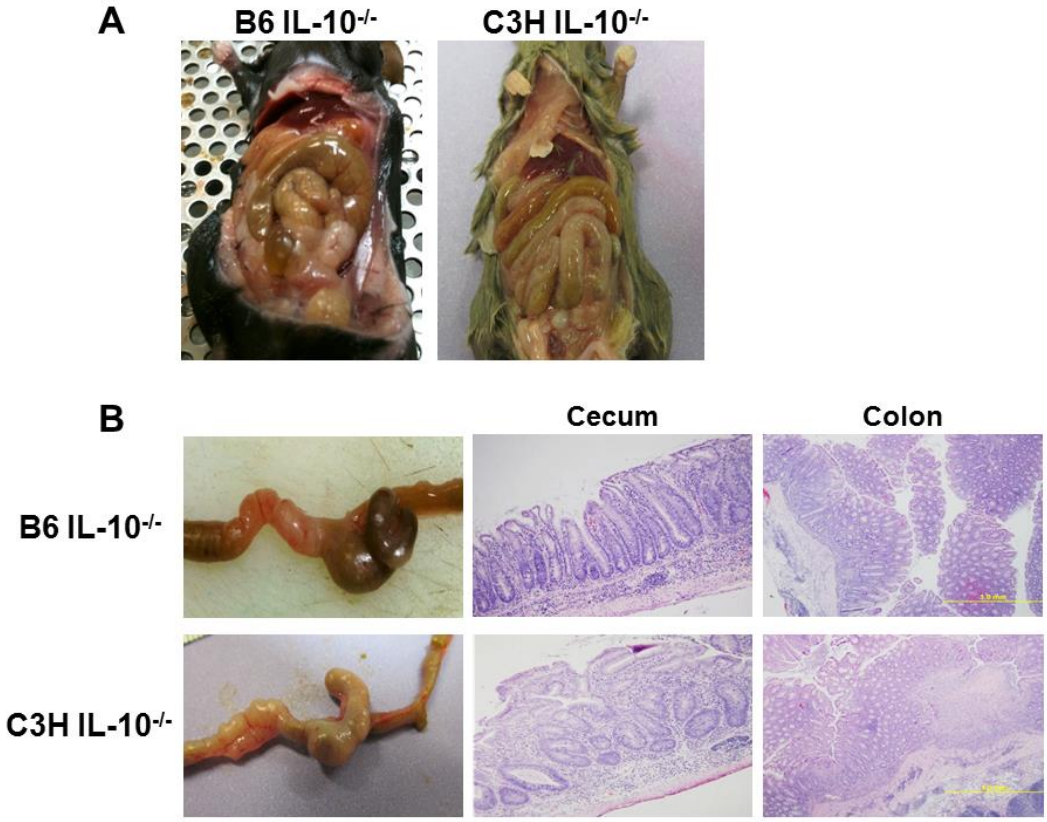

Figure 5.1. Gross and histologic difference in disease characteristics between B6 IL-10-/- and C3H IL-10-/- mouse strains. A) In situ gross comparison of cecum and colon demonstration marked enlargement of the cecum in B6 IL-10-/- mice. B) gross and histologic comparison of cecum and colon illustrating variation in cecal content color, thickness of tissue, and disease severity between B6 IL-10-/- and C3H IL-10-/- mouse strains. (Images at 5x, size bars = 1.0m).

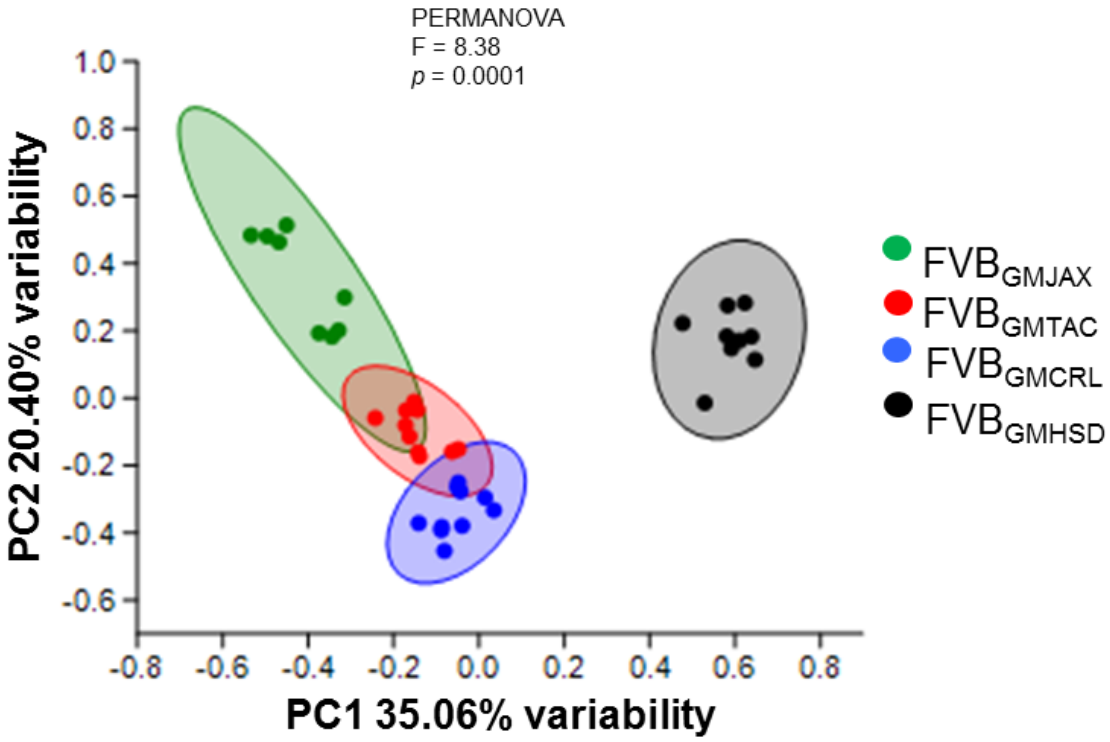

Figure 5.2. Distinct GM profiles of rederived FVB colonies. Unweighted principal component analysis (PCA) of representative fecal samples from 8-10 week old female FVB mice (n = 6-8 per GM profile). Statistical significance determined by one-way PERMANOVA (p = 0.001)

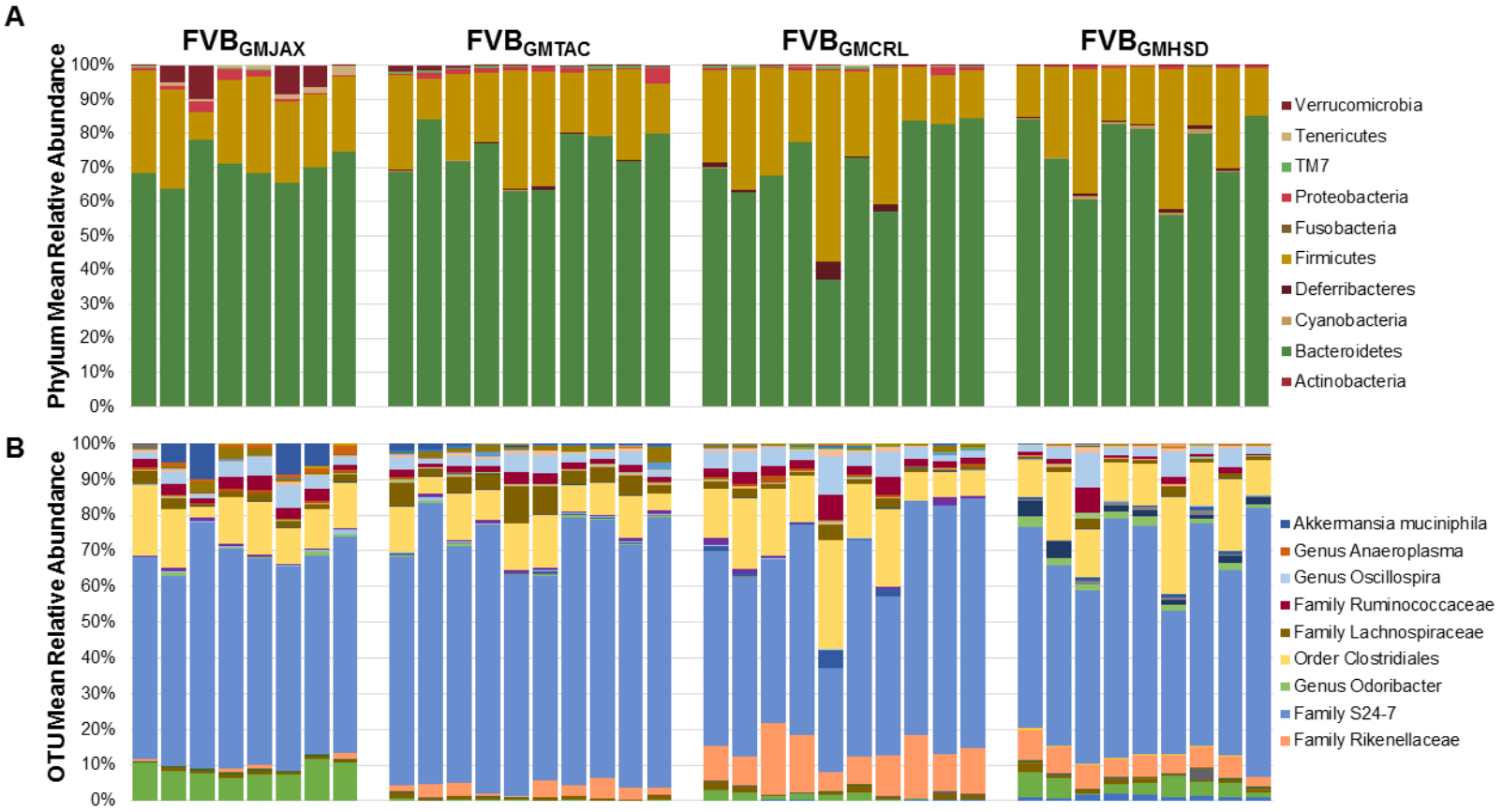

Figure 5.3. Comparison of relative abundance of taxa of rederived FVB mice. Representative samples of 6-8 week old FVB female mice (n = 6-8 per GM profile). A) Bar charts of relative abundance of taxa at phyla level. Legend of phyla at right. B) Bar charts of relative abundance of taxa at OTU level.

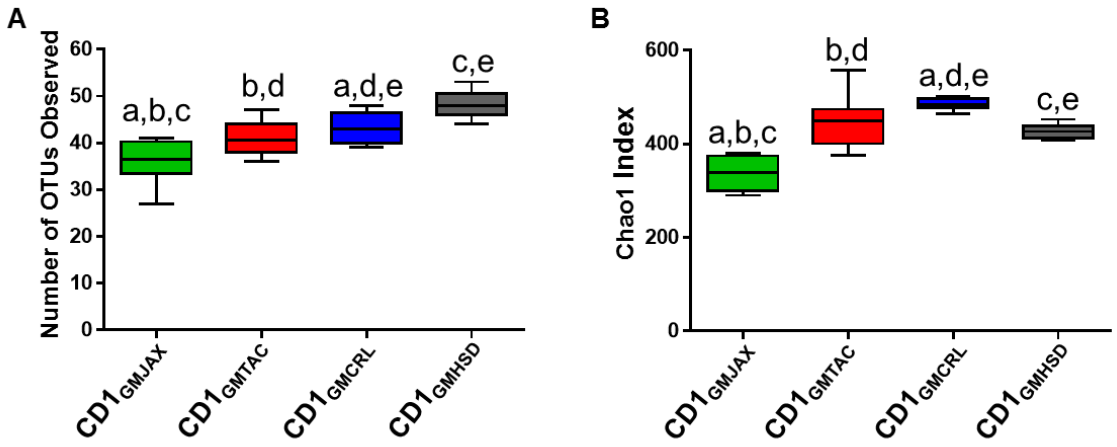

Figure 5.4. Comparison of gut microbiome (GM) richness and diversity of rederived FVB mice. Tukey box and whisker graph of representative samples from 6-8 week old FVB female mice (n = 6-8 per GM profile). Statistical significance comparisons determined by One-way ANOVA with Student Newman Keuls post hoc test. Statistical significance defined by $p \leq 0.05$ and denoted in the figure by lower case letters.

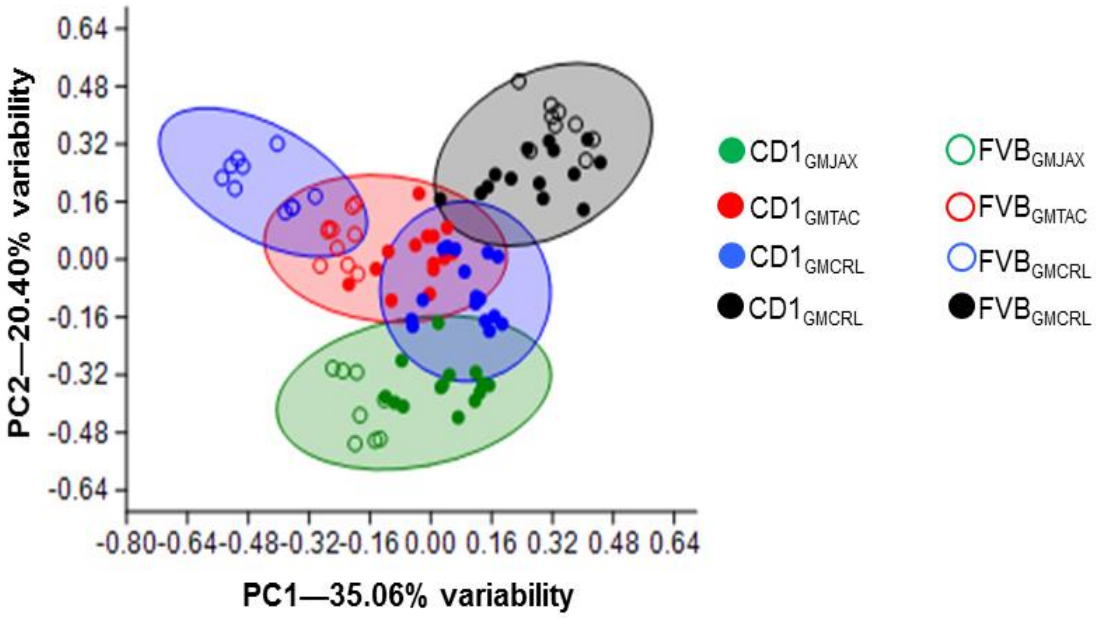

Figure 5.5. Comparison of GM profiles of rederived FVB and CD1 colonies. Unweighted principal component analysis (PCA) of representative fecal samples from 8-10 week old female FVB and CD1 mice (n = 8-10 per GM profile). Statistical significance determined by two-way PERMANOVA (p = 0.001)

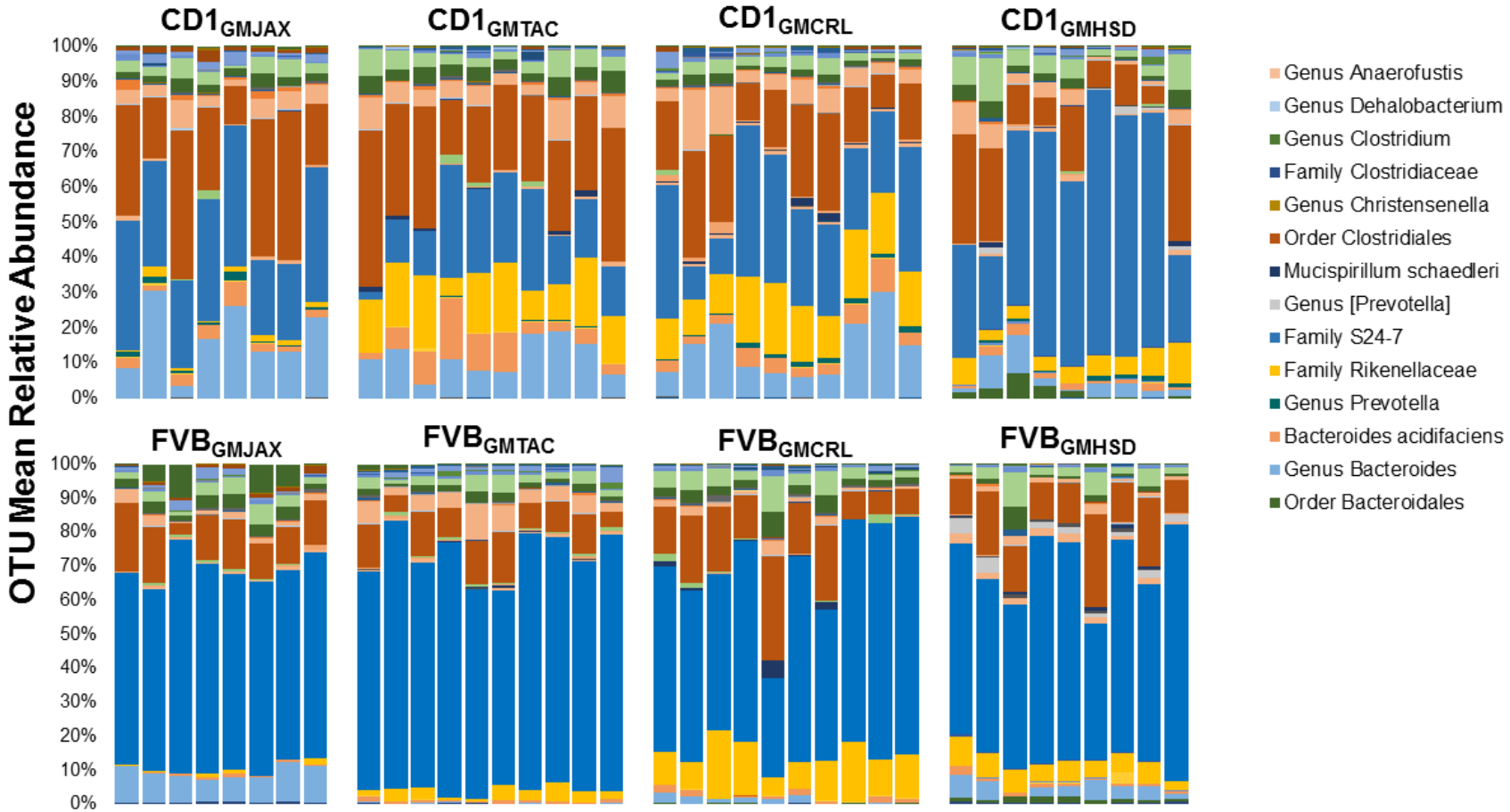

Figure 5.6. Comparison of relative abundance of taxa of rederived FVB and CD1 mice. Representative samples from 8-10 week old FVB and CD1 female mice (n = 8-10 per GM profile). A) Bar charts of relative abundance of taxa at phyla level. Legend of phyla at right. B) Bar charts of relative abundance of taxa at OTU level.

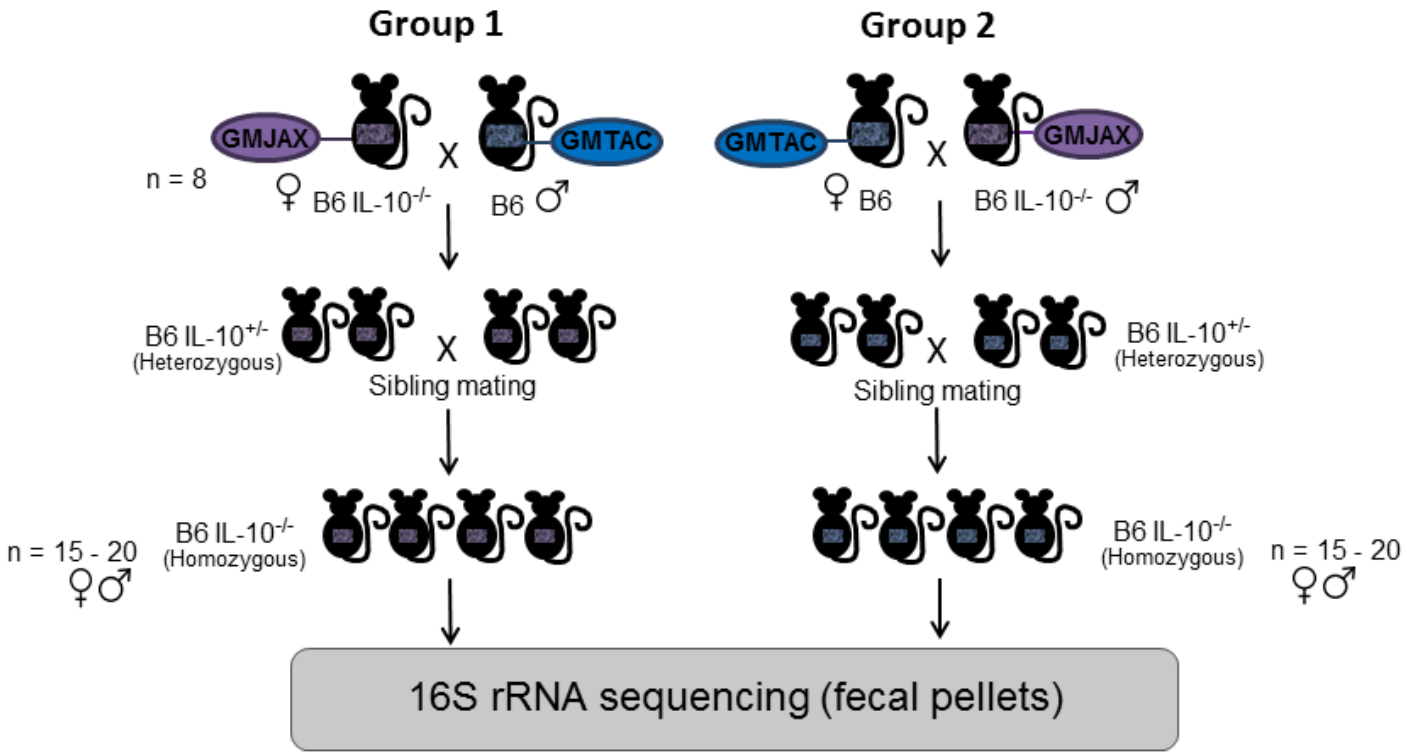

Figure 5.7. Experimental design of co-housing and subsequent mating to generate IL-10$^{-/-}$ pups with different GI microbiota (GM). Schematic diagram showing various combinations of co-housing and mating male and female B6 IL-10$^{-/-}$ mice with wildtype B6 male or female mice. Fecal samples from homozygous F2 generation mice were sequenced and compared for differences in GM composition and complexity.

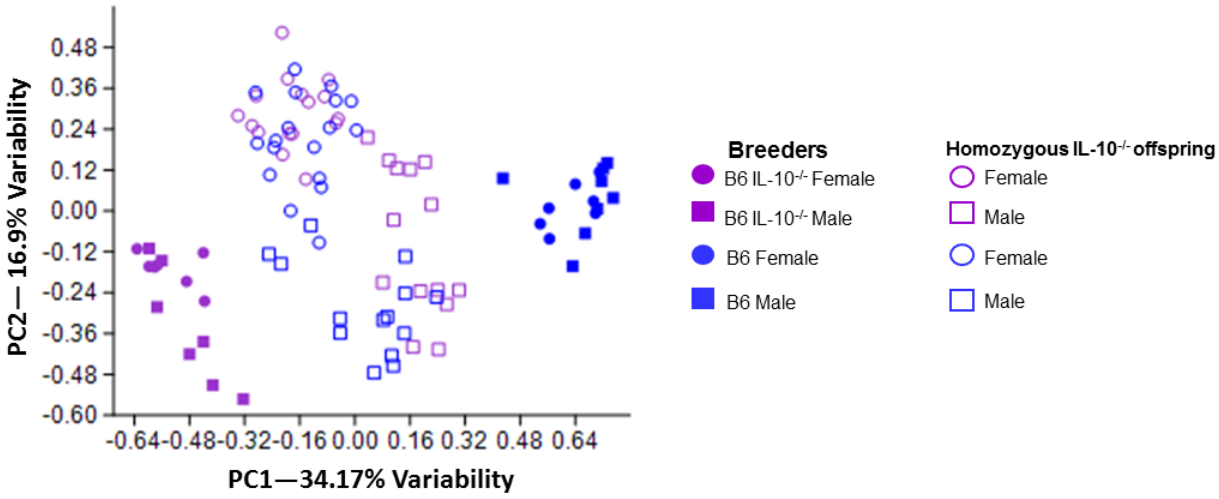

Figure 5.8. Comparison of GM profiles of F2 generation IL-10$^{-/-}$ mice. Unweighted principal component analysis (PCA) of representative fecal samples from 8-10 week old male and female mice (n = 13-15 per GM profile). Samples from male and female IL-10$^{-/-}$ and B6 foundation breeders are provided for reference. Statistical significance determined by two-way PERMANOVA statistical analysis of F2 generation samples.

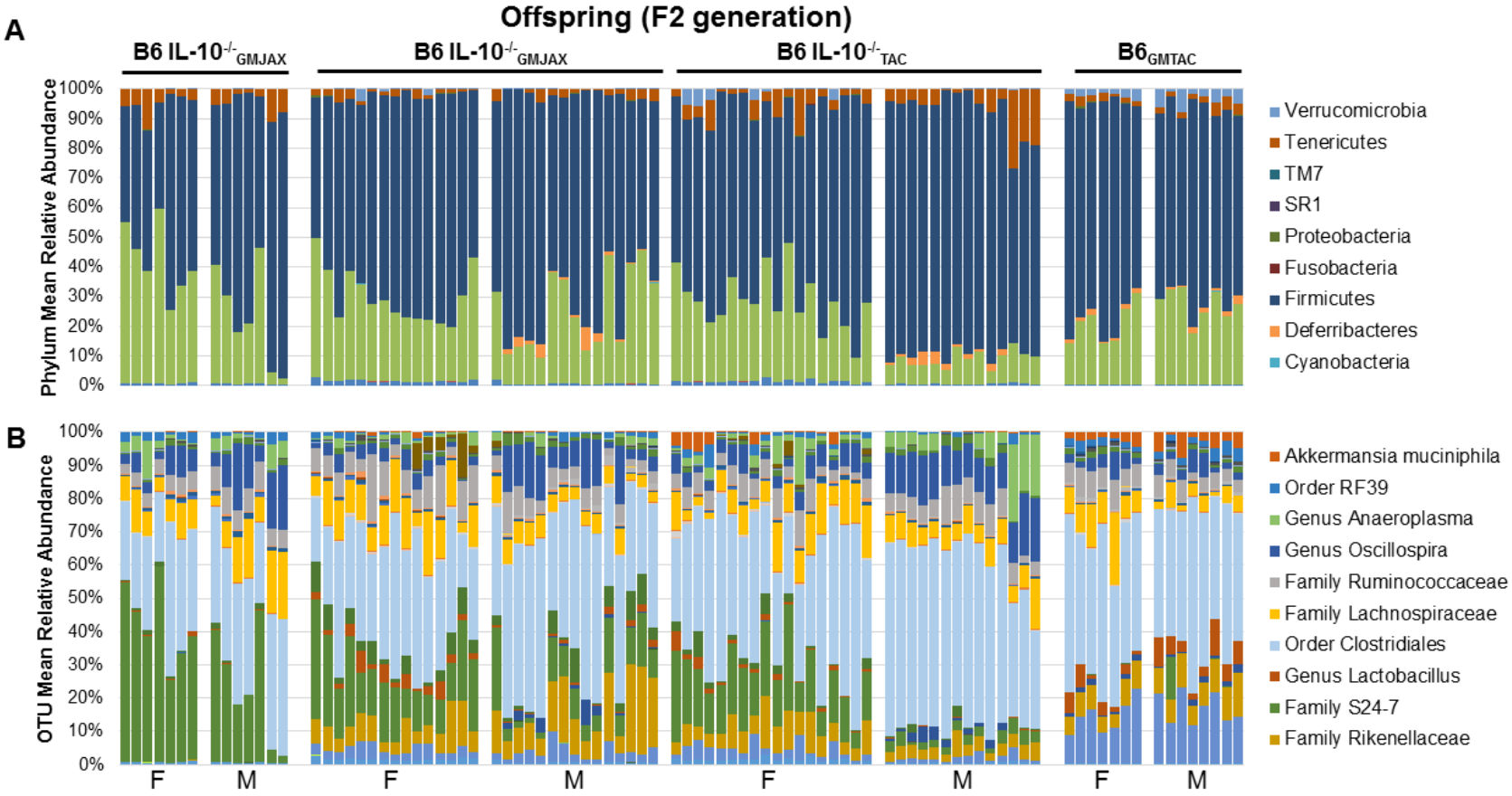

Figure 5.9. Comparison of GM profiles of F2 generation IL-10$^{-/-}$ mice. Representative samples from 8-10 week old male and female mice (n = 13-15 per GM profile). Samples from male and female IL-10$^{-/-}$ and B6 foundation breeders are provided for reference. A) Bar charts of relative abundance of taxa at phyla level. B) Bar charts of relative abundance of taxa at OTU level. Legend of taxa at right.

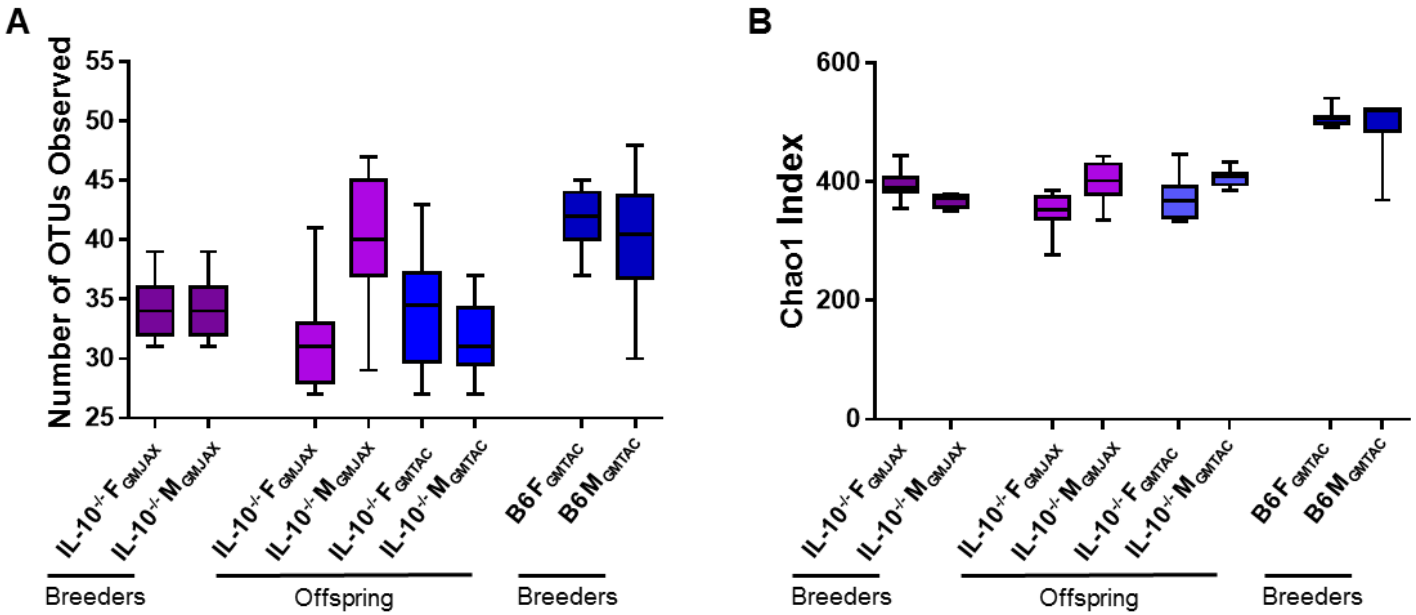

Figure 5.10. Comparison of gut microbiome (GM) richness and diversity of F2 generation IL-10$^{-/-}$ mice. Tukey box and whisker graph of representative samples from 8-10 week old male and female mice (n = 13-15 per GM profile). Samples from male and female IL-10$^{-/-}$ and B6 foundation breeders are provided for reference. Statistical significance determined by two-way PERMANOVA statistical analysis of F2 generation samples. No differences statistical differences were identified between GM profiles.

	B6 IL-10$^{-/-}$			C3H IL-10$^{-/-}$		
	GM_{JAX}	GM_{TAC}	GM_{CRL}	GM_{JAX}	GM_{TAC}	GM_{CRL}
Male	10/14	9/15	11/14	0/14	0/15	2/14
Female	2/15	0/15	2/12	0/15	0/13	0/15

Table 5.1. Incidence of rectal prolapse in IL-10-/- mice. Number of cases of clinical rectal prolapse observed in *Helicobacter hepaticus* inoculated mice. Representative sample of 13-14 mice per GM profile.

CHAPTER 6:

Conclusion and Future Directions

Investigation into the role of the gut microbiome (GM) on host physiology in both health and disease is gaining considerable attention. With the advancement of sequencing technologies, there has been renewed interest into the investigation of the aberration of GM composition and subsequent effects on enteric diseases such as inflammatory bowel disease (IBD). However, translatable *in vivo* methods to fully examine the role of complex GM in diseases such as IBD, remains to be examined. With this in mind, the studies described throughout this body of work have focused on the standardization of DNA extraction methods to improve 16S rRNA sequencing detection of microbial communities that adequately represent true GM composition (chapter 2); development of outbred Crl:CD1 mice with defined, complex GM profiles that can be used for Complex Microbiota Targeted Rederivation (CMTR) (chapter 3); investigation of the utility of CMTR to improve consistency of disease phenotype in the Il-10$^{-/-}$ mouse model of inflammatory bowel disease (chapter 4); and outline smaller projects used to support previous studies (chapter 5).

In chapter 2 we evaluated the performance of several kit and manual based DNA extraction methods with a focus on DNA yield, purity, 16S rRNA sequencing output, and cost. We found that fecal extraction method performance within our testing parameters was dependent on host species examined. In addition, we found that spectrophotometric assessment of DNA elutions prior to PCR had poor predictive value with regard to successful amplification and sequencing indicating that quality of DNA does not

adequately predict successful DNA amplification. Comparison of sequencing results from the same sample subjected to different extraction methods revealed that despite the variable detection of a limited number of rare taxa, the overall community profiles agreed in the majority of samples. Our findings illustrate that careful consideration of the sample species and DNA extraction methods should be considered during study design for complex GM studies.

In chapters 3 and 5 we demonstrate generation of outbred Crl:CD1 and inbred FVB/J mice with defined, complex GM profiles. Using rederivation by surgical embryo transfer, we developed mouse colonies with distinct GM profiles varying in bacterial composition and complexity that can be maintained for at least six generations. The long term GM stability and maintenance of these colonies is an exciting finding, as few studies have investigated the long term maintenance of distinct, complex GM profiles in mice housed in ventilated racks using standard barrier techniques. These mice offer several unique research opportunities to investigate the role of the GM in both isogenic and heterogenic mouse models of localized and systemic disease.

Therefore, these mouse colonies provide a unique opportunity for the research community to further explore the effect of complex GM on host physiology. However, in order to fully utilize these colonies for the purposes of CMTR generation of future mouse models, pups resulting from CMTR will need to be shipped and housed at other institutions. These institutions may have housing conditions that greatly differ from the husbandry practices used to generate our colonies. In order to investigate the stability of these GM profiles under varying housing conditions, we plan to ship adult mice from each microbiome Crl:CD1 colony to various institutions with different geographical

locations. Pre- and post- shipment fecal samples will be collected and analyzed by 16S rRNA sequencing as previously described. While we do anticipate microbial shifts within each GM profile dependent on housing conditions, we expect that all profiles will shift in a similar manner and that previously defined vendor specific profiles will be maintained in accordance with our earlier results. If these results confirm continued stability and maintenance of vendor specific profiles, regardless of change of institution and housing conditions, this will provide further compelling evidence that these GM profiles could be offered for use to the research community at other institutions.

In chapter 4 we investigated the influence of the GM on disease severity in the IL-$10^{-/-}$ mouse model. We hypothesized that the maternal transfer of differing naturally occurring GM using CMTR could be used to design and implement GM-focused studies in this mouse model. To test this hypothesis, we transferred genetically identical C57BL/6 IL-$10^{-/-}$ and C3H/HeJBir IL-$10^{-/-}$ embryos into surrogate CD-1 or C57BL/6 dams from different vendors with varying microbiota complexity and composition. To induce disease, pups were inoculated with *Helicobacter hepaticus* at 24 and 26 days post-weaning. Colonic and cecal lesion scores as well as changes in microbiota were evaluated at 111 days post-inoculation using histopathology and microbial 16S rRNA amplicon sequencing respectively. We found that disease severity was significantly decreased in both the B6 and C3H IL-$10^{-/-}$ mouse strains colonized with the GMCRL profile as compared to the GMJAX and GMTAC groups. In addition, we found that these mice have a significantly lower relative abundance of *H. hepaticus* detected in the cecal contents. These findings are intriguing, as despite all animals being inoculated with the same inoculum, differential *H. hepaticus* colonization suggests GM profile dependent

resistance. In addition to alterations in *H. hepaticus*, statistical differences in the relative abundance of several operational taxonomic units (OTUs) were observed between GM profiles.

Because the initial rederivation was performed using surrogate dams with varying genetic backgrounds, it is possible that differences in maternal care, *in utero* environment, or epigenetic factors could contribute to the observed differential disease severity. To further explore this possibility, we rederived B6 IL-$10^{-/-}$ mice using the Crl:CD1 CMTR colonies with varying complex GM profiles described in chapter 3. Confirming our previous findings in the B6 IL-$10^{-/-}$ model, sequencing of cecal contents revealed that the GMCRL group had decreased disease severity as compared to the GMJAX and GMTAC groups. In addition to differences in the relative abundance of several OTUs between groups, we also found decreased colonization of *H. hepaticus* in the GMCRL mice. It should also be noted that for all mouse strains rederived to surrogate dams with the GMCRL profile, an increase in bacterial diversity was observed as compared to GMJAX and GMTAC colonized mice. Taken as a whole, these findings indicate that the composition of resident GM is a primary determinant of disease severity in IBD and provide proof-of-concept that CMTR can be used to investigate the contribution of GM on disease severity.

Our lab has successfully used CMTR to investigate the influence of GM in mouse models of IBD (described in chapter 4). However, to date, CMTR has not been used in models of systemic disease. Due to recent interest in the influence of GM on the gut:brain axis, we plan to use CMTR to rederive several mouse models of autism spectrum disorder (ASD) to investigate the influence of GM complexity and composition

on disease severity. However, it is not fully understood how the long term effect of maternal genetics, maternal care, and host:microbiome interactions can impact disease in neurodevelopmental mouse models. Although we demonstrate that CMTR using Crl:CD1 mice did not profoundly affect study outcome in IL-$10^{-/-}$ mice, this may not be the case for all mouse models. In order to address this potential experimental variable, we used surgical embryo transfer to develop inbred FVBN/J colonies with GMJAX, GMTAC, GMCRL, and GMHSD profiles that vary in composition and complexity (Chapter 5). We found that the GM profiles of the FVBN/J mice were similar in composition to our previously established Crl:CD1 colonies. As a part of the proposed ASD project, we plan to use both the Crl:CD1 and FVBN/J colonies for CMTR of ASD models. Additionally, the FVBN/J surrogate colonies can be used for CMTR of other mouse models where concerns of the effect of maternal genetics are warranted.

In our hands CMTR offers a great opportunity to investigate the effect of the GM on host physiology. However, not all institutions have the resources necessary to perform surgical embryo transfer or house large breeding surrogate colonies. In order to address this, we evaluated the transfer of complex maternal GM by co-housing $B6_{GMTAC}$ and B6 IL-$10^{-/-}{}_{GMJAX}$ male and female mice. We found that following co-housing resultant offspring were colonized with a combination of both GM profiles. Unfortunately, our results indicate that co-housing at least for purposes of transfer and maintenance of the original profile of the dam is ineffective. One method that might be used to increase the likelihood of maternal colonization with the desired GM is the use of antibiotics to limit the likelihood of GM transfer from the mouse with the undesired GM

profile. However, we have not investigated antibiotic use in the transfer of GM by co-housing.

Bibliography

1. Backhed F, Ley RE, Sonnenburg JL, Peterson DA, Gordon JI. Host-bacterial mutualism in the human intestine. Science. 2005;307(5717):1915-20.
2. Wilson M. The indigenous microbiota of the gastrointestinal tract. Wilson M, editor. Oxfrord, UK: Blackwell Publishing; 2008.
3. Clemente JC, Ursell LK, Parfrey LW, Knight R. The impact of the gut microbiota on human health: an integrative view. Cell. 2012;148(6):1258-70.
4. de Vos WM, de Vos EA. Role of the intestinal microbiome in health and disease: from correlation to causation. Nutr Rev. 2012;70 Suppl 1:S45-56.
5. Hollister EB, Gao C, Versalovic J. Compositional and functional features of the gastrointestinal microbiome and their effects on human health. Gastroenterology. 2014;146(6):1449-58.
6. Hu S, Wang Y, Lichtenstein L, Tao Y, Musch MW, Jabri B, et al. Regional differences in colonic mucosa-associated microbiota determine the physiological expression of host heat shock proteins. Am J Physiol Gastrointest Liver Physiol. 2010;299(6):G1266-75.
7. Harrell L, Wang Y, Antonopoulos D, Young V, Lichtenstein L, Huang Y, et al. Standard colonic lavage alters the natural state of mucosal-associated microbiota in the human colon. PLoS One. 2012;7(2):e32545.
8. Turnbaugh PJ, Ley RE, Hamady M, Fraser-Liggett CM, Knight R, Gordon JI. The human microbiome project. Nature. 2007;449(7164):804-10.
9. Sartor RB. Microbial influences in inflammatory bowel diseases. Gastroenterology. 2008;134(2):577-94.
10. Riedel CU, Schwiertz A, Egert M. The Stomach and Small and Large INtestinal Microbiomes. In: Marchesi JR, editor. The Human Microbiota and Microbiome. Advances in Molecular and Cellular Microbiology. Boston, MA USA: CAB International; 2014. p. 1-19.
11. Whitman WB, Coleman DC, Wiebe WJ. Prokaryotes: the unseen majority. Proc Natl Acad Sci U S A. 1998;95(12):6578-83.
12. Donaldson GP, Lee SM, Mazmanian SK. Gut biogeography of the bacterial microbiota. Nat Rev Microbiol. 2016;14(1):20-32.
13. Cenit MC, Matzaraki V, Tigchelaar EF, Zhernakova A. Rapidly expanding knowledge on the role of the gut microbiome in health and disease. Biochim Biophys Acta. 2014;1842(10):1981-92.
14. Jandhyala SM, Talukdar R, Subramanyam C, Vuyyuru H, Sasikala M, Nageshwar Reddy D. Role of the normal gut microbiota. World J Gastroenterol. 2015;21(29):8787-803.
15. Pflughoeft KJ, Versalovic J. Human microbiome in health and disease. Annu Rev Pathol. 2012;7:99-122.
16. Funkhouser LJ, Bordenstein SR. Mom knows best: the universality of maternal microbial transmission. PLoS Biol. 2013;11(8):e1001631.
17. Jimenez E, Marin ML, Martin R, Odriozola JM, Olivares M, Xaus J, et al. Is meconium from healthy newborns actually sterile? Res Microbiol. 2008;159(3):187-93.
18. DiGiulio DB, Romero R, Amogan HP, Kusanovic JP, Bik EM, Gotsch F, et al. Microbial prevalence, diversity and abundance in amniotic fluid during preterm labor: a molecular and culture-based investigation. PLoS One. 2008;3(8):e3056.
19. Satokari R, Gronroos T, Laitinen K, Salminen S, Isolauri E. Bifidobacterium and Lactobacillus DNA in the human placenta. Lett Appl Microbiol. 2009;48(1):8-12.

20. Jimenez E, Fernandez L, Marin ML, Martin R, Odriozola JM, Nueno-Palop C, et al. Isolation of commensal bacteria from umbilical cord blood of healthy neonates born by cesarean section. Curr Microbiol. 2005;51(4):270-4.
21. Aagaard K, Ma J, Antony KM, Ganu R, Petrosino J, Versalovic J. The placenta harbors a unique microbiome. Sci Transl Med. 2014;6(237):237ra65.
22. Adlerberth I, Wold AE. Establishment of the gut microbiota in Western infants. Acta Paediatr. 2009;98(2):229-38.
23. Ross MG, Nijland MJ. Fetal swallowing: relation to amniotic fluid regulation. Clin Obstet Gynecol. 1997;40(2):352-65.
24. Ardissone AN, de la Cruz DM, Davis-Richardson AG, Rechcigl KT, Li N, Drew JC, et al. Meconium microbiome analysis identifies bacteria correlated with premature birth. PLoS One. 2014;9(3):e90784.
25. Dominguez-Bello MG, Costello EK, Contreras M, Magris M, Hidalgo G, Fierer N, et al. Delivery mode shapes the acquisition and structure of the initial microbiota across multiple body habitats in newborns. Proc Natl Acad Sci U S A. 2010;107(26):11971-5.
26. Biasucci G, Rubini M, Riboni S, Morelli L, Bessi E, Retetangos C. Mode of delivery affects the bacterial community in the newborn gut. Early Hum Dev. 2010;86 Suppl 1:13-5.
27. Salminen S, Gibson GR, McCartney AL, Isolauri E. Influence of mode of delivery on gut microbiota composition in seven year old children. Gut. 2004;53(9):1388-9.
28. Jakobsson HE, Abrahamsson TR, Jenmalm MC, Harris K, Quince C, Jernberg C, et al. Decreased gut microbiota diversity, delayed Bacteroidetes colonisation and reduced Th1 responses in infants delivered by caesarean section. Gut. 2014;63(4):559-66.
29. Barrett E, Kerr C, Murphy K, O'Sullivan O, Ryan CA, Dempsey EM, et al. The individual-specific and diverse nature of the preterm infant microbiota. Arch Dis Child Fetal Neonatal Ed. 2013;98(4):F334-40.
30. Thum C, Cookson AL, Otter DE, McNabb WC, Hodgkinson AJ, Dyer J, et al. Can nutritional modulation of maternal intestinal microbiota influence the development of the infant gastrointestinal tract? J Nutr. 2012;142(11):1921-8.
31. Turnbaugh PJ, Hamady M, Yatsunenko T, Cantarel BL, Duncan A, Ley RE, et al. A core gut microbiome in obese and lean twins. Nature. 2009;457(7228):480-4.
32. Lozupone CA, Stombaugh JI, Gordon JI, Jansson JK, Knight R. Diversity, stability and resilience of the human gut microbiota. Nature. 2012;489(7415):220-30.
33. Hopkins MJ, Sharp R, Macfarlane GT. Variation in human intestinal microbiota with age. Dig Liver Dis. 2002;34 Suppl 2:S12-8.
34. Eckburg PB, Bik EM, Bernstein CN, Purdom E, Dethlefsen L, Sargent M, et al. Diversity of the human intestinal microbial flora. Science. 2005;308(5728):1635-8.
35. Backhed F. Programming of host metabolism by the gut microbiota. Ann Nutr Metab. 2011;58 Suppl 2:44-52.
36. Yatsunenko T, Rey FE, Manary MJ, Trehan I, Dominguez-Bello MG, Contreras M, et al. Human gut microbiome viewed across age and geography. Nature. 2012;486(7402):222-7.
37. Koenig JE, Spor A, Scalfone N, Fricker AD, Stombaugh J, Knight R, et al. Succession of microbial consortia in the developing infant gut microbiome. Proc Natl Acad Sci U S A. 2011;108 Suppl 1:4578-85.
38. Costello EK, Lauber CL, Hamady M, Fierer N, Gordon JI, Knight R. Bacterial community variation in human body habitats across space and time. Science. 2009;326(5960):1694-7.
39. Jalanka-Tuovinen J, Salonen A, Nikkila J, Immonen O, Kekkonen R, Lahti L, et al. Intestinal microbiota in healthy adults: temporal analysis reveals individual and common core and relation to intestinal symptoms. PLoS One. 2011;6(7):e23035.

40. Dethlefsen L, Relman DA. Incomplete recovery and individualized responses of the human distal gut microbiota to repeated antibiotic perturbation. Proc Natl Acad Sci U S A. 2011;108 Suppl 1:4554-61.
41. Walker AW, Ince J, Duncan SH, Webster LM, Holtrop G, Ze X, et al. Dominant and diet-responsive groups of bacteria within the human colonic microbiota. ISME J. 2011;5(2):220-30.
42. Pei Z, Bini EJ, Yang L, Zhou M, Francois F, Blaser MJ. Bacterial biota in the human distal esophagus. Proc Natl Acad Sci U S A. 2004;101(12):4250-5.
43. Yang L, Lu X, Nossa CW, Francois F, Peek RM, Pei Z. Inflammation and intestinal metaplasia of the distal esophagus are associated with alterations in the microbiome. Gastroenterology. 2009;137(2):588-97.
44. Bik EM, Eckburg PB, Gill SR, Nelson KE, Purdom EA, Francois F, et al. Molecular analysis of the bacterial microbiota in the human stomach. Proc Natl Acad Sci U S A. 2006;103(3):732-7.
45. Ley RE, Hamady M, Lozupone C, Turnbaugh PJ, Ramey RR, Bircher JS, et al. Evolution of mammals and their gut microbes. Science. 2008;320(5883):1647-51.
46. Mahowald MA, Rey FE, Seedorf H, Turnbaugh PJ, Fulton RS, Wollam A, et al. Characterizing a model human gut microbiota composed of members of its two dominant bacterial phyla. Proc Natl Acad Sci U S A. 2009;106(14):5859-64.
47. Jeffery IB, Lynch DB, O'Toole PW. Composition and temporal stability of the gut microbiota in older persons. ISME J. 2016;10(1):170-82.
48. Claesson MJ, Jeffery IB, Conde S, Power SE, O'Connor EM, Cusack S, et al. Gut microbiota composition correlates with diet and health in the elderly. Nature. 2012;488(7410):178-84.
49. Biagi E, Nylund L, Candela M, Ostan R, Bucci L, Pini E, et al. Through ageing, and beyond: gut microbiota and inflammatory status in seniors and centenarians. PLoS One. 2010;5(5):e10667.
50. Avershina E, Storro O, Oien T, Johnsen R, Pope P, Rudi K. Major faecal microbiota shifts in composition and diversity with age in a geographically restricted cohort of mothers and their children. FEMS Microbiol Ecol. 2014;87(1):280-90.
51. Palmer C, Bik EM, DiGiulio DB, Relman DA, Brown PO. Development of the human infant intestinal microbiota. PLoS Biol. 2007;5(7):e177.
52. Mardis ER. Next-generation DNA sequencing methods. Annu Rev Genomics Hum Genet. 2008;9:387-402.
53. Goodwin S, McPherson JD, McCombie WR. Coming of age: ten years of next-generation sequencing technologies. Nat Rev Genet. 2016;17(6):333-51.
54. Franzosa EA, Hsu T, Sirota-Madi A, Shafquat A, Abu-Ali G, Morgan XC, et al. Sequencing and beyond: integrating molecular 'omics' for microbial community profiling. Nat Rev Microbiol. 2015;13(6):360-72.
55. Coenye T, Vandamme P. Intragenomic heterogeneity between multiple 16S ribosomal RNA operons in sequenced bacterial genomes. FEMS Microbiol Lett. 2003;228(1):45-9.
56. Weisburg WG, Barns SM, Pelletier DA, Lane DJ. 16S ribosomal DNA amplification for phylogenetic study. J Bacteriol. 1991;173(2):697-703.
57. Neefs JM, Van de Peer Y, De Rijk P, Chapelle S, De Wachter R. Compilation of small ribosomal subunit RNA structures. Nucleic Acids Res. 1993;21(13):3025-49.
58. Kennedy NA, Walker AW, Berry SH, Duncan SH, Farquarson FM, Louis P, et al. The impact of different DNA extraction kits and laboratories upon the assessment of human gut microbiota composition by 16S rRNA gene sequencing. PLoS One. 2014;9(2):e88982.
59. Lagier JC, Million M, Hugon P, Armougom F, Raoult D. Human gut microbiota: repertoire and variations. Front Cell Infect Microbiol. 2012;2:136.

60. Williams CF, Walton GE, Jiang L, Plummer S, Garaiova I, Gibson GR. Comparative analysis of intestinal tract models. Annu Rev Food Sci Technol. 2015;6:329-50.
61. Chung H, Pamp SJ, Hill JA, Surana NK, Edelman SM, Troy EB, et al. Gut immune maturation depends on colonization with a host-specific microbiota. Cell. 2012;149(7):1578-93.
62. Wannemuehler MJ, Overstreet AM, Ward DV, Phillips GJ. Draft genome sequences of the altered schaedler flora, a defined bacterial community from gnotobiotic mice. Genome Announc. 2014;2(2).
63. Turnbaugh PJ, Ridaura VK, Faith JJ, Rey FE, Knight R, Gordon JI. The effect of diet on the human gut microbiome: a metagenomic analysis in humanized gnotobiotic mice. Sci Transl Med. 2009;1(6):6ra14.
64. Kibe R, Sakamoto M, Yokota H, Ishikawa H, Aiba Y, Koga Y, et al. Movement and fixation of intestinal microbiota after administration of human feces to germfree mice. Appl Environ Microbiol. 2005;71(6):3171-8.
65. Atarashi K, Tanoue T, Shima T, Imaoka A, Kuwahara T, Momose Y, et al. Induction of colonic regulatory T cells by indigenous Clostridium species. Science. 2011;331(6015):337-41.
66. Chowdhury SR, King DE, Willing BP, Band MR, Beever JE, Lane AB, et al. Transcriptome profiling of the small intestinal epithelium in germfree versus conventional piglets. BMC Genomics. 2007;8:215.
67. Backhed F, Ding H, Wang T, Hooper LV, Koh GY, Nagy A, et al. The gut microbiota as an environmental factor that regulates fat storage. Proc Natl Acad Sci U S A. 2004;101(44):15718-23.
68. Podolsky DK. Inflammatory bowel disease. N Engl J Med. 2002;347(6):417-29.
69. Loftus EV, Jr. Clinical epidemiology of inflammatory bowel disease: Incidence, prevalence, and environmental influences. Gastroenterology. 2004;126(6):1504-17.
70. Kappelman MD, Rifas-Shiman SL, Kleinman K, Ollendorf D, Bousvaros A, Grand RJ, et al. The prevalence and geographic distribution of Crohn's disease and ulcerative colitis in the United States. Clin Gastroenterol Hepatol. 2007;5(12):1424-9.
71. Molodecky NA, Soon IS, Rabi DM, Ghali WA, Ferris M, Chernoff G, et al. Increasing incidence and prevalence of the inflammatory bowel diseases with time, based on systematic review. Gastroenterology. 2012;142(1):46-54 e42; quiz e30.
72. Rosenstiel P, Sina C, Franke A, Schreiber S. Towards a molecular risk map--recent advances on the etiology of inflammatory bowel disease. Semin Immunol. 2009;21(6):334-45.
73. Ellinghaus D, Bethune J, Petersen BS, Franke A. The genetics of Crohn's disease and ulcerative colitis--status quo and beyond. Scand J Gastroenterol. 2015;50(1):13-23.
74. Wirtz S, Neurath MF. Mouse models of inflammatory bowel disease. Adv Drug Deliv Rev. 2007;59(11):1073-83.
75. Dieleman LA, Arends A, Tonkonogy SL, Goerres MS, Craft DW, Grenther W, et al. Helicobacter hepaticus does not induce or potentiate colitis in interleukin-10-deficient mice. Infect Immun. 2000;68(9):5107-13.
76. Sellon RK, Tonkonogy S, Schultz M, Dieleman LA, Grenther W, Balish E, et al. Resident enteric bacteria are necessary for development of spontaneous colitis and immune system activation in interleukin-10-deficient mice. Infect Immun. 1998;66(11):5224-31.
77. Garrett WS, Lord GM, Punit S, Lugo-Villarino G, Mazmanian SK, Ito S, et al. Communicable ulcerative colitis induced by T-bet deficiency in the innate immune system. Cell. 2007;131(1):33-45.
78. Belkaid Y, Bouladoux N, Hand TW. Effector and memory T cell responses to commensal bacteria. Trends Immunol. 2013;34(6):299-306.

79. Frank DN, St Amand AL, Feldman RA, Boedeker EC, Harpaz N, Pace NR. Molecular-phylogenetic characterization of microbial community imbalances in human inflammatory bowel diseases. Proc Natl Acad Sci U S A. 2007;104(34):13780-5.
80. Andoh A, Kuzuoka H, Tsujikawa T, Nakamura S, Hirai F, Suzuki Y, et al. Multicenter analysis of fecal microbiota profiles in Japanese patients with Crohn's disease. J Gastroenterol. 2012;47(12):1298-307.
81. Sartor RB. Therapeutic manipulation of the enteric microflora in inflammatory bowel diseases: antibiotics, probiotics, and prebiotics. Gastroenterology. 2004;126(6):1620-33.
82. Kaur N, Chen CC, Luther J, Kao JY. Intestinal dysbiosis in inflammatory bowel disease. Gut Microbes. 2011;2(4):211-6.
83. Sokol H, Lay C, Seksik P, Tannock GW. Analysis of bacterial bowel communities of IBD patients: what has it revealed? Inflamm Bowel Dis. 2008;14(6):858-67.
84. Sokol H, Seksik P, Rigottier-Gois L, Lay C, Lepage P, Podglajen I, et al. Specificities of the fecal microbiota in inflammatory bowel disease. Inflamm Bowel Dis. 2006;12(2):106-11.
85. Hold GL, Smith M, Grange C, Watt ER, El-Omar EM, Mukhopadhya I. Role of the gut microbiota in inflammatory bowel disease pathogenesis: what have we learnt in the past 10 years? World J Gastroenterol. 2014;20(5):1192-210.
86. Swidsinski A, Ladhoff A, Pernthaler A, Swidsinski S, Loening-Baucke V, Ortner M, et al. Mucosal flora in inflammatory bowel disease. Gastroenterology. 2002;122(1):44-54.
87. Becker C, Neurath MF, Wirtz S. The Intestinal Microbiota in Inflammatory Bowel Disease. ILAR J. 2015;56(2):192-204.
88. Fox JG. The non-H pylori helicobacters: their expanding role in gastrointestinal and systemic diseases. Gut. 2002;50(2):273-83.
89. On SL, Hynes S, Wadstrom T. Extragastric Helicobacter species. Helicobacter. 2002;7 Suppl 1:63-7.
90. Solnick JV, Schauer DB. Emergence of diverse Helicobacter species in the pathogenesis of gastric and enterohepatic diseases. Clin Microbiol Rev. 2001;14(1):59-97.
91. Mizoguchi A. Animal models of inflammatory bowel disease. Prog Mol Biol Transl Sci. 2012;105:263-320.
92. Kuhn R, Lohler J, Rennick D, Rajewsky K, Muller W. Interleukin-10-deficient mice develop chronic enterocolitis. Cell. 1993;75(2):263-74.
93. Franke A, Balschun T, Karlsen TH, Sventoraityte J, Nikolaus S, Mayr G, et al. Sequence variants in IL10, ARPC2 and multiple other loci contribute to ulcerative colitis susceptibility. Nat Genet. 2008;40(11):1319-23.
94. Franke A, McGovern DP, Barrett JC, Wang K, Radford-Smith GL, Ahmad T, et al. Genome-wide meta-analysis increases to 71 the number of confirmed Crohn's disease susceptibility loci. Nat Genet. 2010;42(12):1118-25.
95. Cahill RJ, Foltz CJ, Fox JG, Dangler CA, Powrie F, Schauer DB. Inflammatory bowel disease: an immunity-mediated condition triggered by bacterial infection with Helicobacter hepaticus. Infect Immun. 1997;65(8):3126-31.
96. Kullberg MC, Ward JM, Gorelick PL, Caspar P, Hieny S, Cheever A, et al. Helicobacter hepaticus triggers colitis in specific-pathogen-free interleukin-10 (IL-10)-deficient mice through an IL-12- and gamma interferon-dependent mechanism. Infect Immun. 1998;66(11):5157-66.
97. Chichlowski M, Sharp JM, Vanderford DA, Myles MH, Hale LP. Helicobacter typhlonius and Helicobacter rodentium differentially affect the severity of colon inflammation and inflammation-associated neoplasia in IL10-deficient mice. Comp Med. 2008;58(6):534-41.

98. Kobayashi T, Okamoto S, Hisamatsu T, Kamada N, Chinen H, Saito R, et al. IL23 differentially regulates the Th1/Th17 balance in ulcerative colitis and Crohn's disease. Gut. 2008;57(12):1682-9.
99. Berg DJ, Davidson N, Kuhn R, Muller W, Menon S, Holland G, et al. Enterocolitis and colon cancer in interleukin-10-deficient mice are associated with aberrant cytokine production and CD4(+) TH1-like responses. J Clin Invest. 1996;98(4):1010-20.
100. Savage DC. Microbial ecology of the gastrointestinal tract. Annu Rev Microbiol. 1977;31:107-33.
101. Martin FP, Dumas ME, Wang Y, Legido-Quigley C, Yap IK, Tang H, et al. A top-down systems biology view of microbiome-mammalian metabolic interactions in a mouse model. Mol Syst Biol. 2007;3:112.
102. Hooper LV, Littman DR, Macpherson AJ. Interactions between the microbiota and the immune system. Science. 2012;336(6086):1268-73.
103. Strober W. Impact of the gut microbiome on mucosal inflammation. Trends Immunol. 2013;34(9):423-30.
104. Kinross JM, Darzi AW, Nicholson JK. Gut microbiome-host interactions in health and disease. Genome Med. 2011;3(3):14.
105. Sekirov I, Russell SL, Antunes LC, Finlay BB. Gut microbiota in health and disease. Physiol Rev. 2010;90(3):859-904.
106. Hugenholtz P. Exploring prokaryotic diversity in the genomic era. Genome Biol. 2002;3(2):REVIEWS0003.
107. Henderson G, Cox F, Kittelmann S, Miri VH, Zethof M, Noel SJ, et al. Effect of DNA extraction methods and sampling techniques on the apparent structure of cow and sheep rumen microbial communities. PLoS One. 2013;8(9):e74787.
108. Li M, Gong J, Cottrill M, Yu H, de Lange C, Burton J, et al. Evaluation of QIAamp DNA Stool Mini Kit for ecological studies of gut microbiota. J Microbiol Methods. 2003;54(1):13-20.
109. Ferrand J, Patron K, Legrand-Frossi C, Frippiat JP, Merlin C, Alauzet C, et al. Comparison of seven methods for extraction of bacterial DNA from fecal and cecal samples of mice. J Microbiol Methods. 2014;105:180-5.
110. Wesolowska-Andersen A, Bahl MI, Carvalho V, Kristiansen K, Sicheritz-Ponten T, Gupta R, et al. Choice of bacterial DNA extraction method from fecal material influences community structure as evaluated by metagenomic analysis. Microbiome. 2014;2:19.
111. Guo F, Zhang T. Biases during DNA extraction of activated sludge samples revealed by high throughput sequencing. Appl Microbiol Biotechnol. 2013;97(10):4607-16.
112. Yuan S, Cohen DB, Ravel J, Abdo Z, Forney LJ. Evaluation of methods for the extraction and purification of DNA from the human microbiome. PLoS One. 2012;7(3):e33865.
113. Wu GD, Lewis JD, Hoffmann C, Chen YY, Knight R, Bittinger K, et al. Sampling and pyrosequencing methods for characterizing bacterial communities in the human gut using 16S sequence tags. BMC Microbiol. 2010;10:206.
114. Ericsson AC, Davis JW, Spollen W, Bivens N, Givan S, Hagan CE, et al. Effects of vendor and genetic background on the composition of the fecal microbiota of inbred mice. PLoS One. 2015;10(2):e0116704.
115. Magoc T, Salzberg SL. FLASH: fast length adjustment of short reads to improve genome assemblies. Bioinformatics. 2011;27(21):2957-63.
116. Kuczynski J, Stombaugh J, Walters WA, Gonzalez A, Caporaso JG, Knight R. Using QIIME to analyze 16S rRNA gene sequences from microbial communities. Curr Protoc Bioinformatics. 2011;Chapter 10:Unit 10 7.

117. Altschul SF, Madden TL, Schaffer AA, Zhang J, Zhang Z, Miller W, et al. Gapped BLAST and PSI-BLAST: a new generation of protein database search programs. Nucleic Acids Res. 1997;25(17):3389-402.
118. DeSantis TZ, Hugenholtz P, Larsen N, Rojas M, Brodie EL, Keller K, et al. Greengenes, a chimera-checked 16S rRNA gene database and workbench compatible with ARB. Appl Environ Microbiol. 2006;72(7):5069-72.
119. Roeselers G, Mittge EK, Stephens WZ, Parichy DM, Cavanaugh CM, Guillemin K, et al. Evidence for a core gut microbiota in the zebrafish. ISME J. 2011;5(10):1595-608.
120. Collins FS, Tabak LA. Policy: NIH plans to enhance reproducibility. Nature. 2014;505(7485):612-3.
121. Shreiner AB, Kao JY, Young VB. The gut microbiome in health and in disease. Curr Opin Gastroenterol. 2015;31(1):69-75.
122. Hammer O, Harper D, Ryan P. PAST: Paleontological statistics software package for educaiton and data analysis. Palaeontologica Electronica. 2001;4(1):9pp.
123. Kang DW, Park JG, Ilhan ZE, Wallstrom G, Labaer J, Adams JB, et al. Reduced incidence of Prevotella and other fermenters in intestinal microflora of autistic children. PLoS One. 2013;8(7):e68322.
124. Manichanh C, Rigottier-Gois L, Bonnaud E, Gloux K, Pelletier E, Frangeul L, et al. Reduced diversity of faecal microbiota in Crohn's disease revealed by a metagenomic approach. Gut. 2006;55(2):205-11.
125. Ott SJ, Musfeldt M, Wenderoth DF, Hampe J, Brant O, Folsch UR, et al. Reduction in diversity of the colonic mucosa associated bacterial microflora in patients with active inflammatory bowel disease. Gut. 2004;53(5):685-93.
126. Comito D, Cascio A, Romano C. Microbiota biodiversity in inflammatory bowel disease. Ital J Pediatr. 2014;40:32.
127. Larsen N, Vogensen FK, van den Berg FW, Nielsen DS, Andreasen AS, Pedersen BK, et al. Gut microbiota in human adults with type 2 diabetes differs from non-diabetic adults. PLoS One. 2010;5(2):e9085.
128. Perrin S. Preclinical research: Make mouse studies work. Nature. 2014;507(7493):423-5.
129. Kappelman MD, Moore KR, Allen JK, Cook SF. Recent trends in the prevalence of Crohn's disease and ulcerative colitis in a commercially insured US population. Dig Dis Sci. 2013;58(2):519-25.
130. Kappelman MD, Rifas-Shiman SL, Porter CQ, Ollendorf DA, Sandler RS, Galanko JA, et al. Direct health care costs of Crohn's disease and ulcerative colitis in US children and adults. Gastroenterology. 2008;135(6):1907-13.
131. Bibiloni R, Mangold M, Madsen KL, Fedorak RN, Tannock GW. The bacteriology of biopsies differs between newly diagnosed, untreated, Crohn's disease and ulcerative colitis patients. J Med Microbiol. 2006;55(Pt 8):1141-9.
132. Beckwith CS, Franklin CL, Hook RR, Jr., Besch-Williford CL, Riley LK. Fecal PCR assay for diagnosis of Helicobacter infection in laboratory rodents. J Clin Microbiol. 1997;35(6):1620-3.
133. Alvarado CG, Kocsis AG, Hart ML, Crim MJ, Myles MH, Franklin CL. Pathogenicity of Helicobacter ganmani in mice susceptible and resistant to infection with H. hepaticus. Comp Med. 2015;65(1):15-22.
134. Fox JG. Helicobacter bilis: bacterial provocateur orchestrates host immune responses to commensal flora in a model of inflammatory bowel disease. Gut. 2007;56(7):898-900.
135. Jergens AE, Wilson-Welder JH, Dorn A, Henderson A, Liu Z, Evans RB, et al. Helicobacter bilis triggers persistent immune reactivity to antigens derived from the commensal bacteria in gnotobiotic C3H/HeN mice. Gut. 2007;56(7):934-40.

136. Watson J, Kelly K, Largen M, Taylor BA. The genetic mapping of a defective LPS response gene in C3H/HeJ mice. J Immunol. 1978;120(2):422-4.
137. Poltorak A, He X, Smirnova I, Liu MY, Van Huffel C, Du X, et al. Defective LPS signaling in C3H/HeJ and C57BL/10ScCr mice: mutations in Tlr4 gene. Science. 1998;282(5396):2085-8.
138. Walters WA, Xu Z, Knight R. Meta-analyses of human gut microbes associated with obesity and IBD. FEBS Lett. 2014;588(22):4223-33.
139. Joossens M, Huys G, Cnockaert M, De Preter V, Verbeke K, Rutgeerts P, et al. Dysbiosis of the faecal microbiota in patients with Crohn's disease and their unaffected relatives. Gut. 2011;60(5):631-7.
140. Sartor RB, Mazmanian SK. Intestinal Microbies in Inflammatory Bowel Diseases. Am J Gastroenterol Suppl. 2012;1:15-21.
141. Baumgart M, Dogan B, Rishniw M, Weitzman G, Bosworth B, Yantiss R, et al. Culture independent analysis of ileal mucosa reveals a selective increase in invasive Escherichia coli of novel phylogeny relative to depletion of Clostridiales in Crohn's disease involving the ileum. ISME J. 2007;1(5):403-18.
142. Gophna U, Sommerfeld K, Gophna S, Doolittle WF, Veldhuyzen van Zanten SJ. Differences between tissue-associated intestinal microfloras of patients with Crohn's disease and ulcerative colitis. J Clin Microbiol. 2006;44(11):4136-41.
143. Yang I, Eibach D, Kops F, Brenneke B, Woltemate S, Schulze J, et al. Intestinal microbiota composition of interleukin-10 deficient C57BL/6J mice and susceptibility to Helicobacter hepaticus-induced colitis. PLoS One. 2013;8(8):e70783.
144. Ericsson AC, Akter S, Hanson MM, Busi SB, Parker TW, Schehr RJ, et al. Differential susceptibility to colorectal cancer due to naturally occurring gut microbiota. Oncotarget. 2015;6(32):33689-704.

Vita

Marcia “Marci” Hart grew up in rural southeast Kansas on a small farm. During those early years she would frequently be found outdoors either helping her dad do chores, riding her horse, or playing with various animals on the farm from cats and dogs to rabbits and sheep. Marcia always loved working with the animals and spent as much time with them as possible. Her parents fondly remember on the rare occasions when Marcia was misbehaving, her punishment was that she wasn’t allowed to do any of her outside chores working with animals. This of course got her to “straighten up” quite quickly.

It is from her early experiences on the farm that Marcia developed a strong interest in biology, animal disease, and veterinary medicine. Marcia completed a Bachelor of Science degree in Animal Science at Kansas State University. During her time at KSU she was able to do a small immunology focused undergraduate project in the lab of Dr. Stephen K. Chapes. It was through this project that Marcia’s interest in the biology behind health and disease strengthened. Following graduation, Marcia had the opportunity to continue to study as a mentee of Dr. Chapes with a primary focus on the role of pulmonary macrophages and opportunistic bacterial infection in an immunocompromised mouse strain. Marcia completed a Master of Science degree for her work entitled *Reconstitution of host immunity with a TLR4-positive macrophage cell line*.

Upon graduation, Marcia moved to Ames, IA where she worked at the National Animal Disease Center for several years initially studying Leptospirosis in cattle and later Paratuberculosis (Johne’s disease) in cattle and sheep. Despite Marcia’s interest in

learning more regarding the mechanisms of disease pathogenesis, veterinary medicine was never far from her heart and in 2008 Marcia was accepted to attend Colorado State University College of Veterinary Medicine. During her time as a veterinary student at CSU, Marcia had the opportunity to continue to do research projects after class and during summer breaks where she worked in the lab of Dr. Craig Webb investigating the effect of probiotics as a potential therapy for inflammatory bowel disease (IBD) in cats. Throughout her burgeoning research career, Marcia had many positive interactions with veterinarians with a variety of different job titles. The influence of these interactions and experiences convinced Marcia that the best career fit to combine her love of veterinary medicine and research was a career in laboratory animal medicine.

Following graduation from CSU Marcia started a Comparative Medicine (lab animal medicine) residency at the University of Missouri. As part of the residency program, Marcia did a first year research project under the mentorship of Dr. Craig Franklin investigating the role of the gut microbiome in a mouse model of inflammatory bowel disease. This project was a huge undertaking with intriguing results, and Marcia was able to focus on this exciting area of research as a PhD project under the co-mentorship of Dr. Craig Franklin and Dr. Aaron Ericsson. The specific results of this project are presented within the body of this dissertation.

Marcia continues to have a strong interest in veterinary medicine and research and is very excited to see where the next step of her career takes her. She is extremely grateful to the guidance that her mentors have given her along the way. Each mentor added something new that piqued Marcia's interest and their encouragement to keep learning new things is what helped guide her along this exciting career path. Her current

future plans are to broaden her research interests and investigate the effect of the gut microbiome on neurologic development and disease. In addition to research Marcia also enjoys teaching and comparative pathology. Marcia hopes to stay in an academic setting where she can incorporate all of her areas of interest into her daily career duties and continue to make an impact on furthering research in both animal and human health.